

## ANNEX B

### Natural sources of radiation

#### CONTENTS

	<i>Paragraphs</i>		<i>Paragraphs</i>
<i>INTRODUCTION</i> .....	1-6	<b>II. INTERNAL IRRADIATION</b> .....	78-209
<b>I. EXTERNAL IRRADIATION</b> .....	7-77	<b>A. Cosmogenic radionuclides</b> .....	81-93
<b>A. Cosmic rays</b> .....	7-38	1. Tritium .....	82-84
1. Primary cosmic rays .....	8-20	2. Beryllium-7 .....	85-86
(a) Primary galactic cosmic rays ..	9-15	3. Carbon-14 .....	87-90
(b) Primary solar cosmic rays ..	16-17	4. Sodium-22 .....	91
(c) Radiation belts .....	18-20	5. Annual doses from internal irradiation by cosmogenic radionuclides .....	92-93
2. Secondary cosmic rays .....	21-25	<b>B. Primordial radionuclides (except radon and its short-lived decay products)</b> .....	94-151
3. Ionization in the atmosphere .....	26-27	1. Potassium-40 .....	95-97
4. Cosmic-ray neutrons in the atmosphere .....	28-29	2. Rubidium-87 .....	98
5. Tissue absorbed doses from cosmic rays .....	30-38	3. Uranium and thorium series .....	99-151
(a) Ionizing component .....	31-33	(a) Uranium .....	102-016
(b) Neutron component .....	34-38	(b) Thorium .....	107-110
<b>B. External radiation from naturally occurring radionuclides (terrestrial radiation)</b> .....	39-77	(c) Radium .....	111-123
1. Source radionuclides .....	39-43	(d) Long-lived decay products of <sup>222</sup> Rn .....	124-151
2. Exposure outdoors .....	44-64	<b>C. Radon-222, radon-220 and their short-lived decay products</b> .....	152-209
(a) Source-exposure relationships ..	44-45	1. Inhalation .....	152-207
(b) Environmental exposure levels .....	46-48	(a) Exposure-dose relationship ..	153-169
(c) Variation of the absorbed dose rate in air with time ..	49-52	(b) Exposure outdoors .....	170-185
(d) Estimate of the average exposure level .....	53-55	(c) Exposure indoors .....	186-204
(e) Variability of the exposure ..	56-57	(d) Recapitulation of tissue absorbed doses from <sup>222</sup> Rn, <sup>220</sup> Rn and their short-lived decay products .....	205-207
(f) Areas with high natural radiation levels .....	58-64	2. Ingestion .....	208-209
3. Exposure indoors .....	65-73	<b>III. RECAPITULATION OF TISSUE ABSORBED DOSES</b> .....	210-213
(a) Activity of building materials ..	66	<b>IV. TECHNOLOGICALLY ENHANCED EXPOSURES TO NATURAL RADIATION</b> .....	214-304
(b) Source-exposure relationship ..	67-71	<b>A. Enhanced exposures to cosmic rays</b> ..	218-236
(c) Estimate of the average indoor level of the air absorbed dose rate in air .....	72	1. Passengers in aircraft .....	218-234
(d) Variability of the absorbed dose in air .....	73	2. Astronauts .....	235-236
4. Tissue absorbed doses from terrestrial radiation .....	74-77	<b>B. Enhanced exposures to naturally occurring radionuclides</b> .....	237-272
		1. Radiation exposures due to coal-fired power plants .....	237-248

	<i>Paragraphs</i>
2. Radiation exposures due to the industrial use of phosphate products . . . . .	249-261
(a) Doses arising from the use of phosphate fertilizers . . . . .	254-256
(b) Doses arising from the use of waste gypsum as a building material . . . . .	257-259
(c) Other pathways of exposure . . . . .	260-261
3. Exposure to <sup>222</sup> Rn in natural gas and natural-gas products . . . . .	262-266
4. Exposure due to the use of building materials containing higher-than-average concentrations of naturally occurring radionuclides . . . . .	267-272

	<i>Paragraphs</i>
C. Summary and conclusions . . . . .	273
<i>Appendix. Radiation exposures from consumer products . . . . .</i>	<i>274-304</i>
Introduction . . . . .	274-276
1. Radioluminous timepieces . . . . .	277-291
2. Other self-luminous devices . . . . .	292
3. Uses of uranium and thorium . . . . .	293-298
4. Electronic and electrical equipment . . . . .	299-302
5. Absorbed doses from disposal of consumer products as waste . . . . .	303
Conclusions . . . . .	304
	<i>Page</i>
<i>References . . . . .</i>	<i>100-114</i>

## Introduction

1. Man has always been exposed to ionizing radiation from various natural sources. A distinguishing characteristic of this natural irradiation is that it involves the entire population of the world and that it has been experienced at a relatively constant rate over a very long period of time. On the other hand, the exposure to natural radiation sources varies substantially from place to place and even locally, for example within one building.

2. The assessment of the radiation doses in man from the natural sources is of particular importance because natural irradiation is the largest contributor to the collective dose of the world population. Furthermore, the study of the extent of the variation of natural radiation with location is of practical interest, since it may influence attitudes towards any additional exposure caused by man-made sources.

3. The various natural radiation sources include:

(a) External sources of extraterrestrial origin (cosmic rays) and external sources of terrestrial origin, i.e., the radioactive nuclides present in the crust of the earth, in building materials and in the air;

(b) Internal sources, comprising the naturally occurring radionuclides which are taken into the human body. The concentration of a few radionuclides in the body, such as naturally occurring <sup>14</sup>C and <sup>40</sup>K, are relatively constant and independent of their concentration in diet or in air, because they are isotopes of elements with practically constant specific activity, which are homeostatically controlled in the human body. For the majority of the natural radionuclides, on the other hand, these two conditions do not apply and their concentrations in the body vary according to the concentrations in the environment.

4. As explained in Annex A, the primary data selected for this document are those that can be used in assessments of absorbed doses in various organs and tissues of the human body. In some instances the data can be used directly in the calculations of dose; in other cases their use is indirect, constituting the basis for the assumptions used for the calculations.

5. In addition to the exposures to natural radiation sources experienced both outdoors and indoors, this

Annex, in chapter IV, discusses situations in which the exposure to natural sources is enhanced as a result of technological developments. It is sometimes difficult to separate normal and technologically enhanced radiation exposure, since this separation depends on what is considered to be a normal exposure. However, because of current interest, chapter IV considers several examples of what might reasonably be deemed technologically enhanced exposures, including those resulting from irradiation by cosmic rays in aeroplanes, the irradiation resulting from the phosphate industry, and the irradiation due to the release of naturally occurring radionuclides from coal-fired power plants.

6. The exposures from widely used consumer products are dealt with in an appendix. While they cannot be described as cases of technologically enhanced exposures to natural sources, they present several similarities to these exposures, and in many cases the radionuclides involved are naturally occurring.

## 1. EXTERNAL IRRADIATION

### A. COSMIC RAYS

7. The high-energy radiations that enter the earth's atmosphere from outer space are known as primary cosmic rays. When they interact with atomic nuclei in the atmosphere, secondary particles and electromagnetic radiation are produced, and these are called secondary cosmic rays.

#### 1. Primary cosmic rays

8. The origin of the primary cosmic rays is still not completely determined. However, it is known that most of the observed radiation originates in our galaxy. In addition to the galactic cosmic rays, the sun produces solar cosmic rays related to solar flares.

##### (a) Primary galactic cosmic rays

9. Primary galactic cosmic rays largely consist of high-energy protons which enter the solar system from interstellar space, together with <sup>4</sup>He ions in the proportion of about 10 per cent. Much smaller

proportions of heavier particles are also present, together with electrons, photons and neutrinos. The energy spectrum of the primary cosmic-ray protons has been measured both in and above the earth's atmosphere by means of instruments carried on balloons and spacecraft. The energy spectrum is peaked around 300 MeV per particle and is very broad, extending from about 1 to  $10^{14}$  MeV. Above about 1000 MeV, the proton flux density decreases markedly with increasing energy. Primary cosmic-ray protons with energies above 100 MeV are believed to be essentially of galactic origin, while those with energies below 20 MeV are of solar origin (187).

10. Although all cosmic rays with energies below  $10^{12}$  MeV have their origin within the galaxy (59), the details of their origin are not yet known. From the elemental distribution present, it is thought that cosmic-ray nuclei are synthesized in supernova events, and are subsequently accelerated by undetermined processes, for which several theories have been postulated. From the abundance in primary cosmic rays of Fe, Co and Ni nuclei, some of which have undergone decay by electron capture, it is inferred that there is a time lapse of more than one year between nucleosynthesis and acceleration to high energy (59). The average "age" of galactic cosmic rays reaching the solar system, which alternatively may be called the escape lifetime from the galaxy, can be estimated from the abundance of  $^{10}\text{Be}$  and  $^{36}\text{Cl}$ . The most recent measurements indicate a lifetime between  $2.5 \cdot 10^6$  and  $33 \cdot 10^6$  y (235).

11. From measurements of the products of the reaction of high-energy cosmic rays with nuclei (spallation products) in meteorites, estimates have been made of the changes in cosmic-ray flux density with time. Within a factor of two, the galactic cosmic-ray flux density has remained constant over the past  $10^9$  y (304). The flux density averaged over the past 400 y is within 10 per cent of that averaged over the past  $4 \cdot 10^5$  y, which in turn is some 50 per cent higher than that averaged over the past  $10^9$  y. This latter variation may be due to a cosmic-ray gradient perpendicular to the galactic plane.

12. Within the solar system, the galactic cosmic-ray flux density increases with increasing distance from the sun. The radial gradient of the flux density has been determined from spallation products in meteorites (304) and more recently by direct measurement on board the Pioneer 10 and 11 spacecraft (225, 227). For cosmic-ray particles with energies above 30 MeV per nucleon, the gradient is about +5 per cent per AU (1 AU =  $149.6 \cdot 10^6$  km).

13. Below  $10^4$  MeV, the primary flux density is modified by two processes. In the first, it is affected by the earth's magnetic field, which deflects lower-energy charged particles back into space. This effect is dependent on the geomagnetic latitude, so that the flux density of low-energy protons at the top of the atmosphere is greater at the poles than in equatorial regions. Thus, the ionization produced at a given altitude in the atmosphere, which is a function of the "atmospheric depth", the mass of air above a unit of area at that altitude, is also latitude dependent (fig. 1).

14. In the second process, the flux density of the galactic low-energy protons in the upper atmosphere varies with the 11-year solar cycle, the flux density being at a minimum during times of maximum solar activity and passing through a maximum during the period of low solar activity. The phenomenon is known as modulation (89, 313). The modulation of galactic cosmic rays with the solar cycle has been observed for many years. It has been proposed that it is due to changes in the flux of magnetic bubbles (large volumes of ionized gas) of solar origin (256). Solar flares blast open the overlying solar magnetic field, thus enabling corona particles access to the interplanetary medium, the large bubbles so formed moving away from the sun with velocities of  $200\text{-}1000 \text{ km s}^{-1}$ .

15. During the 11-year solar cycle the density of these magnetic bubbles in interplanetary space undergoes a cyclical change, reaching a maximum during increased solar activity and a minimum during the period of the quiet sun. Because galactic cosmic-ray particles with energies less than  $10^4$  MeV are deflected away from the inner solar system by these magnetic irregularities, an 11-year modulation of the galactic cosmic-ray flux density is produced at the earth.

#### (b) Primary solar cosmic rays

16. Solar flares are observed as bright flame-like protuberances on the sun's surface which reach maximum brightness in about 10 min and then slowly subside (74). They tend to occur more frequently during periods of sun-spot maximum. Large amounts of energy in the form of visible, ultraviolet and x-radiation are emitted, and in the largest flares large quantities of charged particles, mainly protons and alpha particles, are also released. Measurements indicate that most of the protons have energies in the range 1-40 MeV.

17. Because the solar cosmic rays from solar flares have relatively low energy, they do not usually cause significant increases in radiation doses at the earth's surface. In fact, between 1942 and 1962 only 13 flares produced observable effects in the lower atmosphere (150). However, large flares can increase the absorbed dose index rate in the upper atmosphere by a factor of about 100 for short periods of time.

#### (c) Radiation belts

18. There are two radiation belts, often called the Van Allen belts, situated between 1.2 and 8 earth radii above the equator. The lower belt extends to latitudes between  $30^\circ$  and  $60^\circ$  north and south (3, 129). The outer belt is confined more to low-latitude regions. The energetic particles, mainly protons and electrons, with some alpha particles in the outer belt, are trapped in these belts by the earth's magnetic field. They spiral along the lines of magnetic force, being reflected back and forth owing to the increased convergence of the magnetic field towards the polar regions.

19. The inner radiation belt consists mainly of protons with energies from several to several hundred mega-electronvolts, the peak flux density being at about

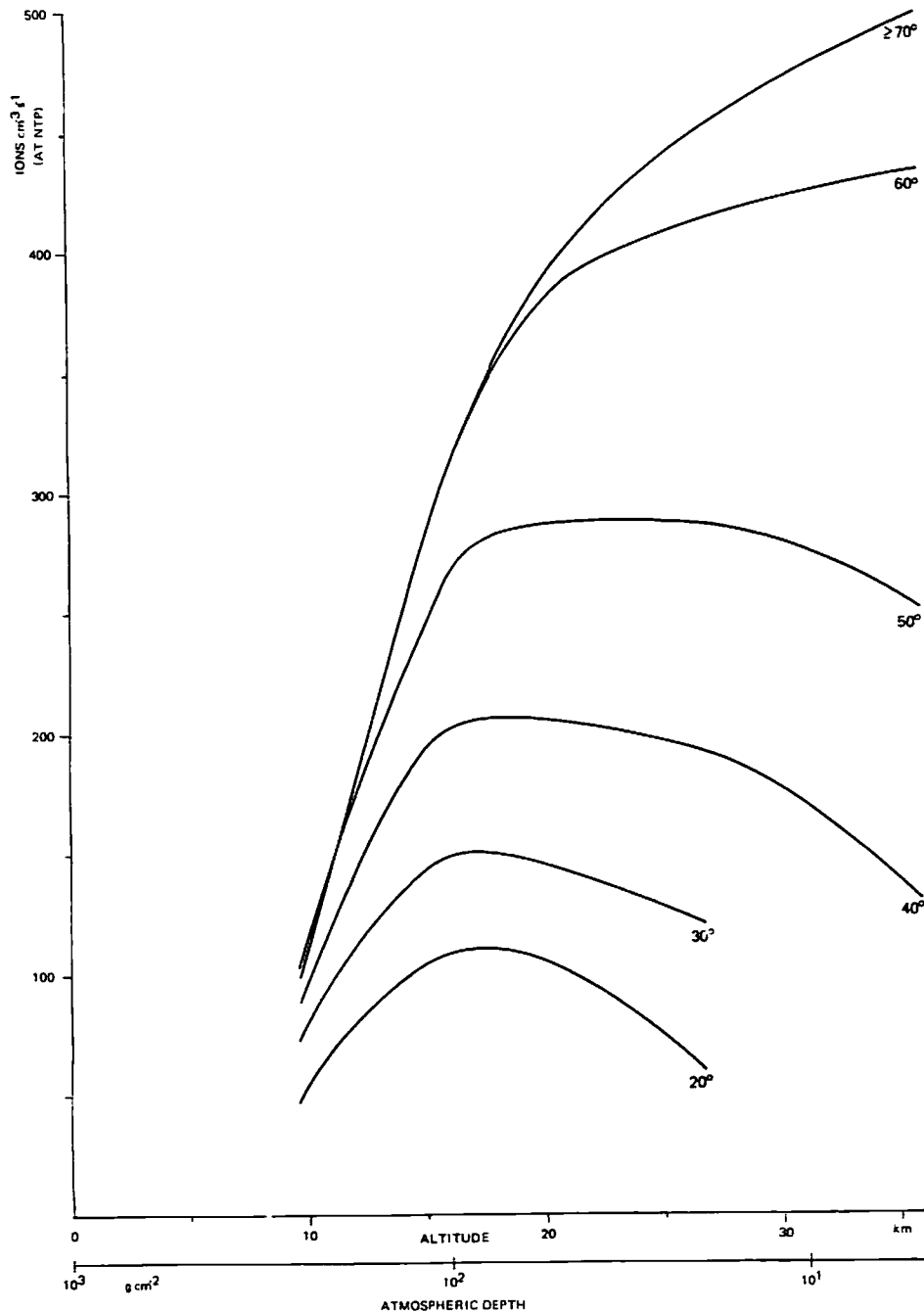


Figure 1. Variation of ionization with altitude and atmospheric depth at different geomagnetic latitudes. Based upon the results of Neher (253)

50 MeV, and electrons with a flux density that is fairly flat over the energy range 100-400 keV. The maximum proton flux density is about  $4 \cdot 10^4$  particles  $\text{cm}^{-2} \text{s}^{-1}$ , and this occurs at a height of about 1.5 earth radii over the equator (3). In the outer belt, the proton energies are mainly in the range 0.1-5 MeV, most of the particles being in the low-energy region. The outer belt also contains electrons and to a lesser extent alpha particles (3, 129). The flux density in the radiation belts is fairly constant in time, but does change with the flux density of primary cosmic rays during the 11-year solar cycle (129).

20. It is believed that the origin of most of the more energetic particles in the inner radiation belt is the decay of cosmic-ray albedo neutrons (233). The high-energy

primary cosmic-ray protons collide with atoms in the air to produce neutrons by knock-on (direct) reactions, with energies between 1 and 1000 MeV, or by compound nuclear reactions that produce evaporation neutrons with energies of about 8 MeV. Many of these neutrons escape from the atmosphere either directly, if their energy is high, or by diffusion, if it is low. These escaping neutrons are called albedo neutrons; they decay to protons and electrons in an average time of 1000 s, and since these particles are charged, they will spiral along the flux lines of the earth's magnetic field. They are reflected back along the magnetic lines of force in high-latitude regions where the magnetic flux lines converge. If the height where the reflection takes place, termed the image height, is above the atmosphere, the particles will remain trapped in the earth's magnetic field

(129). The origin of the particles in the outer belt is less certain. Since there is an alpha-particle component, it is thought that some of the particles are of solar origin.

## 2. Secondary cosmic rays

21. When primary cosmic-ray particles enter the atmosphere, those with higher energy undergo nuclear reactions with nuclei of atoms present in the air, producing neutrons, protons, pions and kaons. Those with lower energy lose energy by causing ionization. Many of the secondary particles have sufficient energy to initiate whole sequences of further nuclear reactions with nitrogen and oxygen nuclei. The initial high-energy reactions are called spallation reactions and quite a variety of reaction products (cosmogenic nuclides) are formed, such as  $^3\text{H}$ ,  $^7\text{Be}$ ,  $^{10}\text{Be}$ ,  $^{22}\text{Na}$  and  $^{24}\text{Na}$ .

22. The important initial secondary cosmic-ray particles are high-energy protons, neutrons and pions, many of which react further with nuclei in the air to form more secondary particles (100, 277). As this process continues, the number of secondary particles builds up; such a process is called a cascade. The pions decay into muons or photons, initiating other cascades.

23. The protons and neutrons contribute significantly to the absorbed dose index rate in the upper atmosphere. The neutrons lose energy by elastic collisions, and when thermalized they are captured by  $^{14}\text{N}$  to form  $^{14}\text{C}$ . Because nucleons rapidly lose energy by ionization and nuclear collisions, the nucleonic flux

density is considerably attenuated in the lower part of the atmosphere and at sea level accounts for only a few per cent of the absorbed dose index rate.

24. At lower altitudes in the atmosphere, the major contribution to the absorbed dose index rate is provided by the muons produced by the decay of charged pions at higher altitudes and by the associated collision electrons. Since muons have only a small cross-section for interaction with atomic nuclei, have a mean life at rest of  $2.2 \mu\text{s}$  before decay into electrons, and move largely at relativistic velocities, they penetrate quite effectively into the lower layers of the atmosphere and through structural building materials (301). Electrons are also produced by muon decay, by ionization due to other charged particles and in electromagnetic cascade processes. Except in the lower layers of the atmosphere, electrons are the main contributor to the absorbed dose index rate.

25. The flux densities of all cosmic-ray particles undergo variations in time due to modulation over the solar cycle, the effects of solar flares and changes in atmospheric pressure or temperature. The approximate amplitude variations expected from these various effects are shown in table 1. It should be noted that the flux densities of various secondary cosmic rays at a given altitude depend primarily on the atmospheric depth (see paragraph 13). However, for the purposes of radiation-dose estimates, atmospheric depth is converted into altitude (in kilometres) in this report, assuming a standard atmosphere.

TABLE 1. AMPLITUDE AND PERIOD OF THE TIME VARIATION OF COSMIC-RAY FLUX DENSITY

Source of variation	Cosmic-ray component	Altitude above sea level (km)	Latitude (N and S)	Relative amplitude ( $100 \Delta N/N_0$ ) <sup>a</sup>	Period	Reference
Solar modulation	Charged particles	9	> 50°	22	11 y	253
	Charged particles	5.5	> 50°	16		253
	Muons	0	> 50°	5		89
	Neutrons	3.5	> 50°	25		313
	Neutrons	0	> 50°	20		313
Solar flares	Muons	0	> 50°	0-400	Hours	74,301
	Neutrons	0	0°-90°	0-10 000	Hours	301
Atmospheric pressure variations	Charged particles	0	0°-90°	< 10	Days	
	Neutrons	0	0°-90°	< 15	Days	
Atmospheric temperature variations	Muons	0	0°-90°	< 5	1 y	54

Source: Reference 249.

<sup>a</sup>Total amplitude of variation relative to "normal" or average flux density  $N_0$ .

## 3. Ionization in the atmosphere

26. Many measurements of cosmic-ray ionization at various altitudes have been reported. The ionization rate per unit volume in free air is a measure of the flux density of the total charged-particle component of the cosmic-ray field and is usually expressed as the number of ion pairs formed per second in each cubic centimetre of air at normal temperature and pressure (NTP) (9, 95, 96, 210, 291, 312). As figure 1 shows, ionization in the atmosphere becomes increasingly latitude-dependent

with increasing altitude. The ionization also varies over the solar cycle, being greatest during solar minimum and smallest during solar maximum (213, 254).

27. For estimating the absorbed dose index rate at altitudes above sea level, use was made of the measurements of Neher (254) over Thule, Greenland, between 1954 and 1959, of Raft *et al.* (291) made at latitude 54°N in 1969, and of George (95), who made measurements at altitudes of 400 and 1500 km in 1969. Lowder and Beck (210) also reported ionization

measurements in the lower atmosphere up to an altitude of about 3 km. In its 1972 report, the Committee discussed inconsistencies in some of the earlier measurements, particularly the differences between the measurements of George (96) and those of Lowder and Beck (210) and Shamos and Liboff (312). A value for the ion-pair production rate of  $2.14 \text{ cm}^{-3} \text{ s}^{-1}$  was used as the average ionization at sea level. Lowder and O'Brien (213) adopted a value of  $2.0\text{-}2.2 \text{ cm}^{-3} \text{ s}^{-1}$ . For the purposes of computing the absorbed dose index rate, a value of  $2.1 \text{ cm}^{-3} \text{ s}^{-1}$  will be assumed in this report.

#### 4. Cosmic-ray neutrons in the atmosphere

28. Most of the dose delivered by low-energy neutrons arise from capture reactions such as  $(n, \gamma)$  and  $(n, p)$ , while for high-energy neutrons it comes from knock-on protons. Since the significant part of the cosmic-ray neutron energy spectrum extends from  $10^{-1}$  to some  $10^9$  electronvolts, some knowledge of its shape is necessary to compute the dose from neutrons.

29. As discussed in the 1972 report, a number of calculations have been made of the neutron differential energy spectrum at different altitudes. In general, these agree with measurements made of neutrons in the range 1-10 MeV at various altitudes. Merker *et al.* (234) have recently reported balloon and aircraft measurements of neutrons in that energy range during the period 1964-1971. These results agree well with the data that was used to compute neutron doses at higher altitudes in the 1972 report. Light *et al.* (201) have carried out Monte Carlo calculations of the neutron energy spectrum and normalized their results using the experimental data of Merker *et al.* (234). These authors assessed the neutron production rate averaged over a solar cycle to be  $4.0 \text{ cm}^{-2} \text{ s}^{-1}$ .

#### 5. Tissue absorbed doses from cosmic rays

30. Traditionally, two quantities that are useful for estimating dose rates from cosmic rays have been measured, the ionization in air and the neutron flux density. Since the radiation quality of these two components is different, the absorbed dose index rates from the ionizing and neutron components will be treated separately. The absorbed dose index rate can be assessed from measured ionization in and above the atmosphere, and from measurements of particle flux density and energy spectrum. The contribution from the neutron component can be calculated from data on the neutron flux density.

##### (a) Ionizing component

31. The estimation of the absorbed dose rate in air from the ionizing component of cosmic rays is straightforward. Assuming each ion pair requires 33.7 eV to be produced, the absorbed dose rate for an ionization rate of  $1 \text{ cm}^{-3} \text{ s}^{-1}$  is  $1.50 \mu\text{rad h}^{-1}$ . Using the value for the ionization rate at sea level of  $2.1 \text{ cm}^{-3} \text{ s}^{-1}$  (para. 27), the absorbed dose rate in air is  $3.2 \mu\text{rad h}^{-1}$ .

This value is quantitatively equal to the absorbed dose index rate at ground level. Using reported values of ionization in the upper atmosphere, absorbed dose index rates have been computed there in a similar manner and are shown in figure II (347). Kolb and Lauterbach (191) have recently reported measurements in the lower atmosphere with both an ionization chamber and a scintillation spectrometer. The ionization chamber results agreed with those reported by Lowder and Beck (210), but the measurements with the scintillator were consistently higher.

32. At sea level about 75 per cent of the ionization is from muon collision electrons, 15 per cent from muon decay electrons and 10 per cent from other electron, proton and neutron processes (249). As the absorbed dose index rate is reduced by about 30 per cent by  $50 \text{ g cm}^{-2}$  of material, mostly due to attenuation of the incident electrons, a building may provide substantial structural shielding.

33. If this structural shielding effect is not taken into account, the annual absorbed dose in human tissues  $D$  is given by

$$D = c_c q \dot{D}_1$$

(see Annex A), where  $c_c = 8.76 \text{ mrad } \mu\text{rad}^{-1} \text{ h}$ ;  $q = 1$ ; and  $\dot{D}_1$  is the outdoor absorbed dose index rate. With a value of  $\dot{D}_1$  of  $3.2 \mu\text{rad h}^{-1}$  (para. 31), the annual absorbed dose in human tissues from the ionizing component of cosmic rays at sea level is approximately 28 mrad.

##### (b) Neutron component

34. The dose rate from the neutron component was derived in the 1972 report from computed absorbed dose rates in 30-cm tissue slabs. As indicated in Annex A, the absorbed-dose index rate is used in this report to describe cosmic-ray irradiation conditions. Hajnal *et al.* (112) found that the variation of dose rate with depth, 0-15 cm, for the bilateral incidence of cosmic-ray neutrons on a 30-cm slab was not very great. The maximum dose rate (at 1 cm) was only 6 per cent greater than the average for 0-15 cm. For a 30-cm sphere, the dose rate would be expected to be even more uniform, and so for cosmic-ray neutrons it can be assumed that the absorbed dose index rate is the same as the average absorbed dose rate computed from the 30-cm slab. The factor to convert neutron flux density to absorbed dose index rate is  $4.93 \mu\text{rad h}^{-1} \text{ cm}^2 \text{ s}$  (112).

35. A number of data on the cosmic-ray neutron flux density at sea level were reported in the 1972 report, varying from  $0.0065$  to  $0.018 \text{ cm}^{-2} \text{ s}^{-1}$ . A neutron flux density of  $0.008 \text{ cm}^{-2} \text{ s}^{-1}$  was adopted for the purpose of estimating doses at high latitudes. Using the conversion factor from the previous paragraph, the absorbed-dose index rate is  $0.04 \mu\text{rad h}^{-1}$ . This value is in good agreement with tissue absorbed dose rates calculated by O'Brien and McLaughlin (263).

36. The annual absorbed dose in human tissues at sea level and at latitudes above  $40^\circ$ , calculated by the

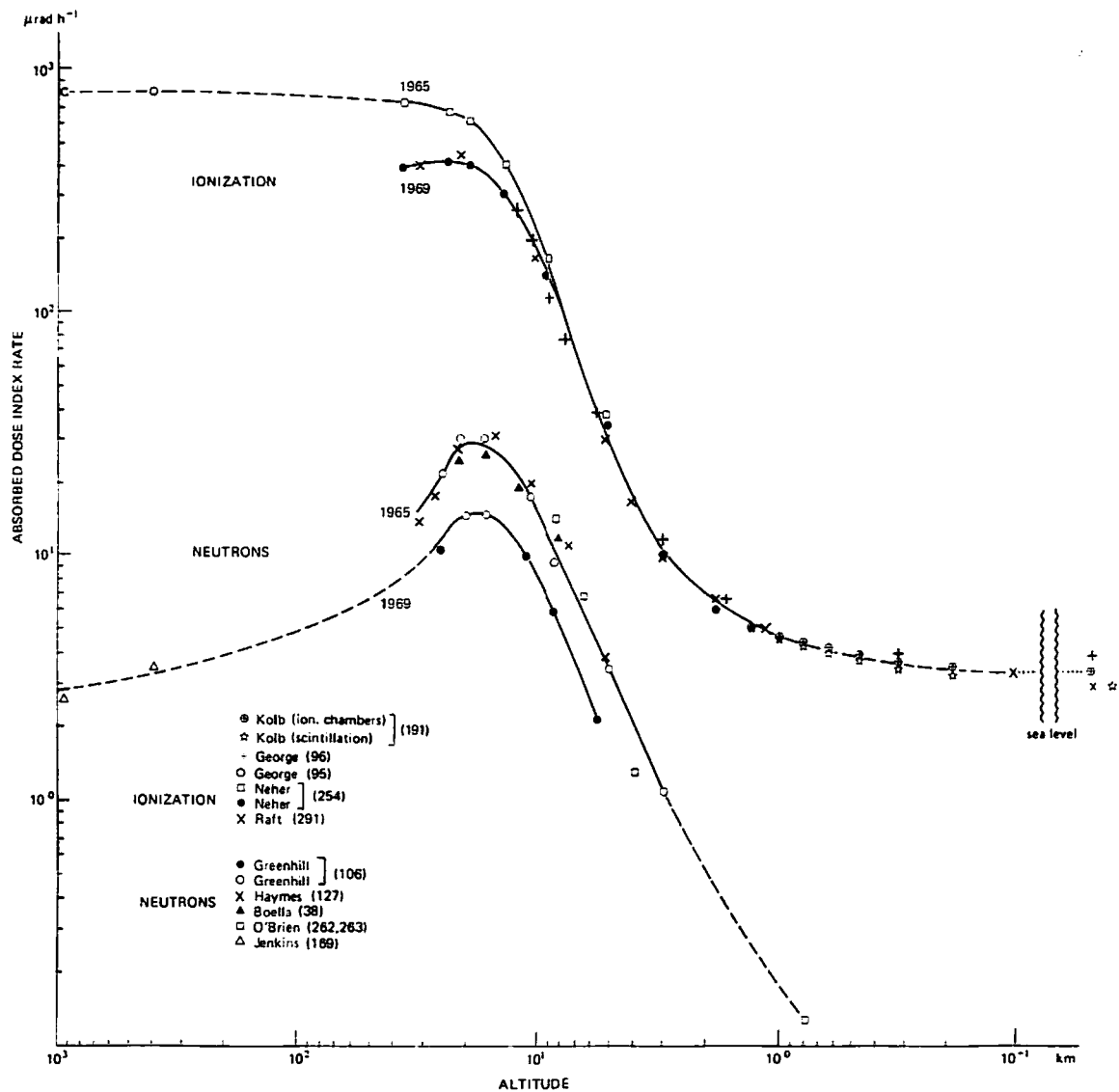


Figure II. Absorbed dose index rates at high geomagnetic latitudes ( $\sim 50^\circ$ ) from the ionizing and neutron components of cosmic rays at different altitudes for 1969 (solar maximum) and 1965 (solar minimum) (347). The ionization component of the absorbed dose rate at  $10^{-1}$  km is inferred from that at ground level

expression given in paragraph 33, is therefore 0.35 mrad. In equatorial regions, the annual absorbed dose in human tissues is about 0.2 mrad (347).

37. Although at sea level the neutron absorbed dose index rate is quite small, it increases rapidly with altitude, reaching a maximum at altitudes between 10 and 20 km. Measured neutron flux densities at various altitudes reported in the literature differ in the energy range they cover, latitude and time in the solar cycle. These reported values were normalized for these factors, using a published energy spectrum (112) to assess the total flux density from the reported values. The absorbed dose index rates were computed using a factor of  $4.93 \mu\text{rad h}^{-1} \text{cm}^2 \text{s}$  to convert the neutron flux density to the absorbed dose index rate, and are shown plotted in figure II versus altitude.

38. Foelsche *et al.* (88) have recently computed the dose-equivalent rate from cosmic-ray neutrons at high altitude using a new energy spectrum that does not drop off so quickly in the high-energy region as that used in the 1972 report. The use of this new spectrum results in

a higher absorbed dose index rate with a much higher contribution from neutrons in the high-energy region above 10 MeV. However, there is some question as to the validity of this spectrum in the high-energy region (88).

## B. EXTERNAL RADIATION FROM NATURALLY OCCURRING RADIONUCLIDES (TERRESTRIAL RADIATION)

### 1. Source radionuclides

39. Radioactive nuclides have always been present in the natural environment. The decay of natural radionuclides produces alpha particles, electrons and electromagnetic radiation. Because the human organs and tissues in which the doses are calculated for the purposes of this document are shielded by at least a few millimetres of tissue, which absorbs practically all of the energy of the alpha particles and electrons given off by the natural radionuclides, only the gamma contribution will be considered here. It is worth noting, however, that

the skin and, to a lesser extent, the lens of the eye, being at or near the surface of the body, receive higher doses than the tissues and organs of primary interest to the Committee.

40. The natural radionuclides in the environment are of two general classes, the primordial and the cosmogenic. The cosmogenic radionuclides are mainly produced through interaction of the cosmic rays with target atoms in the atmosphere and, to a much lesser

extent, in the earth. The three main cosmogenic contributors to external exposure at ground level are  $^7\text{Be}$ ,  $^{22}\text{Na}$  and  $^{24}\text{Na}$ .

41. Among the primordial radionuclides, the main contributors to external exposure are  $^{40}\text{K}$  and the radioactive series headed by  $^{238}\text{U}$  and  $^{232}\text{Th}$ , which are presented in tables 2 and 3. Potassium-40,  $^{238}\text{U}$  and  $^{232}\text{Th}$  are long-lived radionuclides that have existed in the earth's crust throughout its history.

TABLE 2. RADIOACTIVE DECAY PROPERTIES OF THE  $^{238}\text{U}$  SERIES

Nuclide	Historical name	Half-life	Major radiation energies (MeV) and intensities		
			$\alpha$	$\beta$	$\gamma$
$^{238}\text{U}$	Uranium I	$4.51 \cdot 10^9$ y	4.15 (25%) 4.20 (75%)	-	-
$^{234}\text{Th}$	Uranium X <sub>1</sub>	24.1 d	-	0.103 (21%) 0.193 (79%)	0.063 (3.5%) 0.093 (4%)
$^{234\text{m}}\text{Pa}$	Uranium X <sub>2</sub>	1.17 min	-	2.29 (98%)	0.765 (0.30%) 1.001 (0.60%)
$^{234}\text{Pa}$	Uranium Z	6.75 h	-	0.53 (66%) 1.13 (13%)	0.100 (50%) 0.70 (24%) 0.90 (70%)
$^{234}\text{U}$	Uranium II	$2.47 \cdot 10^4$ y	4.72 (28%) 4.77 (72%)	-	0.053 (0.2%)
$^{230}\text{Th}$	Ionium	$8.0 \cdot 10^4$ y	4.62 (24%) 4.68 (76%)	-	0.068 (0.6%) 0.142 (0.07%)
$^{226}\text{Ra}$	Radium	1602 y	4.60 (6%) 4.78 (95%)	-	0.186 (4%)
$^{222}\text{Rn}$	Emanation Radon (Rn)	3.823 d	5.49 (100%)	-	0.510 (0.07%)
$^{218}\text{Po}$	Radium A	3.05 min	6.00 (~100%)	0.33 (~0.019%)	-
$^{214}\text{Pb}$	Radium B	26.8 min	-	0.65 (50%) 0.71 (40%) 0.98 (6%)	0.295 (19%) 0.352 (36%)
$^{218}\text{At}$	Astatine	~2 s	6.65 (6%) 6.70 (94%)	? (~0.1%)	-
$^{214}\text{Bi}$	Radium C	19.7 min	5.45 (0.012%) 5.51 (0.008%)	1.0 (23%) 1.51 (40%) 3.26 (19%)	0.609 (47%) 1.120 (17%) 1.764 (17%)
$^{214}\text{Po}$	Radium C'	164 $\mu\text{s}$	7.69 (100%)	-	0.799 (0.014%)
$^{214}\text{Tl}$	Radium C''	1.3 min	-	1.3 (25%) 1.9 (56%) 2.3 (19%)	0.296 (80%) 0.795 (100%) 1.31 (21%)
$^{210}\text{Pb}$	Radium D	21 y	3.72 (.000002%)	0.016 (85%) 0.061 (15%)	0.047 (4%)
$^{210}\text{Bi}$	Radium E	5.01 d	4.65 (.00007%) 4.69 (.00005%)	1.161 (~100%)	-
$^{210}\text{Po}$	Radium F	138.4 d	5.305 (100%)	-	0.803 (0.0011%)
$^{210}\text{Tl}$	Radium E''	4.19 min	-	1.571 (100%)	-
$^{206}\text{Pb}$	Radium G	Stable	-	-	-

Source: Reference 288.



TABLE 3. RADIOACTIVE DECAY PROPERTIES OF THE  $^{40}\text{K}$  AND THE  $^{232}\text{Th}$  SERIES

Nuclide	Historical name	Half-life	Major radiation energies (MeV) and intensities		
			$\alpha$	$\beta$	$\gamma$
$^{40}\text{K}$		$1.26 \cdot 10^9$ y	-	1.32 (89%)	1.46 (11%)
$^{40}\text{Ar}$		Stable	-		
$^{232}\text{Th}$	Thorium	$1.41 \cdot 10^{10}$ y	3.95 (24%) 4.01 (76%)	-	-
$^{228}\text{Ra}$	Mesothorium I	5.8 y	-	0.055 (100%)	-
$^{228}\text{Ac}$	Mesothorium II	6.13 h	-	1.18 (35%) 1.75 (12%) 2.09 (12%)	0.34 (15%) 0.908 (25%) 0.96 (20%)
$^{228}\text{Th}$	Radiothorium	1.910 y	5.34 (28%) 5.43 (71%)	-	0.084 (1.6%) 0.214 (0.3%)
$^{224}\text{Ra}$	Thorium X	3.64 d	5.45 (6%) 5.68 (94%)	-	0.241 (3.7%)
$^{220}\text{Rn}$	Emanation Thoron (Tn)	55 s	6.29 (100%)	-	0.55 (0.07%)
$^{216}\text{Po}$	Thorium A	0.15 s	6.78 (100%)	-	-
$^{212}\text{Pb}$	Thorium B	10.64 h	-	0.346 (81%) 0.586 (14%)	0.239 (47%) 0.300 (3.2%)
$^{212}\text{Bi}$	Thorium C	60.6 min	6.05 (25%) 6.09 (10%)	1.55 (5%) 2.26 (55%)	0.040 (2%) 0.727 (7%) 1.620 (1.8%)
$^{212}\text{Po}$	Thorium C'	304 ns	8.78 (100%)	-	-
$^{208}\text{Tl}$	Thorium C''	3.10 min	-	1.28 (25%) 1.52 (21%) 1.80 (50%)	0.511 (23%) 0.583 (86%) 0.860 (12%) 2.614 (100%)
$^{208}\text{Pb}$	Thorium D	Stable	-	-	-

Source: Reference 288.

42. The concentration of the primordial radionuclides in soil is determined by the radioactivity of the source rock and by the nature of the processes which had been involved in the formation of the soil. Table 4 shows typical natural concentrations in common rocks (249). In igneous rocks, the concentration of radioactive nuclides is related to the quantity of silicates, being

highest in acidic rocks and lowest in the ultrabasic rocks. Igneous rocks generally exhibit higher radioactivity than sedimentary rocks, while metamorphic rocks have concentrations typical of the rocks from which they were derived. However, certain sedimentary rocks, notably some shales and phosphate rocks, are highly radioactive (249).

TABLE 4. TYPICAL ACTIVITY CONCENTRATION OF  $^{40}\text{K}$ ,  $^{238}\text{U}$  AND  $^{232}\text{Th}$  IN COMMON ROCKS AND ESTIMATED ABSORBED DOSE RATE IN AIR 1 m ABOVE THE SURFACE

Type of rock	Typical activity concentration ( $\mu\text{Ci g}^{-1}$ )			Absorbed dose rate in air ( $\mu\text{rad h}^{-1}$ )
	$^{40}\text{K}$	$^{238}\text{U}$	$^{232}\text{Th}$	
<i>Igneous</i>				
Acidic (e.g. granite)	27	1.6	2.2	12
Intermediate (e.g. diorite)	19	0.62	0.88	6.2
Mafic (e.g. basalt)	6.5	0.31	0.30	2.3
Ultrabasic (e.g. durite)	4.0	0.01	0.66	2.3
<i>Sedimentary</i>				
Limestone	2.4	0.75	0.19	2.0
Carbonate	-	0.72	0.21	1.7
Sandstone	10	0.5	0.3	3.2
Shale	19	1.2	1.2	7.9

Sources: References 1, 353.

43. The concentration of radionuclides in soil, which is directly relevant to the outdoor exposure, is that of the rock from which it is derived, diminished by the leaching action of moving water, diluted by increased porosity and by added water and organic matter, and augmented by sorption and precipitation of radionuclides from incoming water (250). An extensive study of the mean concentration of the natural radionuclides in soils of various types in the Soviet Union (188) shows that there is a regular trend for all the natural radionuclides which partly reflects the extent of bio-geochemical reworking of the original soil-forming rocks (table 5). It should be noted, however, that the

TABLE 5. AVERAGE ACTIVITY CONCENTRATION OF  $^{40}\text{K}$ ,  $^{238}\text{U}$  AND  $^{232}\text{Th}$  IN VARIOUS TYPES OF SOIL AND ABSORBED DOSE RATE IN AIR 1 m ABOVE THE SURFACE

Type of soil	Average activity concentration ( $\mu\text{Ci g}^{-1}$ )			Absorbed dose rate in air ( $\mu\text{rad h}^{-1}$ )
	$^{40}\text{K}$	$^{238}\text{U}$	$^{232}\text{Th}$	
Serozem	18	0.85	1.3	7.4
Gray-brown	19	0.75	1.1	6.9
Chestnut	15	0.72	1.0	6.0
Chernozem	11	0.58	0.97	5.1
Gray forest	10	0.48	0.72	4.1
Sodpodzolic	8.1	0.41	0.60	3.4
Podzolic	4.0	0.24	0.33	1.8
Boggy	2.4	0.17	0.17	1.1
World average	10	0.7	0.7	4.6
Typical range <sup>a</sup>	3-20	0.3-1.4	0.2-1.3	1.4-9

Sources: References 18, 107, 188, 249, 353.

<sup>a</sup>Values based on data contained in references 18, 107 and 353.

main factor influencing the concentration of the natural radionuclides in soil is not the soil-forming process but the corresponding concentration in the soil-forming rocks. Table 5 also includes an estimate of the average soil concentration on a world-wide basis (249), as well as typical ranges of values reported in the literature (18, 107, 353).

## 2. Exposure outdoors

### (a) Source-exposure relationships

44. Methods of calculation of the absorbed dose rate in air<sup>1</sup> from the radionuclides present in the atmosphere and in the soil are discussed in references 26, 86, 142 and 237. Table 6 presents the absorbed dose rates in air 1 m above ground for a representative soil containing unit activity concentrations of the natural radionuclides, assumed to be uniformly distributed with depth. The representative soil is described by its density,  $1.6 \text{ g cm}^{-3}$ , and its constituent concentrations (weight per cent):  $\text{SiO}_2$ , 67.5;  $\text{Al}_2\text{O}_3$ , 13.5;  $\text{Fe}_2\text{O}_3$ , 4.5;  $\text{CO}_2$ , 4.5;  $\text{H}_2\text{O}$ , 10.0. The absorbed dose rates in air have been calculated using the assumption that all the decay products of  $^{238}\text{U}$  and  $^{232}\text{Th}$  are in radioactive equilibrium with

<sup>1</sup>As indicated in Annex A, the absorbed dose rate in air is used in this report to describe environmental exposure situations resulting from gamma-emitting radionuclides and is unambiguously specified, assuming full equilibrium in air.

TABLE 6. ABSORBED DOSE RATE IN AIR 1 m ABOVE GROUND FOR A REPRESENTATIVE SOIL CONTAINING UNIT ACTIVITY CONCENTRATIONS OF  $^{40}\text{K}$ ,  $^{238}\text{U}$  AND  $^{232}\text{Th}$

Radionuclide <sup>a</sup>	Dose rate ( $\mu\text{rad h}^{-1}$ per $\mu\text{Ci g}^{-1}$ )
$^{40}\text{K}$	0.16
$^{238}\text{U}$	1.58
$^{232}\text{Th}$	2.45

Source: Reference 24.

<sup>a</sup>All the decay products of  $^{238}\text{U}$  and  $^{232}\text{Th}$  are assumed to be in radioactive equilibrium with their precursor.

their precursors. This assumption, which is reasonable for rocks, is not strictly valid for soils, since (a) differentiation may result from the soil-forming process and biological reworking and (b) a fraction of the radon produced in the soil escapes into the soil air and diffuses into the atmosphere from the upper soil layers.

45. The conversion factors of table 6 were used to calculate the absorbed dose rates in air above the rocks and soils for which typical concentrations were given in tables 4 and 5 (last column). The main contributors to the absorbed dose rate in air are  $^{208}\text{Tl}$  and  $^{228}\text{Ac}$  in the  $^{232}\text{Th}$  series, while for the  $^{238}\text{U}$  series, about 99 per cent of the dose rate is due to  $^{214}\text{Pb}$  and  $^{214}\text{Bi}$ , which are short-lived decay products of  $^{222}\text{Rn}$ . The gamma rays that these nuclides emit range in energy up to 2.6 MeV and are partly absorbed in the soil. For a typical natural radiation field, the layer of soil which makes the predominant contribution to external irradiation above the ground is about 30 cm thick (fig. III).

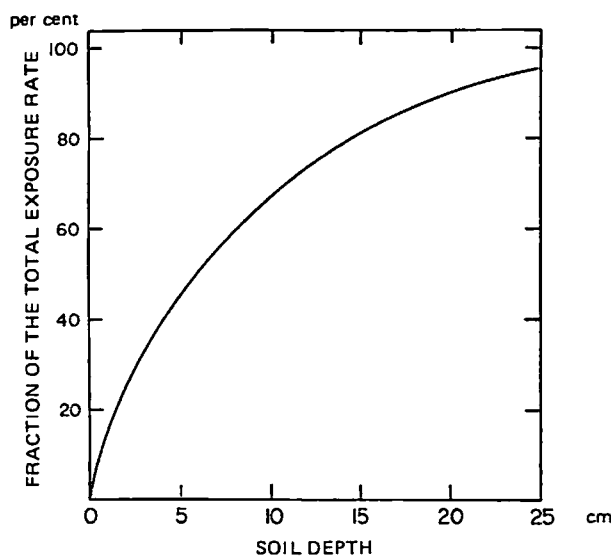


Figure III. Calculated relative contribution of naturally occurring radionuclides to the total exposure rate 1 m above the ground, as a function of soil thickness (24)

### (b) Environmental exposure levels

46. In recent years, several surveys have been performed over whole countries and areas for the purpose of estimating the exposure of the populations of those countries and areas to natural radiation (table 7).

TABLE 7. ESTIMATES OF THE AVERAGE ABSORBED DOSE RATE IN AIR 1 m ABOVE GROUND LEVEL FROM TERRESTRIAL RADIATION

Based on country- and area-wide surveys

Country or area	Estimated population <sup>a</sup> in 1975 (10 <sup>6</sup> )	Area (10 <sup>3</sup> km <sup>2</sup> )	Average absorbed dose rate in air (μrad h <sup>-1</sup> )	Number of measurements	Type of survey and instrumentation used	Reference
Austria	10	84	5.0	> 1 000	Ground survey with a Geiger-Müller counter	343
German Dem. Rep.	17	108	9.1	1 005	Ground survey with an ionization chamber and scintillation dosimeters	264
Germany, Fed. Rep. of	62	246	5.9	> 20 000	Ground survey with scintillation dosimeters	189
India	633	3 282	3.6 <sup>b</sup>	35 stations sampled	Analysis of soil samples by gamma spectrometry	239
Italy	56	301	7.2	1 365	Ground survey with an ionization chamber	53
Japan	110	370	4.1 <sup>b</sup>		Analysis of soil samples by gamma spectrometry	374
Poland	35	312	5.8	16 stations sampled	Ground survey with gamma spectrometers	269
Switzerland	7	41	7.4	Not indicated	Ground survey with an ionization chamber	128
United States	219	7 985	4.5	25 areas covered <sup>c</sup>	Aerial survey with gamma spectrometers	261
Island of Taiwan	12	36	6.0	26	Analysis of soil samples by gamma spectrometry	362

<sup>a</sup>With the exception of the island of Taiwan, the population estimates are taken from table A.6.1 of *United Nations Population Studies No. 53* (348).

<sup>b</sup>Calculated from the average concentration of <sup>40</sup>K, <sup>238</sup>U (or <sup>226</sup>Ra) and <sup>232</sup>Th in soil using the conversion factors given in table 6.

<sup>c</sup>Including approximately 30 per cent of the population.

The results are not altogether coherent as regards the quantity measured, which in practice is the quantity for which the measuring device was calibrated. Some authors report exposure rates, others, absorbed dose rates in air, and still others, "tissue doses in free air". Unless the measuring conditions are well specified, the quantities are often ambiguous, and intercomparisons between different investigations may be difficult.

47. The surveys were conducted using various methods and types of instrumentation. In the United States of America, aerial surveys were made in which an array of large NaI(Tl) crystals was flown in an aircraft at altitudes of 100-150 m above the terrain (50). This method was also used in other large countries, such as Canada (349) and the Union of Soviet Socialist Republics (188), but in these cases the results have not so far been used to estimate the average dose to the country's population.

48. Ground surveys were conducted in the other countries listed in table 7. Direct (or *in situ*) measurements were made in Austria, German Democratic Republic, Germany, Federal Republic of, Italy, Poland and Switzerland, the detectors being Geiger-Müller counters in Austria, ionization chambers in the German Democratic Republic, Italy and Switzerland, gamma spectrometers in Poland, and scintillation dosimeters especially developed for the purpose in the Federal Republic of Germany. In India and Japan and on the island of Taiwan, soil samples were taken over wide areas and then analysed by gamma spectrometry in a laboratory.

(c) *Variation of the absorbed dose rate in air with time*

49. One common aspect of the surveys is that the variation with time of the absorbed dose rate in air was not taken into account. The most significant changes

with time are associated with variations in the amount of snow cover and soil moisture and in the atmospheric concentration of <sup>222</sup>Rn decay products.

50. Snow cover introduces an effective shielding of gamma radiation from ground sources; a 20-cm blanket of typical snow brings about a reduction of about 50 per cent in the exposure rate (250). As a result, a strong seasonal pattern in outdoor exposure rates is observed in regions with significant snowfall (218, 270), as shown in figure IV. It may be noted that, for a given thickness of snow, the value of the absorbed dose rate in air depends on whether the snow is accumulating or melting. The reason is that the soil moisture content is higher during thawing than during the period of snow accumulation (273). The influence of soil moisture content is discussed in paragraph 51.

51. Changes in soil moisture content affect soil bulk density, so that the absorbed dose rate in air above the ground decreases with increasing soil moisture content. For the <sup>238</sup>U series, however, this effect is superimposed on a change of <sup>222</sup>Rn emanation, which generally decreases with increasing soil moisture content. The absorbed dose rate in air from this decay chain is therefore essentially independent of soil moisture, as the shielding effect and the increased source effect roughly compensate (250). For <sup>40</sup>K and the <sup>232</sup>Th series, the absorbed dose rate in air is significantly reduced by soil moisture. Data reported by Beck *et al.* (26) show that the total external terrestrial annual doses in air in a given area during dry years generally average about 20 per cent more than those for wet years.

52. As a result of variations in the stability conditions of the lower atmosphere, the night-time concentrations of <sup>222</sup>Rn decay products in the air near the ground are usually a few times higher than those existing during the day (250). Beck (25) has calculated the gamma absorbed dose rate in air from atmospheric <sup>222</sup>Rn decay products

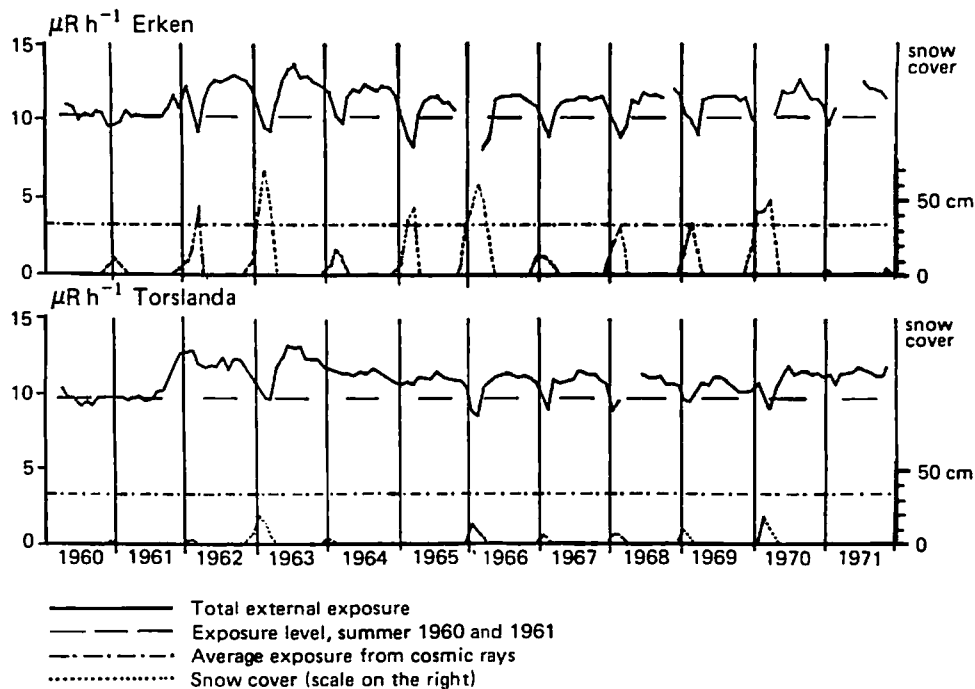


Figure IV. Exposure rates 2.5 m above ground and monthly averages of snow cover in Sweden, 1960-1971 (218, 336)

at 1 m above the ground for four different conditions of atmospheric stability. The values are 0.05, 0.1, 0.3 and  $1 \mu\text{rad h}^{-1}$  for strong mixing, normal turbulence, weak mixing, and strong inversion conditions, respectively. It is believed that usually the absorbed dose rate in air from atmospheric  $^{222}\text{Rn}$  decay products is approximately  $0.1\text{-}0.2 \mu\text{rad h}^{-1}$ .

(d) *Estimate of the average exposure level*

53. The average absorbed dose rates in air at 1 m above the ground given in table 7 are, in the case of Federal Republic of Germany, German Democratic Republic, Italy, Japan and Switzerland, population-weighted, i.e., the values obtained in the subdivisions of the country have been weighted according to their population. In the case of India and Poland, the figures are the reported or arithmetic averages, while for the island of Taiwan, the average absorbed dose rate in air has been calculated from the average concentration of  $^{40}\text{K}$ ,  $^{238}\text{U}$  and  $^{232}\text{Th}$  in surface soil. Although the surveys did not take into account the variation of absorbed dose rate in air with time, and differed widely in the type of instrumentation used and in the number and type of measurements, the average absorbed dose rates in air obtained fall within the relatively narrow range of  $3.6\text{-}9.1 \mu\text{rad h}^{-1}$ .

54. The population-weighted average absorbed dose rate in air for the surveys listed in table 7 is  $4.3 \mu\text{rad h}^{-1}$ . The population involved is about 30 per cent of that of the world, and the value could be considered to be roughly representative of the world population exposure. The areas covered by the surveys, however, represent only 2 per cent of the total land area of the world and all are located in three separate regions of the northern hemisphere. It is conceivable that the rest of the world population might live in areas where

the absorbed dose rate in air is very different from  $4.3 \mu\text{rad h}^{-1}$ . However, the result based on the estimate of the world-wide average concentration of primordial radionuclides in soil is  $4.6 \mu\text{rad h}^{-1}$  (table 6) and thus, in the absence of contradictory evidence, the Committee believes that a value of  $4.5 \mu\text{rad h}^{-1}$  is a reasonable estimate, on a global basis, of the outdoor average absorbed dose rate in air, 1 m above ground, from terrestrial radiation.

55. As to the cosmogenic nuclide contribution to external irradiation, if the concentration of  $^7\text{Be}$ ,  $^{22}\text{Na}$  and  $^{24}\text{Na}$  are taken as  $7 \cdot 10^{-2}$ ,  $10^{-5}$  and  $2 \cdot 10^{-5} \text{ pCi m}^{-3}$ , respectively (168, 378), the corresponding absorbed dose rates in air are about  $3 \cdot 10^{-6}$ ,  $10^{-8}$  and  $6 \cdot 10^{-8} \mu\text{rad h}^{-1}$ . An estimate can also be made of the total dose rate from all the other radionuclides produced by cosmic rays. From the existing experimental determinations of the atmospheric production rate for  $^{24}\text{Na}$ , the estimated production rates for some of the short-lived radionuclides, and the cross-sections for the very short-lived radionuclides of less than 10-s half-life, it can be calculated (250) that for every disintegration of  $^{24}\text{Na}$  at ground level there are  $10^6$  disintegrations of short-lived cosmogenic radionuclides. Assuming an average gamma energy of 1 MeV per disintegration, the absorbed dose in air from the short-lived cosmogenic radionuclides would be of the order of  $0.02 \mu\text{rad h}^{-1}$ . The contribution of all the radionuclides produced by cosmic rays to the absorbed dose rate in air is therefore insignificant compared to the contribution from the primordial nuclides in the ground.

(e) *Variability of the exposure*

56. The variability of the exposure around the mean value can be roughly assessed from data from some of the surveys listed in table 7. The surveys in four of the

countries, each with a population of more than 50 million people, provided the average doses for the populations of their administrative subdivisions: the 11 Länder of the Federal Republic of Germany, the 20 regions of Italy, the 22 districts of Japan, and the 50 states and capital district of the United States. The populations of those subdivisions range from 0.1 to 20 million people.

57. The frequency distribution of the population over absorbed dose rate in air is presented in figure V for each

of the four countries, and in figure VI for the four countries taken together. If the volcanic regions of Lazio and Campania of Italy are excluded, the combined data of figure VI are fitted rather well by a Gaussian distribution, as shown in figure VII. Thus, for the four countries considered, a large fraction of the population lives in areas where the population-weighted distribution of the outdoors absorbed dose rate in air is normally distributed, while another fraction, much smaller, lives in areas outside of the normal distribution. The average absorbed dose rate in air in the "normal" areas of the

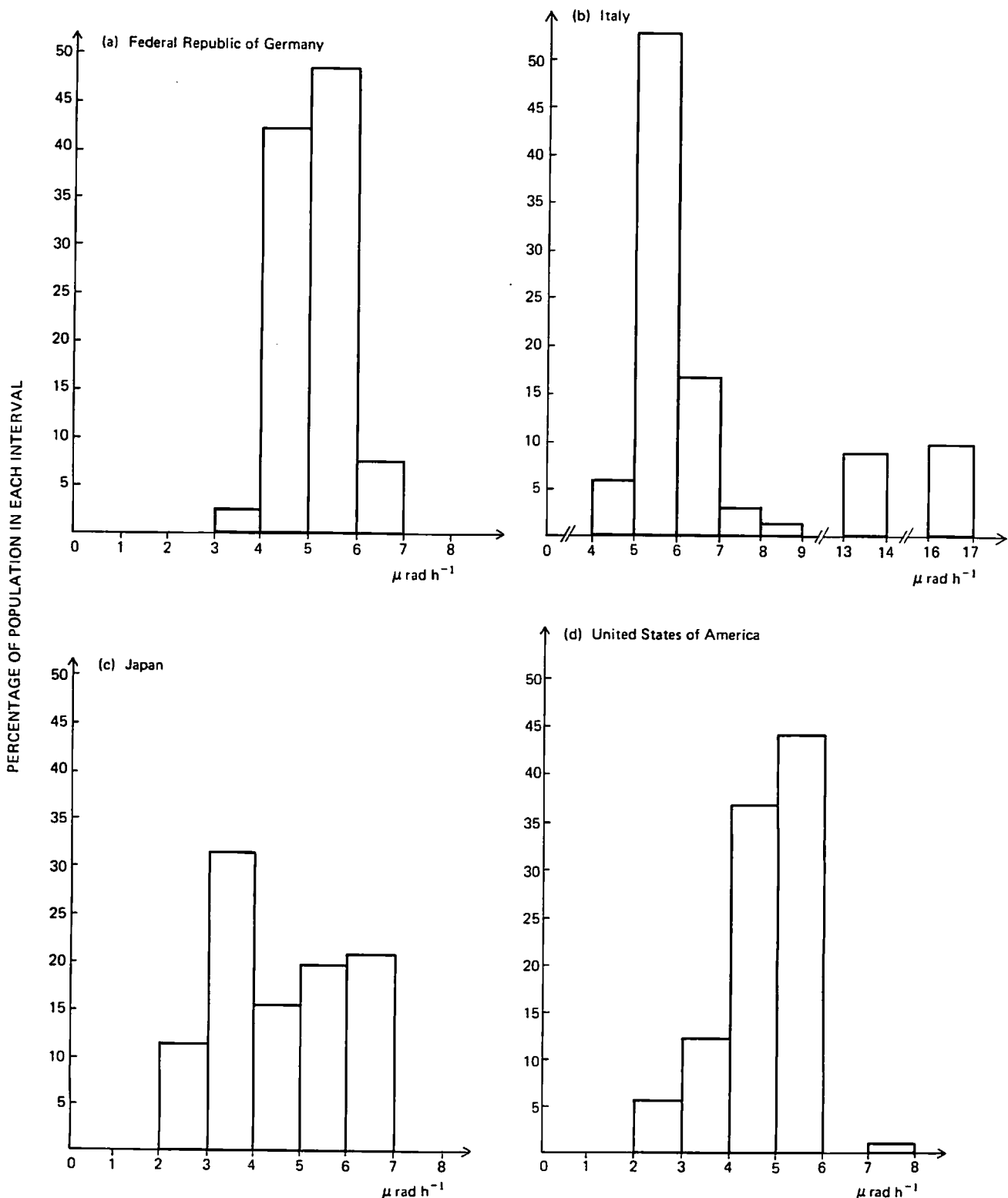


Figure V. Population-weighted distribution of absorbed dose rates in air from terrestrial radiation in four countries

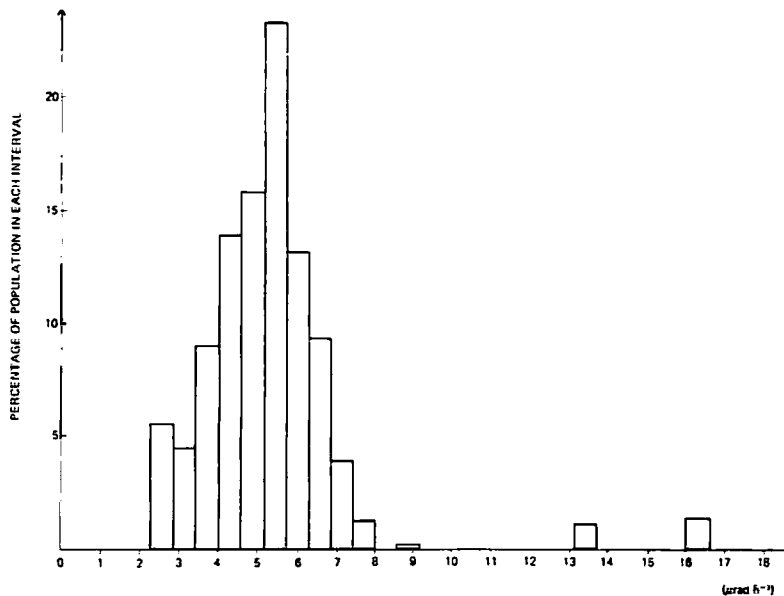


Figure VI. Frequency distribution of outdoor absorbed dose rate in air from terrestrial radiation. Combined data from the Federal Republic of Germany, Italy, Japan and the United States. (The isolated bars on the right represent data from the Italian regions of Lazio and Campania)

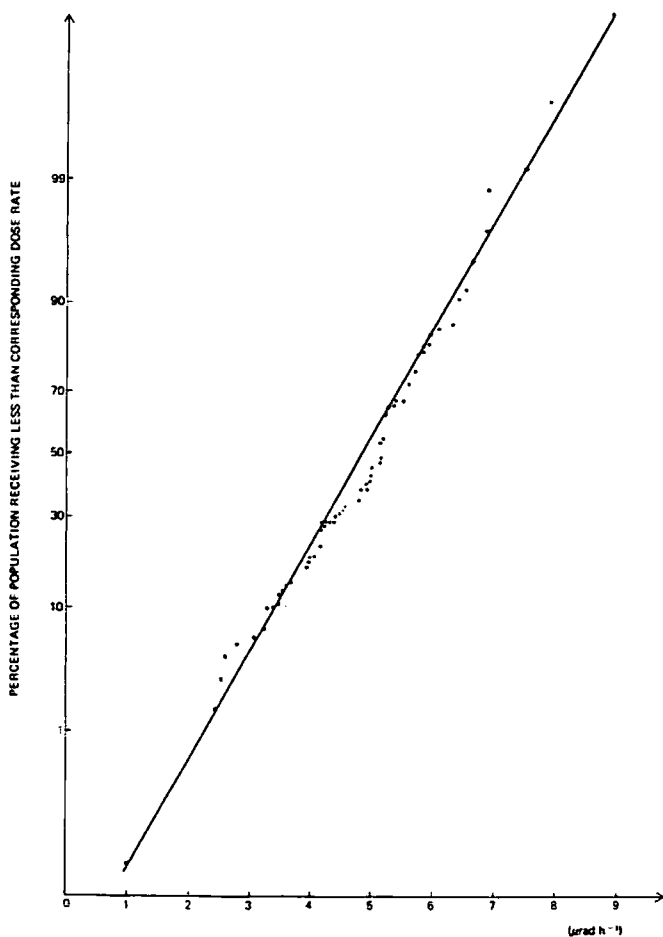


Figure VII. Cumulative frequency distribution of the outdoor absorbed dose rate in air from terrestrial radiation. Combined data from the Federal Republic of Germany, Italy, Japan and the United States. (The data from the Italian regions of Lazio and Campania have not been included)

four countries is  $4.85 \mu\text{rad h}^{-1}$ , with a standard deviation of  $1.1 \mu\text{rad h}^{-1}$ . Assuming that the distribution holds on a global basis, 95 per cent of the world population residing in areas of "normal" natural

radiation would live where the outdoor absorbed dose rate in air from the primordial radionuclides falls between about  $3$  and  $7 \mu\text{rad h}^{-1}$ . However, it should be borne in mind that these values are themselves averages, corresponding to population groups of at least  $10^5$  people.

(f) Areas with high natural radiation levels

58. As indicated above, there are regions in the world where the outdoor absorbed dose rate in air substantially exceeds the range mentioned in paragraph 57. In addition to the Italian provinces of Lazio and Campania, such regions are known to exist in Brazil, France, India, Iran, Madagascar and Nigeria (45). The best known from a dosimetric point of view are those located in Brazil and India.

59. Deposits of radioactive minerals occur in littoral formations along the coastal regions of India. Of particular interest is a stretch about 250 km long and about 0.5 km wide on the south-west coast in the states of Kerala and Tamil Nadu. These deposits are rich in monazite, which contains principally  $^{232}\text{Th}$  and its decay products together with several rare earths; the monazite deposits are admixed with ilmenite, rutile, sillimanite and zircon. The most concentrated deposits along the Kerala coast are located on a 55-km strip populated by about 70 000 persons, where the thorium concentration in the monazite ranges from 8.0 to 10.5 per cent by weight, being the highest known in the world (103). Additional features of this area are that it has definable geographical landmarks, with the backwaters separating this strip from the mainland, and it supports a high density of human population. Further south, another coastal strip about 2.5 km long in the state of Tamil Nadu also has high concentrations of monazite.

60. In a radiometric survey carried out in the late 1950s, measurements of gamma exposure rates were

made at the main entrance of 200 houses selected at random in the 55-km strip of Kerala coast described above. Values varied widely between houses, demonstrating the rather patchy distribution of monazite along the coastal strip. On the basis of these measurements, it was estimated that the average absorbed dose rate in air from terrestrial radiation in the region was about  $130 \mu\text{rad h}^{-1}$  (103).

61. Two types of high-background regions have been found in Brazil: the monazite sand region along the Atlantic coast of the states of Espirito Santo and Rio de Janeiro and the volcanic intrusive anomalies along a geological fracture that extends from the coast through the inland state of Minas Gerais (274). Weathering and decomposition of archeogneisses in the mountain range that parallels a long extension of the Brazilian Atlantic coast produced a natural separation of very insoluble and hard minerals, such as ilmenite, zirconite and monazite. Ground to fine particles and carried downstream by many rivers emptying into the ocean, these minerals underwent stratification and were deposited on fluvial and marine regions (274). The radiation levels in three towns (Guarapari, Meaibe and Cumuruxatiba) built over monazite sands along the Atlantic coast were surveyed in detail by Roser and Cullen (299). Guarapari is a town of 12 000 people which receives an influx of about 30 000 vacationers every summer. In that town, the absorbed dose rates in air were found to range from 100 to  $200 \mu\text{rad h}^{-1}$  in the streets and up to  $2000 \mu\text{rad h}^{-1}$  over selected spots on the beach (275, 299). Meaibe is a fishing village of about 300 people, situated 50 km to the south of Guarapari, where the radiation environment is similar: the average absorbed dose rate in air is about  $100 \mu\text{rad h}^{-1}$  with levels up to  $1000 \mu\text{rad h}^{-1}$  (274). In Cumuruxatiba, the average level is  $50 \mu\text{rad h}^{-1}$  (299).

62. In the state of Minas Gerais, two volcanic regions have been intensively studied, Poços de Caldas and Araxá-Tapira. Near the city of Poços de Caldas stands a hill where absorbed dose rates in air of up to  $2800 \mu\text{rad h}^{-1}$  have been reported. However, this hill is small and uninhabited. The radioactivity of the Araxá-Tapira region originated from an alkaline intrusive, the mineralization consisting mostly of apatite. The radioactive components occur almost exclusively in the form of pyrochlore, a mineral containing up to 60 per cent niobium oxide, 1.9 per cent thorium oxide and 1.3 per cent uranium oxide (274). In Araxá-Tapira, absorbed dose rates in air up to  $400 \mu\text{rad h}^{-1}$  have been measured.

63. Information on the tissue absorbed doses in the populations living in areas of high external terrestrial radiation in Brazil and India are given in paragraphs 76 and 77.

64. Quantitative information on the outdoor absorbed dose rates in air in other areas of high natural radiation levels is very scarce. In the city of Ramsar, Iran, absorbed dose rates in air ranging from 200 to  $5000 \mu\text{rad h}^{-1}$  have been measured within an area of a few square kilometres, characterized by the presence of  $^{226}\text{Ra}$ -rich spring water (181). In France, absorbed dose rates in air of  $200 \mu\text{rad h}^{-1}$  are not uncommon and a very localized value of  $10\,000 \mu\text{rad h}^{-1}$  has been discovered (71).

### 3. Exposure indoors

65. Knowledge of radiation levels in buildings is important in the assessment of population exposure, as most individuals spend a large proportion of their time indoors. However, large-scale surveys of indoor exposure are still relatively few compared to those conducted outdoors.

#### (a) Activity of building materials

66. Information on the radioactivity of building materials is still scarce. Table 8 presents the results of investigations which have been conducted in the Federal Republic of Germany, Sweden, the United Kingdom of Great Britain and Northern Ireland and the USSR. The range of concentrations found in a given type of commonly used building material is very wide, but the average values obtained in the four countries are reasonably close. Wood and materials used for thermal insulation, with the exception of the light-weight aggregate used in Sweden, are of low radioactive content; natural plaster and cement are also relatively low, while granites, bricks and concrete are in the upper part of the range.

#### (b) Source-exposure relationship

67. Estimates of indoor exposure could be derived from the activity concentration of the various building materials, their dimensions and distribution in the building, the geometrical conditions of irradiation and the radiation field outdoors, although it would be extremely difficult to take all those variables into proper account. Furthermore there is not yet sufficient information available on the activity concentrations of natural radionuclides in the various building materials. Therefore, the average absorbed dose rate in air indoors has been estimated from the outdoor values using conversion factors accounting for the type of basic building material used. These conversion factors are based mainly on the results of the few surveys that have involved at least about one hundred dwellings (table 9). The conversion factors take into account that building materials act both as sources of radiation and attenuators of outdoor radiation.

68. The importance of the shielding effect of building materials can be estimated from figure III. If the density of the soil is assumed to be  $1.6 \text{ g cm}^{-3}$ , a wall thickness of  $50 \text{ g cm}^{-2}$  absorbs practically all of the radiation from outdoors and a thickness of  $10 \text{ g cm}^{-2}$  is sufficient to absorb half of it. Therefore, the transmission of radiation through the walls will only play a significant role in light constructions such as wooden or prefabricated houses.

69. The shielding effect is clearly seen in wooden houses, for which the source effect is negligible. Surveys conducted in Australia (377) and in the United States (202, 211, 376) have shown that the indoor absorbed dose rate in air on the ground floor of wooden houses is about 75 per cent of that measured outdoors. One floor above ground level, the values are lower by a further 10-20 per cent (202, 376). In prefabricated houses made

TABLE 8. CONCENTRATION OF <sup>40</sup>K, <sup>226</sup>Ra AND <sup>232</sup>Th IN BUILDING MATERIALS AND ABSORBED DOSE RATE IN AIR

Type of building material	Country	Number of samples	Average activity concentration (pCi g <sup>-1</sup> )			Absorbed dose rate in air (μrad h <sup>-1</sup> ) <sup>a</sup>	Reference
			<sup>40</sup> K	<sup>226</sup> Ra	<sup>232</sup> Th		
Bricks	Germany, Fed. Rep. of	132	16	2.6	2.6	26	327
Bricks	Sweden	21	25	2.6	3.4	33	335
Red bricks	USSR	55	20	1.5	1.0	16	194
Clay bricks	United Kingdom	23	17	1.4	1.2	16	117
Concrete	Germany, Fed. Rep. of	69	15	1.8	1.7	19	327
Heavy concrete	Sweden	15	19	1.3	2.3	21	335
Aerated concrete without alum shale	Sweden	22	9	1.5	1.9	17	335
Heavy concrete	USSR	87	15	0.9	0.8	12	194
Light concrete	USSR	16	14	2.0	0.9	15	194
Concrete	United Kingdom	5	14	2.0	0.8	15	117
Cement	Germany, Fed. Rep. of	19	5.2	1.2	1.2	11	327
Cement	Sweden	8	6.3	1.5	1.5	13	204
Cement	USSR	7	6	1.2	1.2	8	194
Natural plaster	Germany, Fed. Rep. of	23	2	< 0.5	< 0.3	< 4	327
Natural plaster	Sweden	4	0.6	0.09	< 0.04	< 1	335
Plaster	USSR	1	10	0.25	0.17	5	194
Natural plaster	United Kingdom	69	4	0.6	0.2	4	117
Granite	Germany, Fed. Rep. of	34	33	2.6	2.2	30	327
Granite	USSR	2	40	3	4.5	46	194
Granite bricks	United Kingdom	7	28	2.4	2.3	28	117
Pumice stone	Germany, Fed. Rep. of	20	29	3.0	3.4	35	327
Tuff	USSR	13	18	2.6	2.0	24	194
Limestone and marble	Germany, Fed. Rep. of	20	1	< 0.5	< 0.5	< 5	327
Rock aggregate	Sweden	296	22	1.3	1.9	20	111
Rock aggregate	United Kingdom	3	22	1.4	0.1	12	117
Gravel and sand	Germany, Fed. Rep. of	50	7	< 0.4	< 0.5	< 6	327
Natural sand and sand rejects	USSR	32	7.1	0.63	0.5	7	194, 195
Wood	Sweden	1	-	-	-	< 0.4	142
Rock and silica wool	Sweden	2	6	0.4	0.4	5	335
Rock and silica wool	United Kingdom	2	negligible				117
Lightweight aggregate	Sweden	10	27	3.9	4.3	42	335

<sup>a</sup> Assuming 4π-geometry and infinite thickness, and using the conversion factors given in table 6. The values obtained are an index allowing the comparison between building materials and not an estimate of the doses that would be received in dwellings constructed with those building materials.

TABLE 9. RESULTS OF SURVEYS OF THE INDOOR ABSORBED DOSE RATE IN AIR DUE TO TERRESTRIAL RADIATION

Country	Number of dwellings	Type of building	Indoor average absorbed dose rate in air (μrad h <sup>-1</sup> )	Population-weighted average absorbed dose rate in air (μrad h <sup>-1</sup> )	Indoors-to-outdoors ratio	Population-weighted indoors-to-outdoors ratio	Reference
German Democratic Republic	480 in old buildings <sup>a</sup>	Brick (old)	7.2	7.4	}	0.78	264
		Brick (new)	6.5				
		Half-timbered (old)	7.6				
		Store (old)	11.2				
		Mixed construction (new)	5.7				
Germany, Fed. Rep. of	> 20 000	Prefabricated (new)	5.9	6.8	}	1.3	192
		Solid	6.8				
		Frame	6.9				
		Prefabricated (concrete)	4.2				
		Wood	4.2				



Country	Number of dwellings	Type of building	Indoor average absorbed dose rate in air ( $\mu\text{rad h}^{-1}$ )	Population-weighted average absorbed dose rate in air ( $\mu\text{rad h}^{-1}$ )	Indoors-to-outdoors ratio	Population-weighted indoors-to-outdoors ratio	Reference
Norway	823	Wood	7.1				
	594	Concrete	10.5				329
	609	Brick	11.9				
Poland	37	Concrete	4.9		0.73		271
	49	Prefabricated (fly-ash and slag)	6.4		1.1		
	11	Brick	5.7				
Sweden <sup>b</sup>	259	Wood (old)	5.1				142
	126	Wood (new)	4.8				241
	365	Brick (old)	10.6				142
	93	Brick (new)	10.6				241
	43	Concrete (new)	12.5				241
United Kingdom	71	Solid {	sedimentary rock (Dundee)	7.6	1.07		320
	155		sedimentary rock (Edinburgh)	6.8	1.24		
	103		granite (Aberdeen)	9.7	0.82		
	172		granite (Aberdeenshire)	9.4	1.17		
United States	110	Wood	3.9 <sup>c</sup>		0.75		203
	160	Wood			0.70		211

<sup>a</sup>Old: built before 1945. New: built after 1945.

<sup>b</sup>Two surveys have been conducted in Sweden, one in 1956 and one in 1976. The buildings surveyed in 1956 are referred to as old. A large percentage of the buildings surveyed in 1976 are likely to have been built after 1956 and are referred to as new.

<sup>c</sup>Median value.

out of concrete and in wooden houses it has been determined in the study conducted in the Federal Republic of Germany that absorbed dose rates in air indoors are lower than outdoors, the average reduction being 3 per cent for the prefabricated houses and 6 per cent for the wooden houses (189).

70. In the other types of houses, outdoor radiation is almost completely shielded by the walls. This has been demonstrated in various studies (264, 376) in which it has been observed that the levels are about the same on various floors of a given masonry building. Therefore, in these dwellings, the indoor levels cannot be compared to those outdoors unless the building materials are of local origin. If the concentration of radioactive substances in the ground of a given locality is equal to that in building materials, the absorbed dose rate in air might be expected to be somewhat less than twice as large indoors as outdoors, as a result of the change of source geometry. However, correction coefficients should be applied allowing for the presence of windows and doors (195), which makes the ratio much smaller than 2. Direct determinations of these correction coefficients have not been reported.

71. An estimate of the average indoors-to-outdoors dose ratio in masonry buildings may be obtained from the extensive country-wide study from the Federal Republic of Germany, in which nearly 30 000 apartments were surveyed. Preliminary information indicates that the average ratio of the indoors-to-outdoors absorbed dose rate in air is about 1.3 (192). Assuming that, on the average, the radioactive content of the building materials is about the same as that of the soils, roads and pavements around the building, the conversion factor between the indoor and the outdoor absorbed

dose rates in air for masonry buildings would then be about 1.3. This figure is in reasonable agreement with the results of the United Kingdom study (320) but is higher than those obtained in the German Democratic Republic (264) and Poland (271). However, each of these three surveys involved less than 1000 dwellings, and the conversion factors derived from their results might be less representative than that obtained from the country-wide study conducted in the Federal Republic of Germany, where all types of dwellings were included.

(c) *Estimate of the average indoor level of the absorbed dose rate in air*

72. Assuming that the proportion of wooden buildings (dwellings, offices, factories, shops, theatres etc.) is about 20 per cent of the total and taking the average ratio of the indoor to the outdoor absorbed dose rate in air to be 0.7 and 1.3 for wooden and masonry buildings, respectively, the average indoor absorbed dose rate in air would be 18 per cent higher than that outdoors. Therefore, the indoor absorbed dose rate in air, averaged over the world, is estimated to be about  $5.3 \mu\text{rad h}^{-1}$ .

(d) *Variability of the absorbed dose rate in air*

73. Indications on the variability of the indoor dose rates in relation to the average may be derived from the survey conducted in the Federal Republic of Germany (189, 192). As in the case of the outdoor absorbed dose rate in air, the population-weighted distribution seems to be normal (fig. VIII). The mean value of the indoor absorbed dose rate in air is  $6.7 \mu\text{rad h}^{-1}$ , and its standard deviation,  $1.0 \mu\text{rad h}^{-1}$ , while the corresponding values outdoors are 4.9 and  $0.5 \mu\text{rad h}^{-1}$ . The

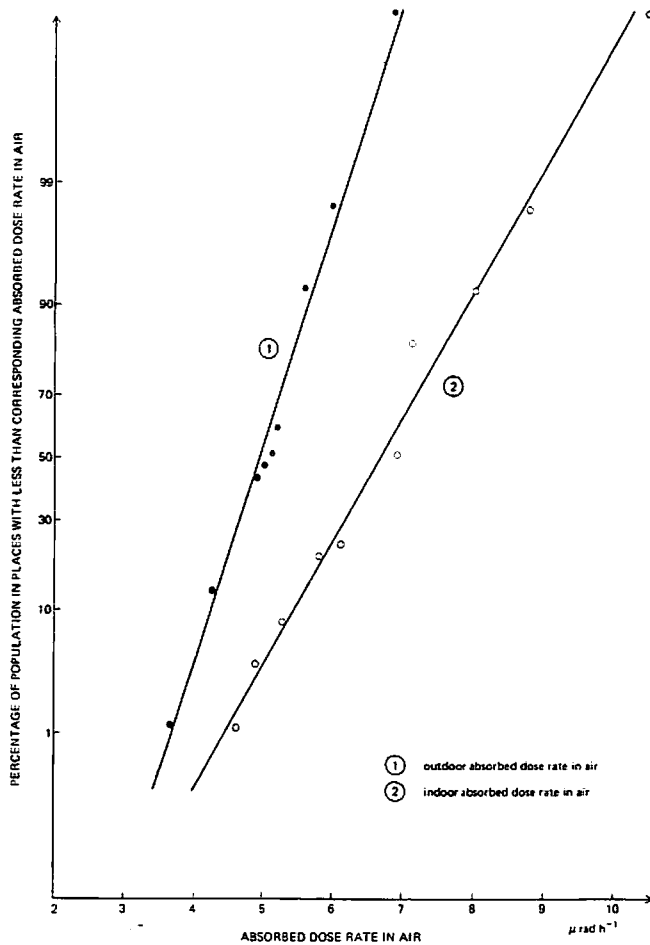


Figure VIII. Cumulative frequency distribution of the absorbed dose rate in air measured in the Federal Republic of Germany (189, 192)

outdoor coefficient of variation in the Federal Republic of Germany is about half of the value derived for global conditions (para. 5'). Assuming that the same relation applies to the indoor coefficient of variation, it is tentatively estimated that 95 per cent of the world population would be subject to indoor absorbed dose rates in air ranging from 2 to 9  $\mu\text{rad h}^{-1}$ .

#### 4. Tissue absorbed doses from terrestrial radiation

74. From the analysis contained in Annex A, the annual gonad absorbed dose  $D$  can be derived from the absorbed dose rate in air  $\dot{D}_a$  as

$$D = (cq\dot{D}_a)_{\text{outdoors}} + (cq\dot{D}_a)_{\text{indoors}}$$

where  $c$ , the conversion factor from the absorbed dose rate in air to the gonad annual absorbed dose, is taken as 7.2  $\text{mrad } \mu\text{rad}^{-1} \text{ h}$  for outdoor exposure and 6.0  $\text{mrad } \mu\text{rad}^{-1} \text{ h}$  for indoor exposure, and  $q$ , the occupancy factor, is estimated in a later paragraph to be 0.8 indoors, and thus 0.2 outdoors.

75. From  $\dot{D}_a = 4.5 \mu\text{rad h}^{-1}$  outdoors and  $5.3 \mu\text{rad h}^{-1}$  indoors, it can be estimated that the annual gonad absorbed dose from external terrestrial radiation is, on average, 32 mrad; 95 per cent of the world population would receive annual gonad doses in the

range of 21 to 43 mrad. The doses in other organs of interest to the Committee are nearly equal to the gonad dose. The annual collective dose from terrestrial radiation, for the present size of the world population, is of the order of  $10^8$  man rad.

76. Populations living in areas of high external terrestrial radiation, such as those of Brazil and India, incur much greater tissue doses. Relevant information has been obtained in both countries by means of thermoluminescent dosimeters distributed to a fraction of the population. Gopal-Ayengar *et al.* (102, 103) carried out a dosimetric survey on the 55-km long coastal strip described in paragraphs 59 and 60, which was selected on the basis of high exposure rate, definable geographical boundaries and high population density. From results for a sample of 8513 individuals, the average annual tissue absorbed dose for the 70 000 people residing in the region was estimated at 380 mrad. It was estimated that about 24 per cent of the people experienced annual doses in excess of 0.5 rad, about 6 per cent exceeded 1 rad and about 0.7 per cent exceeded 2 rad.

77. On the Brazilian coast (see paragraph 61), Cullen (63) determined the average annual tissue dose from external terrestrial irradiation for a group of 317 inhabitants of Guarapari to be 0.55 rad, with a range of 0.09-2.8 rad.

## II. INTERNAL IRRADIATION

78. Radioactive nuclides occurring in the biosphere enter the human body through ingestion and inhalation. In order to assess the doses from internal exposure in the organs and tissues of interest to the Committee (lung, gonads, red bone marrow, and endosteal cells), two types of information are necessary: (a) the concentration of radionuclides in the organs and tissues mentioned above and also in neighbouring tissues, such as bone and yellow marrow, and (b) the dosimetric factors linking the concentrations to the dose rates. The following paragraphs deal with the estimation of the relevant dosimetric factors and their application.

79. If a radionuclide emits only one type of monoenergetic particle per disintegration, the dose rate  $\dot{D}_i$  in an organ or tissue  $i$ , can be assessed from the expression:

$$\dot{D}_i = \sum_j \phi_E(i, j) C_j$$

where  $E$  is the energy of the particle,  $C_j$  the activity concentration of the radionuclide in organ or tissue  $j$  that may contribute to dose in tissue  $i$ , and  $\phi_E(i, j)$  is the dosimetric factor, quantitatively equal to the dose-rate contribution in tissue  $i$  from a unit activity concentration in organ  $j$ . In the case of beta decay, the same expression is valid, provided that there is only one transition in the decay scheme. The energy  $E$ , in this case, would be the average energy of the beta particles emitted in the transition. In the most general case, several types of radiation with several energies are emitted. The dose rate in organ  $i$  becomes

$$\dot{D}_i = \sum_k \sum E f_{k, E} \sum_j \phi_{k, E}(i, j) C_j$$

where  $f_{k,E}$  is the yield of particles including photons of type  $k$  of energy  $E$  per disintegration, and  $\varphi_{k,E}(i, j)$  represents that contribution to the dose rate in organ or tissue  $i$  from a unit activity concentration in organ  $j$  which is due to particles of type  $k$  and energy  $E$ .

80. The dosimetric factors, symbolized as  $\varphi(i, j)$ — $i$  and  $j$  being the target and the source organs, respectively—are given as a function of energy in figures IX, X, XI and XII, separately for the three types of radiation (alpha, beta, gamma) encountered in internal exposure from natural radionuclides. Four target organs have been considered, namely, the lung, the gonads, the red bone marrow, and the bone lining cells, which are defined as the cells lying on endosteal surfaces of bone (mainly trabecular), assumed to form a layer  $10 \mu\text{m}$  thick. In the case of the alpha emitters, the dosimetric factors relating the activity concentration in bone to the dose rates in red bone marrow and in bone lining cells have been estimated for two types of distribution, (a) distribution

throughout the bone matrix and (b) deposition on bone surfaces. For gamma emitters, two types of distribution in the human body have been considered; (a) uniform distribution over the whole body and (b) preferential distribution in the skeleton. In the latter case, which is that of the bone seekers, the dosimetric factors have been calculated using the assumption that the low activity present in the soft tissues is distributed over the whole body and is superimposed over the distribution in the skeleton. Although most of the dosimetric factors given here can be used for humans of any age and sex, they apply strictly to adult man. They have been derived from published models (147, 318, 319, 321).

#### A. COSMOGENIC RADIONUCLIDES

81. Very little of the dose from natural background is contributed by the cosmogenic radionuclides. Of the many nuclides produced by cosmic rays, only  $^3\text{H}$ ,  $^7\text{Be}$ ,

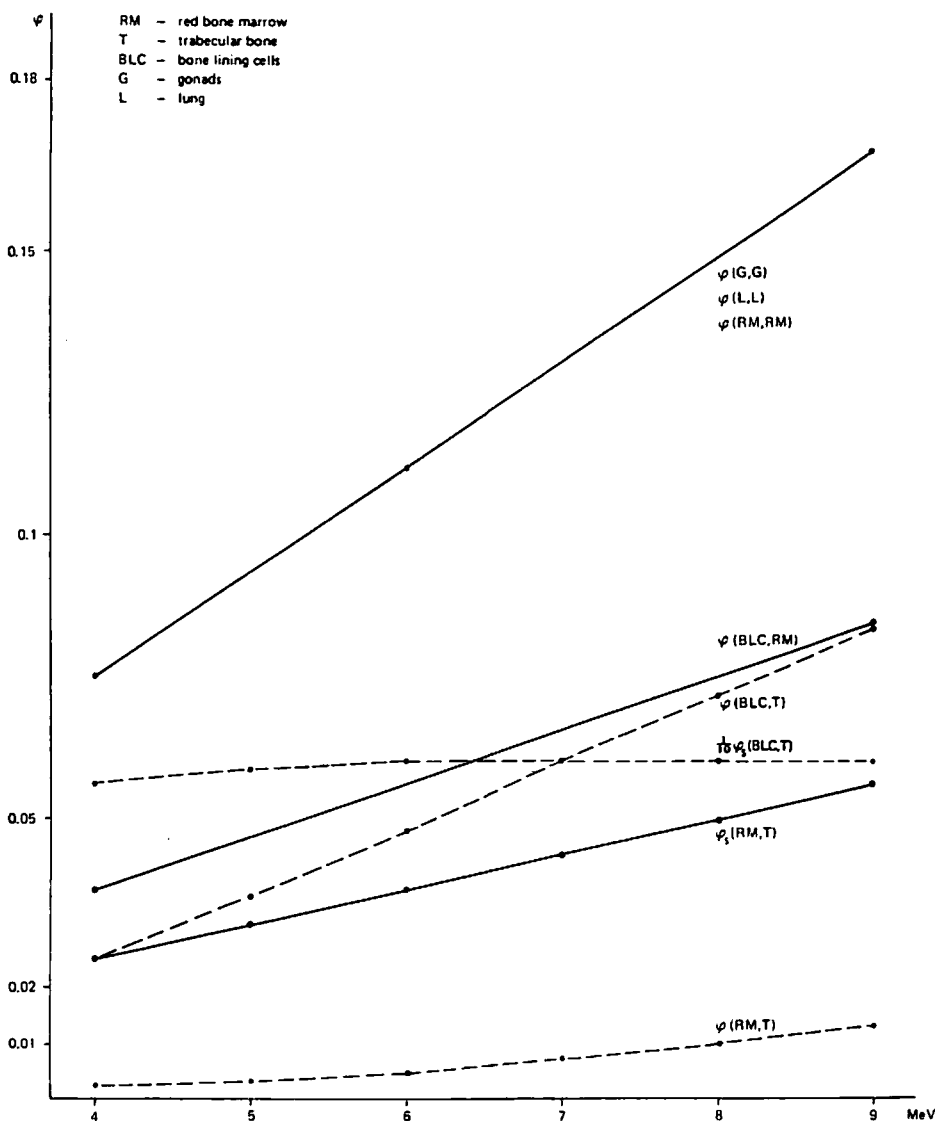


Figure IX. Dosimetric factors for alpha-emitting radionuclides ( $\text{mrad y}^{-1}$  per  $\text{pCi kg}^{-1}$ )

The subscript  $s$  denotes that the alpha emitter is assumed to be distributed on the bone surfaces. The absence of subscript indicates that the alpha emitter is assumed to be uniformly distributed throughout the whole matrix

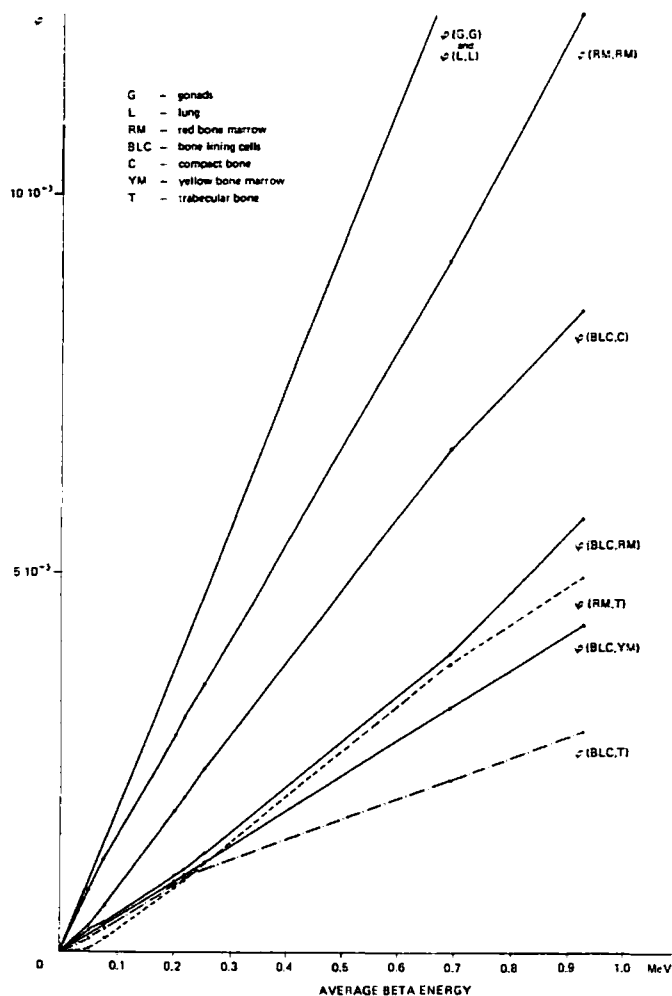


Figure X. Dosimetric factors for beta-emitting radionuclides (mrad  $y^{-1}$  per pCi  $kg^{-1}$ )

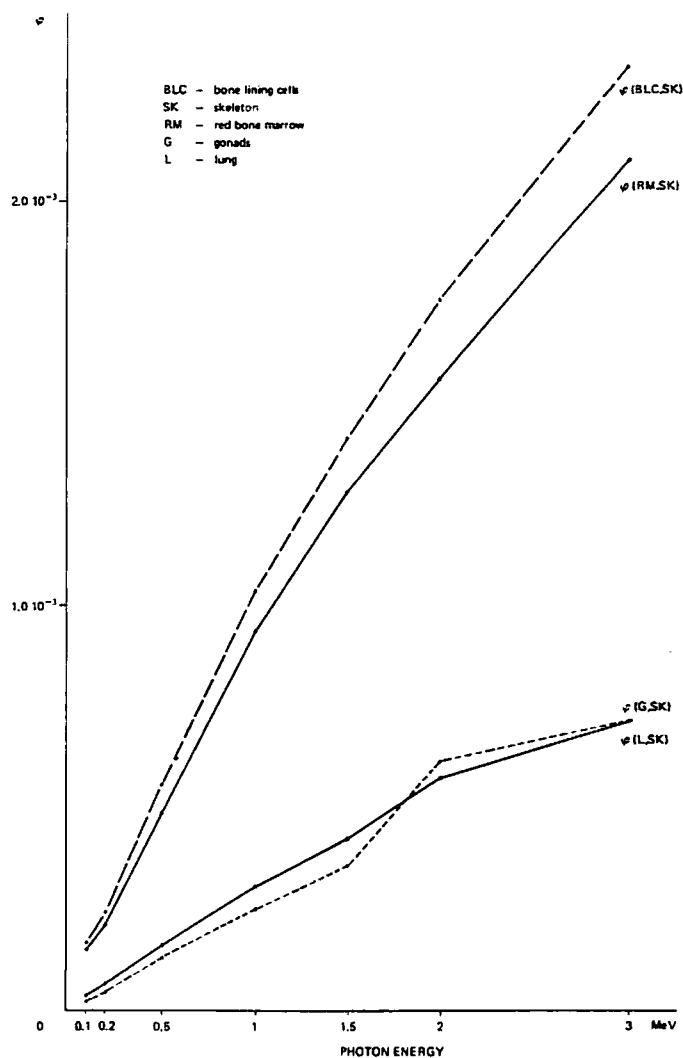


Figure XII. Dosimetric factors for several tissues for gamma-emitting radionuclides located in the skeleton (mrad  $y^{-1}$  per pCi  $kg^{-1}$ )

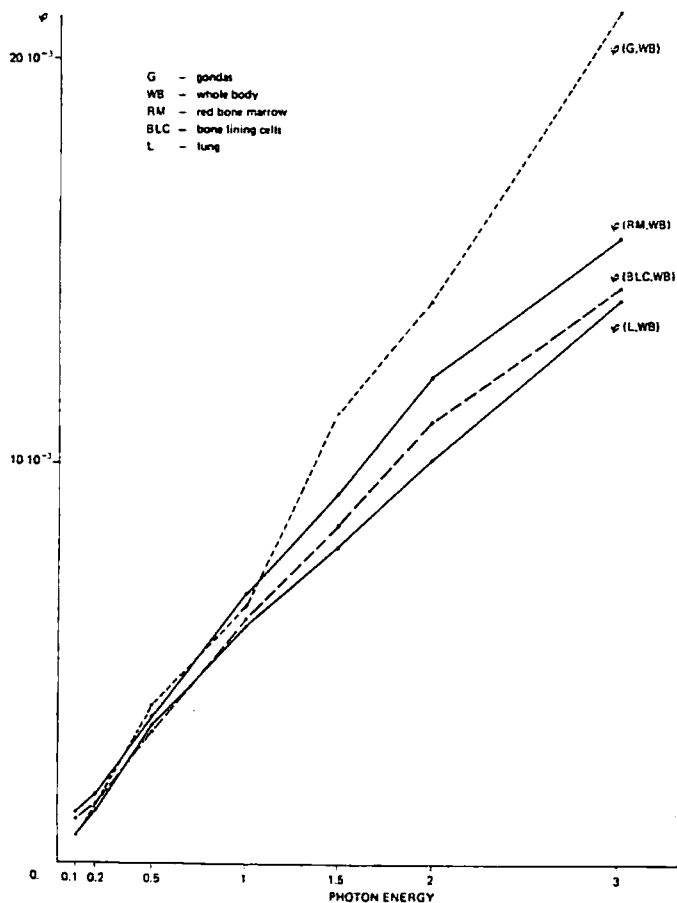


Figure XI. Dosimetric factors for gamma-emitting radionuclides distributed uniformly over the whole body (mrad  $y^{-1}$  per pCi  $kg^{-1}$ )

$^{14}C$  and  $^{22}Na$  contribute appreciably to the dose. The production and distribution of these nuclides in the environment is presented in table 10.

### 1. Tritium

82. Tritium.  $^3H$ , is produced naturally in the atmosphere, lithosphere and hydrosphere. The production of man-made  $^3H$  in nuclear explosions and nuclear reactors is discussed in Annexes C and D. The major source of natural  $^3H$  is the atmosphere, where it results from the interaction of cosmic-ray protons and neutrons with nitrogen, oxygen, and argon, the main reaction being  $^{14}N + n \rightarrow ^{12}C + ^3H$  for  $E_n > 4.4$  MeV. Estimates of the inventory, calculated from published values of the production rate, range from 17 to 170 MCi (table 11), the most recent estimates being 34 MCi and  $28 \pm 7$  MCi (197, 340). It has been suggested that  $^3H$  might also be ejected from the sun during solar flares (199) and from stars (83), but the contribution to the inventory from these sources has not been evaluated.

83. About 99 per cent of the  $^3H$  inventory is converted to HTO and participates in the normal water cycle. According to the data contained in table 10, most of the  $^3H$  inventory, which is taken to be 34 MCi, would be in the oceans, as a result of transport by rain and by

TABLE 10. DATA ON THE PRODUCTION AND DISTRIBUTION OF NATURALLY OCCURRING  $^3\text{H}$ ,  $^7\text{Be}$ ,  $^{14}\text{C}$  AND  $^{22}\text{Na}$

	$^3\text{H}$	$^7\text{Be}$	$^{14}\text{C}$	$^{22}\text{Na}$
Half-life	12.3 y	53.6 d	5 730 y	2.62 y
Number of atoms produced per unit time and per unit area of the earth's surface ( $\text{cm}^{-2} \text{s}^{-1}$ ) in the:				
Troposphere	$8.4 \cdot 10^{-2}$	$2.7 \cdot 10^{-2}$	1.1	$2.4 \cdot 10^{-5}$
Total atmosphere	0.25	$8.1 \cdot 10^{-2}$	$2.3^a$	$8.6 \cdot 10^{-5}$
Global inventory (MCi)	34	1	300	0.01
Distribution as a percentage of inventory in the:				
Stratosphere	6.8	60	0.3	25
Troposphere	0.4	11	1.6	1.7
Land surface and biosphere	27	8	4	21
Mixed oceanic layers	35	20	2.2	44
Deep ocean	30	0.2	92	8
Oceanic sediments			0.4	
Activity concentration in surface air ( $\text{pCi m}^{-3}$ ) <sup>b</sup>		$7 \cdot 10^{-2}$		$10^{-5}$
Activity concentration in continental surface waters ( $\text{pCi l}^{-1}$ ) <sup>c</sup>	6-24			
Specific activity in terrestrial biosphere ( $\text{pCi g}^{-1}$ ) <sup>d</sup>			6.1	

Source: Reference 197.

<sup>a</sup>Reference 200.

<sup>b</sup>Reference 190.

<sup>c</sup>References 52, 178.

<sup>d</sup>Reference 330a.

TABLE 11. PUBLISHED RATES OF PRODUCTION AND CORRESPONDING INVENTORIES OF NATURAL  $^3\text{H}$

	Number of atoms produced per unit time and per unit area of the earth's surface ( $\text{cm}^{-2} \text{s}^{-1}$ )	Inventory (MCi)	Year of publication	Reference
Atmosphere	0.10-0.20	14-28	1953	83
	0.12	17	1954	178
	0.14	20	1955	52
	1.2	170	1957	29
	1.2	170	1957	60
	1.06	150	1958	27
	0.9	130	1958	40
	0.75	100	1958	99
	0.6-1.3	80-180	1960	367
	0.25-0.35	35-150	1961	61
	0.6	80	1962	28
	0.25	34	1967	197
	$0.20 \pm 0.05$	$28 \pm 7$	1967	340
Lithosphere	$10^{-3}$	0.1	1954	178
Hydrosphere	$10^{-6}$	0.0001	1953	83

direct exchange of water vapour between air and sea water. Once in the ocean,  $^3\text{H}$  is dispersed through mixing processes. Measured concentrations of natural  $^3\text{H}$  in ocean surface water average about  $3 \text{ pCi l}^{-1}$  (178).

84. The land areas seem to contain about 30 per cent of the natural  $^3\text{H}$  inventory (table 10). Tritium concentrations in fresh water are usually higher than in sea water. Activity concentrations of continental surface waters, measured before nuclear explosions began, were found to be in the range  $6-24 \text{ pCi l}^{-1}$  (178). Assuming that the specific activity of  $^3\text{H}$  in the body is the same as that in the continental surface waters, and using the

distribution of hydrogen in the Reference Man of ICRP (152), the annual doses from natural  $^3\text{H}$ , calculated with the dosimetric factors given in figure X, are found to be of the order of  $1 \mu\text{rad}$  in each of the four organs and tissues considered by the Committee.

## 2. Beryllium-7

85. Mainly because of its short half-life, most of the  $^7\text{Be}$  inventory is in the atmosphere (table 10). As exemplified by measurements in the Federal Republic of Germany (190), the surface-air concentration of  $^7\text{Be}$  in the temperate zones shows a regular seasonal variation with maximum values of about  $100 \text{ fCi m}^{-3}$  in spring and minimum values of about  $40 \text{ fCi m}^{-3}$  in late autumn. Using these concentrations, the annual lung absorbed dose in adults from inhalation would be about  $2 \mu\text{rad}$ .

86. Reported concentrations in rain range from 2 to  $130 \text{ pCi l}^{-1}$  with an average value of about  $20 \text{ pCi l}^{-1}$  (199). In the diet, leafy vegetables have been estimated to constitute the main source of  $^7\text{Be}$ , with a resulting annual whole-body absorbed dose in adults of  $8 \mu\text{rad}$  (250).

## 3. Carbon-14

87. Natural  $^{14}\text{C}$  is produced in the upper atmosphere by the reaction  $^{14}\text{N}(n, p) \rightarrow ^{14}\text{C}$  induced by cosmic-ray neutrons. The specific activity of biological carbon, as measured in wood samples grown in the nineteenth century, was  $6.13 \pm 0.03 \text{ pCi per gram of carbon}$  (341), corresponding to an atmospheric inventory of 3.8 MCi. During the present century the specific activity of  $^{14}\text{C}$

in air has decreased due to the diluting effect of releases into the atmosphere of carbon dioxide from the burning of fossil fuels. By 1954 the specific activity of atmospheric carbon had been reduced some 2.5 per cent due to this process (16). The contributions of  $^{14}\text{C}$  in the environment from nuclear explosions and from nuclear power production are discussed in Annexes C and D. According to Nydal *et al.* (260),  $^{14}\text{C}$  activity in the human body follows that in the atmosphere with a delay of about 1.4 y.

88. Measurements of the natural  $^{14}\text{C}$  in tree rings and in lake and ocean sediments have shown that  $^{14}\text{C}$  levels in the atmosphere have remained fairly constant for many thousands of years, although there is a fluctuating change of 10 per cent over a period of 10 000 y (66), in addition to smaller, more random fluctuations over periods of the order of a hundred years (236). The long-term fluctuation over a period of 10 000 y is attributed to a cyclical change of the dipole strength of the earth's magnetic field, which results in a cyclical change of the cosmic-ray flux, which in turn changes the  $^{14}\text{C}$  production rate. The causes of the fluctuations over periods of the order of a hundred years are not known.

89. Knowledge of the natural production rate of  $^{14}\text{C}$  is useful for determining dose commitments from artificial releases into the environment. Since the Committee's 1972 report, a new estimate for the  $^{14}\text{C}$  natural production rate has been reported. Averaged over the 11-year solar cycle, it is 2.28 atoms  $\text{cm}^{-2} \text{s}^{-1}$  (201), which is equivalent to an activity production rate of 0.038  $\text{MCi y}^{-1}$  and is within the range of values given previously (1.6-2.5 atoms  $\text{cm}^{-2} \text{s}^{-1}$  or 0.027-0.042  $\text{MCi y}^{-1}$ ). An independent estimate of the production rate can be computed from the total inventory of natural  $^{14}\text{C}$  on the earth. In units of atmospheric content (which is 6.17  $10^{17}$  g of  $^{12}\text{C}$ ), the biosphere, atmosphere and oceans contain 67 units of carbon (16). Noting that the specific activities of  $^{14}\text{C}$  in surface ocean and deep ocean are lower than in the atmosphere by 4 and 17 per cent, respectively (46), the inventory of  $^{14}\text{C}$  in the above reservoirs is 56 units (of the atmospheric content of  $^{14}\text{C}$ , which is 3.8  $\text{MCi}$ ). From the estimates of Broecker (47) that the slow movement of carbon from the oceans into sediments takes place over a time scale of 100 000 years, it is inferred that about 8 per cent of the  $^{14}\text{C}$  inventory is in sediments. The total inventory is therefore estimated to be 60 units, equivalent to some 230  $\text{MCi}$ . This inventory is in equilibrium with a production rate of natural  $^{14}\text{C}$  of 0.028  $\text{MCi y}^{-1}$ . Considering the uncertainties involved in determining both the production rate and also the total  $^{14}\text{C}$  inventory of the earth, the estimates are in reasonable agreement, particularly since no account is taken of  $^{14}\text{C}$  entering the humus reservoir.

90. Taking the natural specific activity of  $^{14}\text{C}$  as 6.1 pCi per gram of carbon and using the dosimetric factors presented in figure X and the concentrations of carbon, as well as the masses of organs and tissues in the Reference Man of ICRP (152), the annual absorbed doses in man are found to be 1.3 mrad in the whole body, 0.6 mrad in the lung, 0.5 mrad in the gonads, 2.0 mrad in the bone lining cells and 2.2 mrad in the red bone marrow.

#### 4. Sodium-22

91. Even though the production rate and the atmospheric concentration of  $^{22}\text{Na}$  are very small (table 10), the doses in man given in table 12, are higher than those arising from  $^3\text{H}$  and  $^7\text{Be}$  because of both the metabolic behaviour of sodium and the decay properties of  $^{22}\text{Na}$ .

#### 5. Annual doses from internal irradiation by cosmogenic radionuclides

92. Table 12 summarizes the data given above on the internal doses from the four cosmogenic radionuclides considered. It should be mentioned that the annual lung dose received from all the other radionuclides produced by cosmic rays has been estimated to be  $10^{-3}$  mrad (250).

TABLE 12. ANNUAL DOSE FROM INTERNAL IRRADIATION BY COSMOGENIC  $^3\text{H}$ ,  $^7\text{Be}$ ,  $^{14}\text{C}$  AND  $^{22}\text{Na}$

Radio-nuclide	Annual dose (mrad)				
	Gonads	Lung	Bone lining cells	Red bone marrow	Whole-body average
$^3\text{H}$	0.001	0.001	0.001	0.001	0.001
$^7\text{Be}$	—	0.002	—	—	0.008
$^{14}\text{C}$	0.5	0.6	2.0	2.2	1.3
$^{22}\text{Na}$	0.02	0.02	0.02	0.02	0.02

93. As can be seen from table 12, the major part of the annual dose from cosmogenic radionuclides is delivered by  $^{14}\text{C}$ . With the present size of the world population, the annual collective dose is in the range of (2-8)  $10^6$  man rad for the tissues mentioned in table 12.

#### B. PRIMORDIAL RADIONUCLIDES (EXCEPT RADON AND ITS SHORT-LIVED DECAY PRODUCTS)

94. The primordial radionuclides include those belonging to the  $^{235}\text{U}$ ,  $^{238}\text{U}$  and  $^{232}\text{Th}$  series and some other nuclides, among which only  $^{40}\text{K}$  and  $^{87}\text{Rb}$  are significant sources of radiation.

##### 1. Potassium-40

95. Potassium-40, which is the major naturally occurring source of internal radiation dose, enters the body through diet. Being an essential element, potassium is under close homeostatic control in the body. The dose rates from  $^{40}\text{K}$  can be calculated from its isotopic abundance in the biosphere and the concentration of potassium in human tissues.

96. The mass of potassium contained in the whole body varies as a function of age and sex. The mass concentration of potassium is highest in adolescent males and lowest in elderly females, the ratio of the two values being about 2. An average value for an adult male would be about 2 g of potassium per kilogram of body weight (10a, 347). According to Kaul *et al.* (179), the

mass concentration of potassium in various organs and tissues of interest to the Committee are 0.5 g kg<sup>-1</sup> in bone, 4.4 g kg<sup>-1</sup> in red marrow, 2.2 g kg<sup>-1</sup> in lungs, 2.1 g kg<sup>-1</sup> in testes and 1.35 g kg<sup>-1</sup> in ovaries. The annual absorbed doses corresponding to these concentrations can be assessed using the dosimetric factors

presented in figures IX to XII, the masses of organs and tissues in the Reference Man of ICRP (152) and the isotopic ratio of <sup>40</sup>K (0.0118 per cent). The annual absorbed doses are found to be 27 mrad in red bone marrow and 15-17 mrad in the lungs, gonads, bone lining cells and whole body (table 13).

TABLE 13. TISSUE CONCENTRATION AND ANNUAL ABSORBED DOSE DUE TO <sup>40</sup>K AND <sup>87</sup>Rb

Organ or tissue	Potassium			Rubidium		
	Mass concentration of element (g kg <sup>-1</sup> )	Activity concentration of <sup>40</sup> K (pCi kg <sup>-1</sup> )	Annual absorbed dose (mrad)	Mass concentration of element (mg kg <sup>-1</sup> )	Activity concentration of <sup>87</sup> Rb (pCi kg <sup>-1</sup> )	Annual absorbed dose (mrad)
Lung	2.1	1 700	17	9.2	220	0.4
Testes	2.1	1 700	17	20	480	0.8
Ovaries	1.35	1 100	12	—	—	—
Bone	0.5	400	—	26.7	640	—
Red marrow	4.4	3 600	27	7.8	190	0.4
Yellow marrow	0.6	500	6	7.8	190	0.3
Bone lining cells	—	—	15	—	—	0.9
Whole-body average	2	1 600	17	9.7	230	0.4

97. Yamagata (373) studied the variability of the mass of potassium in adult man. He found a normal distribution with an average of 136 g and a standard deviation of 28 g. Using these values, 95 per cent of the adult males would receive annual absorbed doses in the following ranges (mrad): gonads and endosteal cells, 9-21; lung, 10-24; red bone marrow, 16-38.

## 2. Rubidium-87

98. Very little is known about the behaviour of rubidium in man's environment. The doses from <sup>87</sup>Rb have been calculated from the mass concentrations of rubidium in the ICRP Reference Man (152), which are 9.2 µg g<sup>-1</sup> in the lung, 20 µg g<sup>-1</sup> in the testes and 26.7 µg g<sup>-1</sup> in the bone. The value for red bone marrow has been assumed to be equal to the average concentration in soft tissues, which is 7.8 µg g<sup>-1</sup>. The annual absorbed doses obtained range from 0.4 to 0.9 mrad in the organs and tissues of interest to the Committee (table 13).

## 3. Uranium and thorium series

99. Uranium-238 and thorium-232 are each the head of a series of more than ten nuclides (tables 2 and 3). In the same way as in the 1972 report, the <sup>238</sup>U and the <sup>232</sup>Th series can be classified in the subseries in which the activity of the precursor to a large degree controls the activities of the decay products. For the <sup>238</sup>U series, the subseries include: (a) <sup>238</sup>U, two short-lived nuclides and <sup>234</sup>U; (b) <sup>226</sup>Ra, which is frequently separated in the environment from its precursor, <sup>230</sup>Th, of little dosimetric significance in natural background, and from its decay product, <sup>222</sup>Rn, which is an isotope of a noble gas; (c) <sup>222</sup>Rn and its short-lived decay products (through <sup>214</sup>Po) a subseries which is important both for external radiation because of the energetic gamma rays emitted through decay of <sup>214</sup>Bi, and for internal radiation, and is discussed in section C of this chapter;

(d) the long-lived <sup>222</sup>Rn decay products <sup>210</sup>Pb, <sup>210</sup>Bi and <sup>210</sup>Po.

100. The <sup>232</sup>Th series has also been classified in three subseries: (a) <sup>232</sup>Th itself; (b) the sequence of <sup>228</sup>Ra, <sup>228</sup>Ac, <sup>228</sup>Th and <sup>224</sup>Ra; (c) <sup>220</sup>Rn and its decay products. Because of their similarities, <sup>232</sup>Th and <sup>230</sup>Th will be discussed together, the sequences headed by <sup>228</sup>Ra and <sup>226</sup>Ra will be treated in the same section and <sup>220</sup>Rn and its decay products will be considered with <sup>222</sup>Rn. The decay chain of <sup>235</sup>U is not of dosimetric significance and will not be dealt with here.

101. Since all the long-lived (half-life >1 y) radionuclides of the <sup>238</sup>U and <sup>232</sup>Th series are bone seekers, an important parameter for dose assessment is the average activity concentration of those radionuclides in human bone. The comparison of the reported concentrations in the skeleton is complicated since results are given per unit of various quantities such as wet, fresh, dry-fat-free, ash or calcium mass and the relationships between these quantities cannot always be readily assessed. In this report, the conversion factors that have been adopted are derived from data published by the ICRP (151, 152). The weight of the skeleton of an adult man is taken to be 10 kg (wet or fresh weight), including 5 kg of bone (dry or dry-fat-free weight), which yields 2.7 kg of ash. The total mass of calcium in the skeleton is 1 kg. Unless otherwise indicated, the activity concentrations in this document are expressed per unit mass of dry bone. The following information has also been used for dose calculations: the 5 kg of bone comprise 4 kg of compact bone and 1 kg of cancellous bone; the total bone surface in an adult man is 10 m<sup>2</sup> with 5 m<sup>2</sup> in compact bone and 5 m<sup>2</sup> in cancellous bone (151).

### (a) Uranium

102. In this Annex, uranium is assumed to consist of <sup>238</sup>U in radioactive equilibrium with <sup>234</sup>Th, <sup>234</sup>Pa and <sup>234</sup>U, so that 1 g of uranium contains 0.33 µCi of each

of the four radionuclides. In fact, it is known that a disequilibrium state between  $^{238}\text{U}$  and  $^{234}\text{U}$  is rather common in nature. The mechanism by which the isotopes  $^{238}\text{U}$  and  $^{234}\text{U}$  can be fractionated in the ground is the Szilard-Chalmers effect. In the three-step decay of  $^{238}\text{U}$  to  $^{234}\text{U}$ , the daughter atom ( $^{234}\text{U}$ ) is displaced from the crystal lattice. The recoil atom  $^{234}\text{U}$  is liable to be oxidized to the hexavalent stage and therefore can be leached into the water phase more easily than its parent nuclide  $^{238}\text{U}$  (56). Depending on the origin of the water sample, the  $^{234}\text{U}$  to  $^{238}\text{U}$  activity concentration ratio can vary greatly, and values ranging from 0.66 up to 9 have been reported (56, 337).

103. In the atmosphere, the main natural source of uranium are the dust particles resuspended from the

earth. Assuming a dust loading of about  $100 \mu\text{g m}^{-3}$  in surface air of populated areas, and taking an average  $^{238}\text{U}$  activity concentration in soil of  $0.7 \text{ pCi g}^{-1}$  (table 5), the activity concentrations in air are estimated to be about  $7 \cdot 10^{-5} \text{ pCi m}^{-3}$ . Measured values in ground-level air (114, 160, 226) are in good agreement with this estimate. This average concentration corresponds to a daily intake by adults through inhalation of  $1.4 \cdot 10^{-3} \text{ pCi}$ .

104. The dietary intake of  $^{238}\text{U}$  has been measured in several countries (116, 186, 259, 311, 361) and found to lie in the relatively narrow range of  $0.3\text{-}0.5 \text{ pCi d}^{-1}$  in areas of "normal" natural radioactivity (table 14). The activity concentration of  $^{238}\text{U}$  in tap water being usually less than  $0.03 \text{ pCi l}^{-1}$  (14, 186), the contri-

TABLE 14. URANIUM-238 IN THE HUMAN DIET AND BODY IN VARIOUS COUNTRIES

Country	Dietary intake ( $\text{pCi d}^{-1}$ )	Urinary excretion ( $\text{pCi d}^{-1}$ )	Activity in skeleton ( $\text{pCi}$ )	Activity in whole body ( $\text{pCi}$ )	Reference
France	0.2-0.9				311
Japan					
Kyoto and Sapporo	0.50				186
Okayama <sup>a</sup>	1.2	0.03			375
Control area	0.3	0.003			375
United Kingdom	0.40	0.13	21	33	69, 115, 116
United States					
New York	0.43	0.05	18	26	361
Chicago	0.46				361
San Francisco	0.43				361
USSR	about 0.3				186

<sup>a</sup>Mean of the values observed in two villages located near a uranium mine and its refinery.

bution of drinking water to the total dietary intake is in general small. However, it should be mentioned that very high concentrations of uranium in tap water have been reported. In the USSR, activity concentrations as high as  $70 \text{ pCi l}^{-1}$  have been observed (31); in Helsinki, Finland, concentrations of the order of  $1000 \text{ pCi l}^{-1}$  have been measured in several wells, the highest concentration being about  $5000 \text{ pCi l}^{-1}$  (176). According to the authors (176), the very high concentrations of uranium in the water of those wells are probably caused by small, localized uranium-rich deposits.

105. There is experimental evidence (332) that the fraction of uranium absorbed in the gastro-intestinal tract is a few per cent of the amount ingested. As the intake through inhalation is only about  $1 \text{ fCi d}^{-1}$ , the blood uptake through inhalation is small compared to that from ingestion. This is confirmed by the data contained in table 14 which show that the daily urinary excretion, expected to be approximately equal to the daily uptake (145), exceeds substantially the intake by inhalation.

106. In man, the results of measurements of activity concentration of  $^{238}\text{U}$  in soft tissues range from 0.03 to

$0.3 \text{ pCi kg}^{-1}$ , while those in bone are from 4 to  $5 \text{ pCi kg}^{-1}$  (116, 361). From the data contained in table 14 it can be estimated that a daily dietary intake of  $0.4 \text{ pCi}$  of  $^{238}\text{U}$  leads to concentrations in soft tissues of  $0.2 \text{ pCi kg}^{-1}$  and to a bone concentration of  $4 \text{ pCi kg}^{-1}$ . These values have been used to calculate the absorbed doses (table 15). In bone, uranium has been taken to be homogeneously distributed throughout the volume. This has been shown to be approximately true by neutron-induced autoradiographic studies, although higher concentrations were found on bone surfaces (307, 370).

#### (b) Thorium

107. From a dust loading of  $100 \mu\text{g m}^{-3}$  and a  $^{232}\text{Th}$  activity concentration in soil of  $0.7 \text{ pCi g}^{-1}$  (table 5), the activity intake through inhalation per unit time is about  $1 \text{ fCi d}^{-1}$ . There is no direct information on the dietary activity intake of  $^{232}\text{Th}$  per unit time but an indirect estimate of about  $0.1 \text{ pCi d}^{-1}$  has been proposed (250). The contribution of this route to the body content is probably negligible because of the very low absorption of thorium through the gastro-intestinal tract.



TABLE 15. TISSUE ACTIVITY CONCENTRATION AND ANNUAL ABSORBED DOSE DUE TO RADIONUCLIDES OF THE  $^{238}\text{U}$ - $^{234}\text{U}$  SUBSERIES

Organ or tissue	Activity concentration of $^{238}\text{U}$ , $^{234}\text{Th}$ , $^{234\text{m}}\text{Pa}$ or $^{234}\text{U}$ ( $\text{pCi kg}^{-1}$ )	Annual absorbed dose (mrad)					
		$^{238}\text{U}$	$^{234}\text{Th}$	$^{234\text{m}}\text{Pa}$	$^{234}\text{U}$	Total	
		(a)	( $\beta$ , $\gamma$ )	( $\beta$ , $\gamma$ )	(a)	(a) ( $\beta$ , $\gamma$ )	
Lung	0.2	0.02	0.0002	0.003	0.02	0.04	0.003
Testes	0.2	0.02	0.0002	0.003	0.02	0.04	0.003
Ovaries	0.2	0.02	0.0002	0.003	0.02	0.04	0.003
Bone	4	—	—	—	—	—	—
Red marrow	0.2	0.02	0.0006	0.02	0.03	0.05	0.02
Yellow marrow	0.2	—	—	—	—	—	—
Bone lining cells	0.2	0.12	0.003	0.04	0.14	0.3	0.04

108. Measured levels in rib bone show a linear increase with age (216). The average activity concentration in ash would be about  $1 \text{ fCi g}^{-1}$  in adults, which is about 10 times less than the corresponding values for  $^{238}\text{U}$ . However, thorium is known to deposit on the endosteum, and the dose rates in this tissue per unit activity of thorium in bone are much higher than those for uranium, because the latter element is distributed over the total mass of bone. The calculated dose rates to bone tissues from  $^{232}\text{Th}$  are shown in table 16.

TABLE 16. TISSUE ACTIVITY CONCENTRATION AND ANNUAL ABSORBED DOSE DUE TO  $^{230}\text{Th}$  AND  $^{232}\text{Th}$

Organ or tissue	Activity concentration of $^{230}\text{Th}$ or $^{232}\text{Th}$ ( $\text{pCi kg}^{-1}$ )	Annual absorbed dose (mrad)	
		$^{230}\text{Th}$	$^{232}\text{Th}$
Lung	0.5	0.04	0.04
Gonads	0.05	0.004	0.004
Bone (average)	0.5	—	—
Trabecular bone	1.3	—	—
Red marrow	0.05	0.05	0.04
Bone lining cells	—	0.8	0.7

109. Pavlovskaya (268) measured the activity concentration of  $^{232}\text{Th}$  in soft tissues and found it to be one fifth to one fourth of that in the skeleton and thus about one tenth of that in dry bone. Taking the activity concentration in bone to be  $0.5 \text{ pCi kg}^{-1}$ , the activity concentration in soft tissues would therefore be about  $0.05 \text{ pCi kg}^{-1}$ . It has been suggested by Wrenn (370), on the basis of Budinger's measurements (48), that the  $^{232}\text{Th}$  concentration could be much higher in lung tissue than in the other soft tissues. Using an intake per unit time through inhalation of  $1 \text{ fCi d}^{-1}$ , a deposition of 25 per cent in the pulmonary region, and a biological half-life of 4 y, the equilibrium activity concentration in lung tissue would be about  $0.5 \text{ pCi kg}^{-1}$ . The resulting annual absorbed dose to soft tissue is presented in table 16.

110. The Committee is not aware of any study dealing with concentrations of  $^{230}\text{Th}$  in man. However, it is likely that the  $^{230}\text{Th}$  and the  $^{232}\text{Th}$  levels in man are

very similar, because their activity concentrations in soil are about equal and their physical half-lives are very much longer than man's life span. The annual absorbed doses in several tissues from  $^{230}\text{Th}$  are given in table 16.

### (c) Radium

111. Radium has 13 known radioactive isotopes, whose atomic weights range from 213 to 230 and whose radioactive half-lives range from  $10^{-3}$  s to 1600 y. From the point of view of human radiation exposure from natural background only  $^{226}\text{Ra}$  and  $^{228}\text{Ra}$ , which gives rise to  $^{224}\text{Ra}$ , are of significance.

112. *Inhalation.* As in the case of uranium and thorium, the main natural source of radium in the atmosphere is the resuspension of soil particles; this corresponds to a calculated activity intake of about  $1 \text{ fCi d}^{-1}$ .

113. *Ingestion.* Food consumption is a much more important source of radium intake and fractional blood uptake than inhalation. The average dietary activity intake per unit time of  $^{226}\text{Ra}$  in areas of normal radiation background is of the order of  $1 \text{ pCi d}^{-1}$  (table 17). Typical  $^{226}\text{Ra}$  levels in most components of the diet range from 0.1 to  $5 \text{ pCi kg}^{-1}$ , but some individual foods, such as Brazil nuts and Pacific salmon, contain much larger concentrations of  $^{226}\text{Ra}$ . Although much less documented, the dietary activity intake of  $^{228}\text{Ra}$  in areas of normal radiation background seems to be about the same as that of  $^{226}\text{Ra}$  (278).

114. The contribution of water to the total intake is in general small when the drinking-water supplies are drawn from surface waters. However,  $^{226}\text{Ra}$  levels of 1 to  $10 \text{ pCi l}^{-1}$  are not exceptional in well and mineral waters (5, 176, 296, 316). Available information on the concentrations of  $^{228}\text{Ra}$  in water is limited, but it seems that they are of an order of magnitude lower than the corresponding concentrations of  $^{226}\text{Ra}$  (14, 176).

115. Two well known populated areas with high concentrations of thorium and uranium in their soil are located along the coast of Kerala in India and in the Araxá-Tapira region in Brazil. The estimated average daily intakes of  $^{226}\text{Ra}$  and  $^{228}\text{Ra}$  of the Indian population along the Kerala coast are 3 and 160 pCi, respectively (58, 240). In Brazil, a survey in the

TABLE 17. RADIUM-226 IN THE HUMAN DIET AND DRY BONE IN VARIOUS AREAS

Area	Dietary intake		Mean activity concentration in dry bone <sup>a</sup> (pCi kg <sup>-1</sup> )	Bone/diet <sup>b</sup>		Reference
	(pCi d <sup>-1</sup> )	pCi (gCa) <sup>-1</sup>		pCi kg <sup>-1</sup> per pCi d <sup>-1</sup>	Observed ratio	
<i>Areas of normal external radiation background</i>						
Argentina	0.8	1.1	6.6	8.2	0.030	30
Australia			5.4			357
Canada			3.2			357
Chile			2.2			357
Congo			12			357
France	1.1	1.1				311
Germany, Fed. Rep. of			7.0			324
Guatemala			2.7			357
India						
Bombay	0.8	1.6	4.3	5.4	0.013	58
Tarapur	0.5	1.0				177
Israel			19			357
Italy	1.4	2.8				42
Japan						
Sapporo	0.4	0.8	1.6	4.0	0.016	113a
Kyoto	1.0	2.9	7.5	7.5	0.019	113a
Poland						
Eastern			7.7			} 163
Northern			5.3			
Southern			6.5			
Western			32.6			
Puerto Rico 1	0.7	1.3	3.4	4.8	0.013	113
Puerto Rico 2			2.7			357
South Africa			5.9			357
Ukrainian SSR			21			245
United Kingdom	1.2	1.1	8.1	6.7	0.037	357, 314
United States						
Boston			7.6			357
Houston			12			357
Illinois			20			135
New England			8.6			143
New York 1	1.7	1.7	7.2	4.2	0.021	85
New York 2			5.4			357
San Francisco	0.8	0.8	6.2	7.7	0.039	85
Wisconsin			6.5			222
<i>Arithmetic mean</i>	0.9	1.5	8.5	6.1	0.024	
<i>Area of high external radiation background</i>						
Kerala, India	3.3	6.6	77	23	0.058	58

<sup>a</sup>The data have been either taken directly from the references or converted in terms of dry bone using the factors of paragraph 101.

<sup>b</sup>The left-hand column gives the bone-to-diet quotient, the units used being pCi kg<sup>-1</sup> for the activity concentration in dry bone and pCi d<sup>-1</sup> for the dietary intake. The right-hand column gives the corresponding values of the bone-to-diet observed activity ratio, the unit used being pCi per gram of Ca for both bone and diet.

Araxá-Tapira region showed that, out of a population of 1670 people living in and around the radioactive anomalies of Barreiro and Tapira, only 196 individuals are ingesting alpha emitters at a level five times or more than that of a similar group living in Rio de Janeiro. Their intake of radium per unit time ranged from 10 to 40 pCi d<sup>-1</sup> of <sup>226</sup>Ra and from 60 to 240 pCi d<sup>-1</sup> of <sup>228</sup>Ra (347).

116. *Distribution in man and dose rates.* When radium is taken into the body, its metabolic behaviour is similar to that of calcium, and an appreciable fraction is deposited on bone surfaces and in areas of active bone turnover (82). Rowland (300) has shown that, after high

intakes, approximately half of the initial activity in man is deposited in "hot spots" and half in the diffuse component. The initial deposition in hot spots is due presumably to the fact that these are areas of actively growing bone where mineralization is occurring. Even in the case of relatively low-level dietary intake, the same hot-spot accumulation is thought to occur, but at a lower activity level (125). About 70-90 per cent of the radium in the body is contained in bone (151), the remaining fraction being distributed approximately uniformly in soft tissues. In the areas of normal radiation background, the <sup>226</sup>Ra concentrations in bone range roughly from 2 to 20 pCi kg<sup>-1</sup> (table 17), with an arithmetic mean of about 8 pCi kg<sup>-1</sup>. Several studies

(see, for example, reference 325) have shown that the  $^{226}\text{Ra}$  concentration in bone seems to be independent of age.

117. The relationship between the dietary intake and the skeletal content can be estimated from measurements in countries where both the concentrations in bone and the dietary intake have been published (table 17). The bone-to-diet quotient, expressed in  $\text{pCi kg}^{-1}$  per  $(\text{pCi d}^{-1})$ , ranges from 4.0 to 8.2 with an average of 6.1. The "observed ratio" between the activity per gram of calcium in the bone and in the diet ranges from 0.013 to 0.039, with an average of 0.024.

118. Another way to estimate the bone-to-diet relationship is to use the model developed by ICRP on the metabolism of alkaline earths in adult man (151). According to that model, a blood uptake of 1  $\text{pCi}$  of  $^{226}\text{Ra}$  yields a time-integral of the bone activity of 126.3  $\text{pCi d}$ , and a time-integral of the whole-body activity of 143.7  $\text{pCi d}$ . Therefore, a continuous blood uptake of 1  $\text{pCi d}^{-1}$  would yield an equilibrium activity of 126  $\text{pCi}$  in the skeleton corresponding to an average bone activity concentration of 25  $\text{pCi kg}^{-1}$ . Since the fractional blood uptake for radium is 0.15-0.20 (125), an intake of about 6  $\text{pCi d}^{-1}$  corresponds to a blood uptake of 1  $\text{pCi d}^{-1}$ . The bone-to-diet quotient is therefore calculated to be 4.2  $\text{pCi kg}^{-1}$  per  $\text{pCi d}^{-1}$ , which is in reasonable agreement with the value of 6.1 given in paragraph 117.

119. If all the values of the daily dietary intake and of the activity concentrations in bone shown in table 17 are taken into account, the averages are 0.9  $\text{pCi d}^{-1}$  and 8.5  $\text{pCi kg}^{-1}$ , respectively, corresponding to a bone-to-diet quotient of 9  $\text{pCi kg}^{-1}$  per  $\text{pCi d}^{-1}$ , which is somewhat higher than the two estimates in the previous paragraphs. The difference may be due to the high concentrations in bone found in the Congo, Israel, western Poland, the United States (Houston and Illinois) and the Ukrainian Soviet Socialist Republic. The  $^{226}\text{Ra}$  dietary intake in these regions might be higher than average. If they are excluded, the bone-to-diet quotient becomes 6  $\text{pCi kg}^{-1}$  per  $\text{pCi d}^{-1}$ .

120. The fraction of  $^{226}\text{Ra}$  distributed in the soft tissues will be taken to be 17 per cent, as given in ICRP Publication 20 (151). The average activity of human soft tissues would thus be 0.13  $\text{pCi kg}^{-1}$ .

121. The concentration of  $^{228}\text{Ra}$  in human bone could be expected to be lower than that of  $^{226}\text{Ra}$  because of the shorter half-life of the former and the estimated biological half-life of radium in the body, which is of the order of 10 years (151, 363). Thus, the  $^{228}\text{Ra}$  activity would be limited by its physical half-life to about 30 per cent of the  $^{226}\text{Ra}$  activity. This is consistent with the ICRP model (151), from which a figure of 27 per cent can be derived. In fact, in the few studies dealing with the determination in bone of  $^{228}\text{Th}$ , which can be assumed to be in radioactive equilibrium with  $^{228}\text{Ra}$ , the average ratio of  $^{228}\text{Th}$  to  $^{226}\text{Ra}$  in bone ash was found to vary between 0.25 and 0.5 (143, 215, 324). Using a value of 0.3, the average  $^{228}\text{Ra}$  activity in bone would be 2.4  $\text{pCi kg}^{-1}$  in areas of normal background radiation. Since no measurement of  $^{228}\text{Ra}$  in soft tissues could be found in the literature, the figure of 0.1  $\text{pCi kg}^{-1}$  derived from the ICRP model (151) is used in this Annex.

122. The dose rates in bone lining cells and bone marrow presented in tables 18 and 19 have been calculated using the same assumptions as in the 1972 report: (a) an average retention factor in the skeleton and in the soft tissues of 0.33 for  $^{222}\text{Rn}$  and of 1.0 for  $^{220}\text{Rn}$  and (b) a uniform concentration of radium and its decay products over the total mass of mineral bone. In fact, with respect to  $^{228}\text{Ra}$  and its decay products, it is known that a fraction of  $^{228}\text{Th}$ , which is the long-lived alpha emitter of the radioactive sequence, migrates to the endosteum (330). Furthermore, direct intake of  $^{228}\text{Th}$  and  $^{224}\text{Ra}$ , although contributing to a small extent to the skeletal activity, leads to deposition of those radionuclides on bone surfaces. Because a fraction of the activity of the decay products of  $^{228}\text{Ra}$  is surface distributed, the doses from that sequence in bone marrow and in bone lining cells may therefore be somewhat higher than indicated in table 19.

123. Data on the activity of radium in the skeleton of the populations living in the high radiation areas of Brazil and India are very scarce. In Brazil, the mean  $^{226}\text{Ra}$  concentration in the teeth of the population living in the Araxá-Tapira region has been estimated as 85  $\text{fCi}$  per gram of ash, which corresponds to an activity in the skeleton of about 230  $\text{pCi}$ , if it is assumed that the concentration in teeth is the same as that in bone. In India, the analysis of a femur bone yielded a  $^{226}\text{Ra}$  concentration per unit mass of ash of 143  $\text{fCi g}^{-1}$ , which corresponds to a skeletal activity of about 400  $\text{pCi}$  (58).

TABLE 18. TISSUE ACTIVITY CONCENTRATION AND ANNUAL ABSORBED DOSE DUE TO  $^{226}\text{Ra}$  AND ITS SHORT-LIVED DECAY PRODUCTS

Organ or tissue	Activity concentration of $^{226}\text{Ra}$ ( $\text{pCi kg}^{-1}$ )	Activity concentration of the decay products of $^{226}\text{Ra}$ ( $\text{pCi kg}^{-1}$ )	Annual tissue absorbed dose (mrad)						Total	
			$^{226}\text{Ra}$	$^{222}\text{Rn}$	$^{218}\text{Po}$	$^{214}\text{Pb}$	$^{214}\text{Bi}$	$^{214}\text{Po}$		
			(a)	(a)	(a)	( $\beta, \gamma$ )	( $\beta, \gamma$ )	(a)	(a)	( $\beta, \gamma$ )
Lung	0.13	0.043	0.01	0.004	0.005	0.0003	0.001	0.006	0.03	0.001
Gonads	0.13	0.043	0.01	0.004	0.005	0.0004	0.001	0.006	0.03	0.001
Bone	8	2.6	—	—	—	—	—	—	—	—
Red marrow	0.13	0.043	0.03	0.01	0.02	0.003	0.009	0.03	0.09	0.01
Yellow marrow	0.13	0.043	—	—	—	—	—	—	—	—
Bone lining cells	—	—	0.27	0.11	0.13	0.009	0.02	0.18	0.7	0.03

TABLE 19. ANNUAL TISSUE ABSORBED DOSE

Organ or tissue <sup>a</sup>	Annual				
	<sup>228</sup> Ra (β)	<sup>228</sup> Ac (β, γ)	<sup>228</sup> Th (α)	<sup>224</sup> Ra (α)	<sup>220</sup> Rn (α)
Lung	3 10 <sup>-5</sup>	1 10 <sup>-3</sup>	1.0 10 <sup>-2</sup>	1.1 10 <sup>-2</sup>	1.2 10 <sup>-2</sup>
Gonads	3 10 <sup>-5</sup>	1 10 <sup>-3</sup>	1.0 10 <sup>-2</sup>	1.1 10 <sup>-2</sup>	1.2 10 <sup>-2</sup>
Red marrow	6 10 <sup>-5</sup>	8 10 <sup>-3</sup>	2.5 10 <sup>-2</sup>	2.8 10 <sup>-2</sup>	3.4 10 <sup>-2</sup>
Bone lining cells	2 10 <sup>-4</sup>	1 10 <sup>-2</sup>	1.7 10 <sup>-1</sup>	1.8 10 <sup>-1</sup>	2.1 10 <sup>-1</sup>

<sup>a</sup>The activity concentration in the lung, gonads and red marrow is assumed to be 0.1 pCi kg<sup>-1</sup>. The activity concentration in bone is taken to be 4 pCi kg<sup>-1</sup> for cancellous bone and 2 pCi kg<sup>-1</sup> for

#### (d) Long-lived decay products of <sup>222</sup>Rn

124. The <sup>210</sup>Pb-<sup>210</sup>Bi-<sup>210</sup>Po chain is a significant component of the dose from internal irradiation by natural alpha emitters. When the three radionuclides are in radioactive equilibrium, the dose from <sup>210</sup>Po is much higher than from <sup>210</sup>Pb and <sup>210</sup>Bi, and on this basis <sup>210</sup>Po could be considered separately. However, the activity concentrations of <sup>210</sup>Po, in the environment as well as in man, are usually closely related to those of <sup>210</sup>Pb, which is its long-lived precursor and acts as a carrier. For that reason, <sup>210</sup>Po and <sup>210</sup>Pb will be dealt with together. The half-life of <sup>210</sup>Bi is short compared to that of <sup>210</sup>Pb. Therefore, <sup>210</sup>Bi will almost always be assumed to be in equilibrium with <sup>210</sup>Pb in the various compartments of the environment and of the human body.

#### (i) Sources and levels in the environment

125. *Air.* The main source of <sup>210</sup>Pb and <sup>210</sup>Po in the atmosphere is <sup>222</sup>Rn emanation from the ground. The amount of atmospheric <sup>210</sup>Pb produced in this way has been estimated to be 0.6 MCi y<sup>-1</sup> (164), which would lead to an equilibrium activity of <sup>210</sup>Pb and <sup>210</sup>Po in the atmosphere of about 20 MCi if the air concentrations were governed by radioactive decay only. However, tropospheric aerosols to which these radionuclides are attached are scavenged from the atmosphere through wash-out and dry deposition with a mean residence time of about 10 d (91). The inventories are therefore about 20 kCi for <sup>210</sup>Pb (164) and 2 kCi for <sup>210</sup>Po. The concentrations of these nuclides in surface air depend mainly on the rate of emanation of <sup>222</sup>Rn from the ground and on the latitudinal distribution of land and sea areas. Consequently, they are highest in the subtropical and temperate latitudes of the northern hemisphere, as illustrated in figure XIII for <sup>210</sup>Pb (295). In the middle latitudes of the northern hemisphere, the average concentrations of <sup>210</sup>Pb and <sup>210</sup>Po have been estimated to be 14 fCi m<sup>-3</sup> (162) and 3.3 fCi m<sup>-3</sup> (267), respectively. It has been suggested (244) that a significant source of <sup>210</sup>Po in surface air could be vegetative transpiration.

126. *Rain and drinking water.* The global distribution of <sup>210</sup>Pb and <sup>210</sup>Po in rain water follows the same pattern as that in surface air, being highest in the middle latitudes (fig. XIV). The annual averages of the

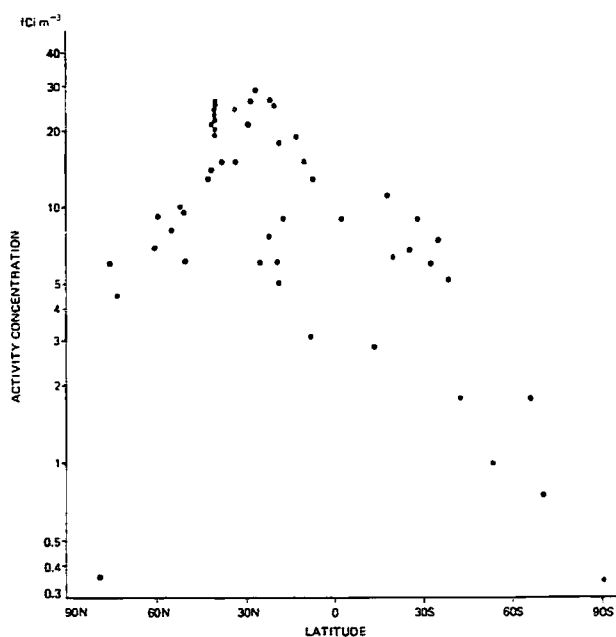


Figure XIII. Latitudinal distribution of <sup>210</sup>Pb in surface air (295)

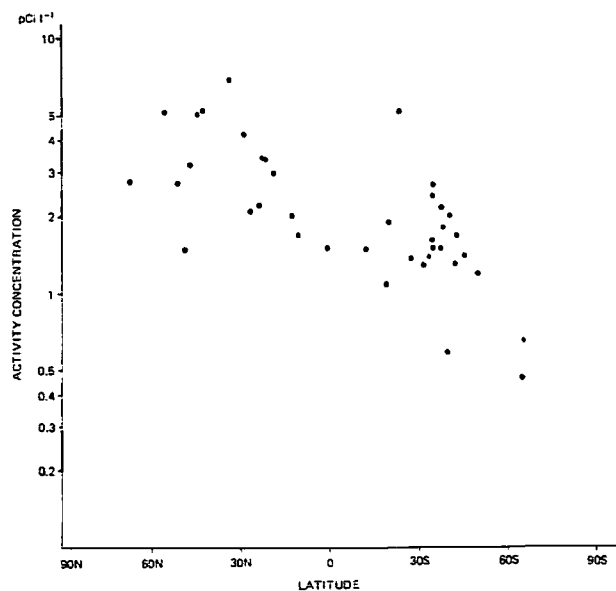


Figure XIV. Latitudinal distribution of <sup>210</sup>Pb in rain water (295)

tissue absorbed dose (mrad)

$^{210}\text{Po}$	$^{210}\text{Pb}$	$^{212}\text{Bi}$		$^{212}\text{Po}$	$^{210}\text{Pb}$	Total	
		( $\alpha$ )	( $\beta, \gamma$ )			( $\alpha$ )	( $\beta, \gamma$ )
$1.3 \cdot 10^{-2}$	$4 \cdot 10^{-4}$	$4 \cdot 10^{-3}$	$8 \cdot 10^{-4}$	$1.0 \cdot 10^{-2}$	$2 \cdot 10^{-3}$	$6 \cdot 10^{-2}$	$4 \cdot 10^{-3}$
$1.3 \cdot 10^{-2}$	$3 \cdot 10^{-4}$	$4 \cdot 10^{-3}$	$8 \cdot 10^{-4}$	$1.0 \cdot 10^{-2}$	$2 \cdot 10^{-3}$	$6 \cdot 10^{-2}$	$4 \cdot 10^{-3}$
$3.9 \cdot 10^{-2}$	$2 \cdot 10^{-3}$	$1.2 \cdot 10^{-2}$	$1 \cdot 10^{-2}$	$4.3 \cdot 10^{-2}$	$7 \cdot 10^{-3}$	$18 \cdot 10^{-2}$	$3 \cdot 10^{-2}$
$2.4 \cdot 10^{-1}$	$5 \cdot 10^{-3}$	$6.5 \cdot 10^{-2}$	$1.5 \cdot 10^{-2}$	$2.1 \cdot 10^{-1}$	$1 \cdot 10^{-2}$	$10.8 \cdot 10^{-1}$	$4 \cdot 10^{-2}$

compact bone, yielding an average concentration per unit mass of bone of  $2.4 \text{ pCi kg}^{-1}$ ; the activity concentration in yellow marrow is assumed to be  $0.1 \text{ pCi kg}^{-1}$ , the same as in other soft tissues.

concentration of  $^{210}\text{Pb}$  in rain at various locations have been found to vary between  $0.2$  and  $7 \text{ pCi l}^{-1}$  (295), a typical value for the continental stations of the middle northern latitudes being  $3 \text{ pCi l}^{-1}$ . Reported values of the  $^{210}\text{Po}/^{210}\text{Pb}$  activity concentration ratio in rain water range from  $0.1$  to  $0.54$  (267). Activity concentrations in drinking water are usually less than  $0.1 \text{ pCi l}^{-1}$ . However, concentrations in mineral water or in well water may reach the levels observed in rain water.

127. *Soil.* The activity concentrations of  $^{210}\text{Pb}$  and  $^{210}\text{Po}$  in the top layer of soil are not strictly equal to those of  $^{226}\text{Ra}$  because (a) a fraction of  $^{222}\text{Rn}$  diffuses through soil into the atmosphere and (b)  $^{210}\text{Pb}$  and  $^{210}\text{Po}$  are deposited on the soil surface through dry and wet fallout. Assuming a deposition velocity of  $5 \cdot 10^{-3} \text{ m s}^{-1}$  and an atmospheric concentration of  $14 \text{ fCi m}^{-3}$ , the dry deposition of  $^{210}\text{Pb}$  in the northern middle latitudes would occur at the rate of  $2.2 \text{ mCi km}^{-2} \text{ y}^{-1}$ , corresponding to an equilibrium activity in the deposit of  $68 \text{ mCi km}^{-2}$ . With a mean annual precipitation of  $800 \text{ mm}$  and a concentration in rain or snow of  $3 \text{ pCi l}^{-1}$ , the rate of wet deposition of  $^{210}\text{Pb}$  would be  $1.2 \text{ mCi km}^{-2} \text{ y}^{-1}$ , leading to an equilibrium value of the deposit of  $37 \text{ mCi km}^{-2}$ . Assuming that the amount deposited is contained within the top  $20 \text{ cm}$  of soil, the  $^{210}\text{Pb}$  activity concentration in that layer, at equilibrium, would be  $0.2 \text{ pCi g}^{-1}$  from dry deposition and  $0.1 \text{ pCi g}^{-1}$  from wet deposition. The average activity concentration of  $^{226}\text{Ra}$  in soil being about  $0.7 \text{ pCi g}^{-1}$  (table 5), the activity of  $^{210}\text{Pb}$  in the top  $20 \text{ cm}$  of soil is expected to be about  $30$  per cent higher than that of  $^{226}\text{Ra}$  if the fraction of  $^{222}\text{Rn}$  retained in soil is taken to be  $0.9$ . Measurements of  $^{210}\text{Pb}$  and  $^{226}\text{Ra}$  in the top layers of soil which have been conducted in several countries confirm that the relative importance of fallout  $^{210}\text{Pb}$ , as assessed above, is reasonably correct. In Massachusetts (United States),  $^{210}\text{Pb}$  from fallout was found to migrate to a depth of  $40 \text{ cm}$  (121); over that depth, the average  $^{210}\text{Pb}/^{226}\text{Ra}$  activity ratio was  $1.9$ . In another sample of soil taken in Maryland (United States), the migration of  $^{210}\text{Pb}$  seemed to extend up to  $30 \text{ cm}$ , the average  $^{210}\text{Pb}/^{226}\text{Ra}$  over that layer being about  $1.2$  (4). In New Zealand, the results of measurements carried out on four types of soil show that that portion of  $^{210}\text{Pb}$  which is due to fallout tends to remain within the top  $15 \text{ cm}$  of the soil and that this portion constitutes from  $18$  to  $34$  per cent of the total  $^{210}\text{Pb}$  in this depth (17). In Poland, similar

measurements, limited to a depth of  $10 \text{ cm}$ , show that in inland areas the excess  $^{210}\text{Pb}$  is  $23$  per cent while in coastal areas, where the  $^{210}\text{Pb}$  deposition is smaller, the excess  $^{210}\text{Pb}$  is only  $6$  per cent over the top  $10 \text{ cm}$  of soil (166).

128. *Plants.* The concentration of  $^{210}\text{Pb}$  and  $^{210}\text{Po}$  in plants is a function of both direct deposition on the leaves and root uptake from the soil. The relative importance of these two pathways is controversial. Francis *et al.* (90) have studied tobacco and vegetables under greenhouse and field conditions. They found that under greenhouse conditions little  $^{210}\text{Pb}$  or  $^{210}\text{Po}$  was detected in the plants, while under field conditions the  $^{210}\text{Pb}$  and  $^{210}\text{Po}$  levels increased. They concluded that the major source of  $^{210}\text{Po}$  in vegetation is from fallout of  $^{210}\text{Pb}$  with decay to  $^{210}\text{Po}$ . A similar conclusion has been reached by Hansen and Watters (118), who compared the concentrations obtained in plants grown in control soil and in  $^{210}\text{PoO}_2$ -contaminated soil. The  $^{210}\text{Po}$  activity concentrations per unit mass of dry weight measured in the vegetables grown in control soil ranged from  $10$  to  $100 \text{ pCi kg}^{-1}$ . On the other hand, studies of tobacco by Tso *et al.* (344) suggest the source of  $^{210}\text{Po}$  in plants may be root uptake of  $^{210}\text{Pb}$ . Tobacco plants exposed to a  $500$ -fold increase of  $^{222}\text{Rn}$  in a greenhouse only exhibited a  $2$ -fold increase in  $^{210}\text{Po}$  content. In a study of the transfer of  $^{210}\text{Pb}$  and  $^{210}\text{Po}$  added to soil as nitrate, Tso and Fisenne (345) state that the principal route of entry of  $^{210}\text{Pb}$  and  $^{210}\text{Po}$  in the tobacco plant is probably root absorption.

#### (ii) Human intake

129. *Inhalation.* The average concentrations in surface air given above are  $14 \text{ fCi m}^{-3}$  for  $^{210}\text{Pb}$  and  $3.3 \text{ fCi m}^{-3}$  for  $^{210}\text{Po}$ . Assuming that an adult inhales  $20 \text{ m}^3$  of air daily (152), the intakes of non-smokers are estimated to be  $0.3 \text{ pCi d}^{-1}$  of  $^{210}\text{Pb}$  and  $0.07 \text{ pCi d}^{-1}$  of  $^{210}\text{Po}$ . Since a cigarette contains about  $0.6 \text{ pCi}$  of  $^{210}\text{Pb}$  and  $0.4 \text{ pCi}$  of  $^{210}\text{Po}$  (267) and both nuclides are volatile at the burning temperature of tobacco, cigarette smoking will lead to a substantial increase in the intake of  $^{210}\text{Pb}$  and  $^{210}\text{Po}$  through inhalation. About  $10$  per cent of the  $^{210}\text{Pb}$  and  $20$  per cent of the  $^{210}\text{Po}$  contained in the cigarette will enter the lung with the main smoke stream (267). Therefore, for a person smoking  $20$  cigarettes a day, the values of the estimated intakes are  $1.2 \text{ pCi}$  for  $^{210}\text{Pb}$  and  $1.6 \text{ pCi}$  for  $^{210}\text{Po}$ .

However, it should be pointed out that the conditions of inhalation while smoking are very different from those in normal respiration.

130. *Ingestion.* For non-smokers, consumption of food is usually the most important route by which  $^{210}\text{Pb}$  and  $^{210}\text{Po}$  enter the human organism. The dietary intake is presented in table 20. In cereal products, vegetables and meat, the typical concentration of  $^{210}\text{Pb}$  is 2.5 pCi  $\text{kg}^{-1}$ , and the  $^{210}\text{Po}/^{210}\text{Pb}$  ratio is in the range 0.5-1.0. The concentration in milk is lower by an order of magnitude. These products are the main components of the diet in the areas of normal intake (table 20). In these areas the values of the intake of  $^{210}\text{Pb}$  and  $^{210}\text{Po}$  lie between 1 and 10 pCi  $\text{d}^{-1}$ , the contribution of drinking water to the intake being only a few per cent. A value of 3 pCi  $\text{d}^{-1}$  will be taken as representative of the intake of  $^{210}\text{Pb}$  and  $^{210}\text{Po}$  in areas of normal radiation background. The actual value of the intake in a given area depends to a certain extent upon the concentration of these nuclides in surface air and rain water. However, the published values of the dietary intake of  $^{210}\text{Pb}$  and its average concentration in surface air and rain water in the same regions (table 21) do not seem to be correlated.

131. High concentrations of  $^{210}\text{Po}$  are observed in the edible portions of aquatic organisms, for which it is now well established that the  $^{210}\text{Po}/^{210}\text{Pb}$  activity concentration ratio is greater than 1 (57). The  $^{210}\text{Po}$  concentrations in the muscles of fish and in molluscs are approximately 20 and 500 pCi  $\text{kg}^{-1}$  (267). The intakes of  $^{210}\text{Pb}$  and  $^{210}\text{Po}$  in populations consuming large

TABLE 20. COMPARISON OF THE DIETARY INTAKE OF  $^{210}\text{Pb}$  AND  $^{210}\text{Po}$  IN AREAS OF NORMAL AND HIGH INTAKE

Area	Dietary intake (pCi $\text{d}^{-1}$ )		Ref- erence
	$^{210}\text{Pb}$	$^{210}\text{Po}$	
<i>Areas of normal dietary intake</i>			
Argentina		1.3	347
Germany, Federal Republic of	4.6	4.6	347
USSR		3.8	267
Rostov	6.2	4.1	196
United Kingdom <sup>a</sup>	3.2	3.2	347
United States	1.4	1.8	250, 140
<i>Areas of high dietary intake</i>			
High seafood consumption			
Japan	17		347
High reindeer and caribou consumption			
Canada		100	132
Finland (Inari)	8.6	69	180
Sweden (Lake Rogen district)	3.6-9	72-180	276
USSR		30-70	267
Murmansk region <sup>b</sup>	44	79	267, 258
Yamalo-Nenetskii National Area			
		344	267
United States (Alaska)		60	35

<sup>a</sup>The range of the dietary intake of  $^{210}\text{Pb}$  and  $^{210}\text{Po}$  in the United Kingdom is estimated to be 1-10 pCi  $\text{d}^{-1}$  (347).

<sup>b</sup>The  $^{210}\text{Pb}$  dietary intake is based on measurements of excreta (258).

TABLE 21. ACTIVITY CONCENTRATION OF  $^{210}\text{Pb}$  IN THE ENVIRONMENT, THE HUMAN DIET AND HUMAN BONE ASH

Location	Surface air <sup>a</sup> (fCi $\text{m}^{-3}$ )	Rain water (pCi $\text{l}^{-1}$ )	Dietary intake (pCi $\text{d}^{-1}$ )	Human bone ash <sup>b</sup> (fCi $\text{g}^{-1}$ )	Ref- erence
<i>Continental</i>					
Finland	7 (3-15)			78 C	180, 295
Germany, Federal Republic of	10 (3-38)	3.0	4.6	110 C	101, 137, 295
India, Bombay	18 (5-49)	3.0		321 T	182, 295
Poland				148 T	161
				91 T	32
USSR, Rostov	17	5.2 <sup>c</sup>	6.2	134 M	196, 295
United States					
Palmer, Alaska	9 (5-16)	0.8	1.7		219, 295
Los Angeles, California	15 (6-25)	0.8, 3.2	1.5		219, 295
Chicago, Illinois	21 (11-76)	1.3-2.5	1.8	184 T	} 135, 219, 295
				146 M	
				105 C	
New Orleans, Louisiana	21 (12-35)		1.8		219, 295
Boston, Massachusetts	14 (10-22)		1.7		219, 295
New York, New York	21 (7-43)		1.2	200 T	39, 219, 295
<i>Island</i>					
Japan					
Sapporo				96 T	113a
Kyoto				218 T	113a
New Zealand	5 <sup>d</sup>	1.4-1.8		61 M	252, 295
United Kingdom, England	6 (2-13)	2.7	3.2	96 T	134, 295
Puerto Rico	9 (4-15)	2.2 <sup>e</sup>		118 T	137, 295
United States					
Honolulu, Hawaii	5 (4-7)	1.1	1.6		219, 295

<sup>a</sup>The range of observed values is given within parentheses.

<sup>b</sup>T = trabecular bone, C = cortical bone, M = mean bone value.

<sup>c</sup>Concentration measured in Moscow.

<sup>d</sup>Concentration measured in Melbourne.

<sup>e</sup>Concentration measured in Nassau.

proportions of seafood are therefore expected to be higher than those of populations with other types of diet. This assumption is confirmed by the value of the  $^{210}\text{Pb}$  intake in Japan (table 20).

132. A well documented case of elevated intakes is that of the tens of thousands of reindeer and caribou eaters in the arctic and sub-arctic regions of the northern

hemisphere. Their main food is the meat of these animals, which contains unusually high concentrations of  $^{210}\text{Po}$  because in the winter they graze on lichens which accumulate  $^{210}\text{Pb}$  and  $^{210}\text{Po}$ .

133. Table 22 presents information on the concentrations of  $^{210}\text{Pb}$  and  $^{210}\text{Po}$  in the lichen-reindeer-man food-chain. Lichens, which do not have a root system,

TABLE 22. MEASUREMENTS OF THE CONCENTRATION OF  $^{210}\text{Pb}$  AND  $^{210}\text{Po}$  IN THE LICHEN-REINDEER-MAN FOOD-CHAIN

<i>Link in chain and location of measurement</i>	$^{210}\text{Pb}$	$^{210}\text{Po}$	<i>Comments</i>	<i>Reference</i>
<i>Lichen</i>				
	(pCi kg <sup>-1</sup> dry weight)			
Canada		7 300		139
Finland, Lapland	7 900	7 300		180
Sweden	7 200	6 400		276
USSR, Murmansk	9 200			258
USA, Alaska, Bethel	5 800	5 800		35
<i>Reindeer or caribou</i>				
	(pCi kg <sup>-1</sup> fresh weight)			
<i>Bone</i>				
Finland, Inari	4 600	2 000		180
Sweden	5 800	3 700		276
USSR, Murmansk	1 500			258
USA, Alaska, Anaktuvuk Pass		5 000		35
<i>Meat</i>				
	(pCi kg <sup>-1</sup> )			
Canada	11	280		139
Finland, Lapland	6	160		276
Sweden	18	360		276
USSR	38	80		293
USA, Alaska, Anaktuvuk Pass	15	200		138
<i>Man</i>				
	(fCi g <sup>-1</sup> ash)			
<i>Bone</i>				
Finland, Inari	160	160	Levels in teeth	180
Sweden	500	370	Inferred from blood concentration	276
USSR, Nenetskii National Area	430	220		258, 267
USA, Alaska	300	220		36
<i>Soft tissues</i>				
	(pCi kg <sup>-1</sup> )			
<i>Blood</i>				
Finland	6.8	12	Concentrations measured in southern Finns are 2.7 for $^{210}\text{Pb}$ and 0.7 for $^{210}\text{Po}$	180
Sweden	M <sup>a</sup> 4.7 F 3.3	M 9.4 F 5.0	Corresponding levels in "normal" populations are about 2 pCi kg <sup>-1</sup>	276
<i>Placenta</i>				
Canada	2.5	29		139
Finland	1.9	36	Concentrations measured in southern Finns are 0.8 for $^{210}\text{Pb}$ and 2.9 for $^{210}\text{Po}$	180

<sup>a</sup>M = male, F = female.

derive their nutrition preferentially from the air. As they present a high sorption area, live for a long time (as long as 300 y), and eliminate  $^{210}\text{Pb}$  very slowly (effective half-time estimated to be  $7 \pm 2$  y), they concentrate  $^{210}\text{Pb}$  and  $^{210}\text{Po}$  to much higher levels than other

plants. Lichens also accumulate other long-lived natural radionuclides, such as  $^{226}\text{Ra}$  or  $^{228}\text{Th}$  (258), but because of their much lower concentration in surface air and rain water, the absolute concentrations reached by those radionuclides in lichens are also much lower.

134. As reindeer consume 3-4 kg of lichen per day (276, 292), their daily intake of  $^{210}\text{Pb}$  and  $^{210}\text{Po}$  is of the order of 10 000 pCi. The concentrations in reindeer bone and meat presented in table 22 clearly show the different biological behaviour of polonium and lead. Lead-210 concentrates in the skeleton, where it gives rise to  $^{210}\text{Po}$  through radioactive decay. Polonium-210 concentrates mainly in the soft tissues, where it is clearly in excess of its equilibrium value with  $^{210}\text{Pb}$ . It is worth mentioning that the  $^{210}\text{Po}$  concentration in reindeer meat varies seasonally by a factor of 4 (180), being lowest in early autumn because of the greater availability of forage other than lichens during the warm summer months.

135. The daily intakes of  $^{210}\text{Pb}$  and  $^{210}\text{Po}$  by the populations living on reindeer or caribou meat are given in table 20. Most of the estimates were inferred from the measured concentration in reindeer or caribou meat, using a daily rate of consumption of 0.2-0.5 kg. The  $^{210}\text{Pb}$  intake is not much higher than that of the populations of other areas, but the  $^{210}\text{Po}$  intake is about one order of magnitude higher, a typical value being  $100 \text{ pCi d}^{-1}$ .

(iii) *Distribution in man and absorbed doses*

136. Lead-210, bismuth-210 and polonium-210, being the last radionuclides of the  $^{226}\text{Ra}$  decay chain, would be present in the human body even in the absence of direct intake. However, under normal conditions, the decay of  $^{226}\text{Ra}$ ,  $^{222}\text{Rn}$  and their short-lived products in the body does not play a major role in the accumulation of  $^{210}\text{Pb}$  and  $^{210}\text{Po}$  in the body (133, 135). Only in occupational exposure, such as in uranium mining, is the role of the precursors important.

137. Lead is a bone seeker which is found incorporated in bone mineral, from where it seems to be eliminated by the process of long-term skeletal remodelling (144, 162, 208). About 70 per cent of the body content of  $^{210}\text{Pb}$  is found in the skeleton (162). According to Holtzman's study (135), in which 128 bone samples were examined for  $^{210}\text{Pb}$  content, the concentration in males is higher than in females. In both sexes, the level in cancellous bone was found to be 70 per cent higher than in compact bone. No clear correlation could be found in that study between the age of the subject and the  $^{210}\text{Pb}$  concentration in bone, but it is worth mentioning that stable lead concentrations increase with age (167, 308).

138. The  $^{210}\text{Pb}$  activity concentrations in bone ash presented in table 21 show that, in continental areas of the northern latitudes, a typical value could be  $0.15 \text{ pCi g}^{-1}$ , corresponding to a skeletal content of 400 pCi. In island areas the concentrations in human bone appear to be somewhat lower than in continental regions.

139. Assuming that the rate of elimination of  $^{210}\text{Pb}$  from bone is described by a single exponential, the total activity in the skeleton  $A$  due to both inhalation and ingestion may be estimated from the relationship

$$A = (T_e/0.693) (I_{\text{inh}}f_{\text{inh}} + I_{\text{ing}}f_{\text{ing}})$$

where  $I$  is the daily activity intake ( $I_{\text{inh}}$  from inhalation and  $I_{\text{ing}}$  from ingestion),  $f$  the fraction of the intake which is deposited in the skeleton, and  $T_e$  is the effective half-life of  $^{210}\text{Pb}$ , taken here to be 3300 d (135). In the case of ingestion, assuming a blood uptake from the gastro-intestinal tract of 0.08 and a fractional deposition in the skeleton from blood of 0.28, a daily intake of 3 pCi leads to a bone deposition of  $0.067 \text{ pCi d}^{-1}$  and to a contribution to the equilibrium skeletal activity of 320 pCi. With respect to inhalation, if it is assumed that one half of the activity is deposited in the respiratory tract and that one third of the activity deposited is absorbed into the blood and the remaining two thirds are subsequently ingested, a daily intake by inhalation of  $0.3 \text{ pCi d}^{-1}$  corresponds to a bone deposition of  $0.016 \text{ pCi d}^{-1}$  and a skeletal content of 76 pCi. The sum of the contributions from inhalation and ingestion to the skeletal content is thus estimated to be about 400 pCi.

140. Polonium, in contrast to all the other natural alpha emitters, is not a bone seeker but rather accumulates in soft tissues. Therefore, the greatest part of the  $^{210}\text{Po}$  bone activity arises from the decay of deposited  $^{210}\text{Pb}$  (131, 370). Average measured ratios of  $^{210}\text{Po}$  and  $^{210}\text{Pb}$  activity concentrations in bone range from 0.5 to 1.1 (35, 135, 180, 196, 246). A value of 0.8 is assumed to be representative for the purposes of this report. Using an average  $^{210}\text{Pb}$  activity concentration per unit mass of ash of  $0.15 \text{ pCi g}^{-1}$  and a  $^{210}\text{Po}/^{210}\text{Pb}$  ratio of 0.8, the  $^{210}\text{Po}$  concentration in bone ash would be  $0.12 \text{ pCi g}^{-1}$  for the populations living in continental areas in temperate regions of the northern hemisphere.

141. With respect to the soft tissues,  $^{210}\text{Pb}$  and  $^{210}\text{Po}$  are distributed relatively uniformly throughout the body. From measured concentrations the total amount of  $^{210}\text{Po}$  in soft tissues has been estimated to be 72 pCi by Kauranen and Miettinen (180), 160 pCi by Parfenov (267), and 250 pCi by Ladinskaya *et al.* (196), while the corresponding estimates for  $^{210}\text{Pb}$  were 60, 156, and 266 pCi, respectively. Although there is a factor of more than 3 between the extreme values regarding a given radionuclide, it is worth noting that in the three studies the  $^{210}\text{Po}/^{210}\text{Pb}$  activity ratio is found to be about 1. Assuming that 70 per cent of the whole-body content of  $^{210}\text{Pb}$  is in bone, the representative value of 400 pCi for the  $^{210}\text{Pb}$  skeletal activity corresponds to an activity of 170 pCi of  $^{210}\text{Pb}$  and a like amount of  $^{210}\text{Po}$  in the soft tissues.

142. Typical concentrations of  $^{210}\text{Pb}$  and  $^{210}\text{Po}$  in the gonads seem to be about  $6 \text{ pCi kg}^{-1}$  (19, 35, 196). In the lung, the concentrations in non-smokers are around  $3 \text{ pCi kg}^{-1}$  for  $^{210}\text{Po}$  and  $6 \text{ pCi kg}^{-1}$  for  $^{210}\text{Pb}$  (35, 139). In red bone marrow, Baratta and Ferri (19) reported  $^{210}\text{Po}$  concentrations of  $26 \text{ pCi kg}^{-1}$  in men and  $21 \text{ pCi kg}^{-1}$  in women, but a more recent study by Ladinskaya *et al.* (196) found a much lower value of  $3.8 \text{ pCi kg}^{-1}$  and a  $^{210}\text{Po}/^{210}\text{Pb}$  activity ratio of 0.8, which will be used in this Annex for the purpose of assessing doses.

143. It is interesting to estimate how much  $^{210}\text{Po}$  in soft tissues is due to the decay of  $^{210}\text{Pb}$  in soft tissues, to the elimination of  $^{210}\text{Po}$  from bone, and to the direct dietary intake of  $^{210}\text{Po}$ . Assuming a  $^{210}\text{Po}$  dietary



intake of 3 pCi d<sup>-1</sup>, a blood uptake of 0.35 (196, 294) and an effective half-life in the body of 50 d (309), the contribution to the <sup>210</sup>Po inventory in soft tissues from the <sup>210</sup>Po dietary intake would be about 75 pCi. As inhalation of <sup>210</sup>Po, at least for non-smokers, does not lead to a substantial activity in the body, the rest of the <sup>210</sup>Po inventory would result from the decay of <sup>210</sup>Pb. An average <sup>210</sup>Po/<sup>210</sup>Pb ratio of 0.8 in bone yields a contribution of about 30 pCi from the elimination of <sup>210</sup>Pb in bone. Finally, the decay of <sup>210</sup>Pb in soft tissues leads to an amount of 85 pCi if it is assumed that the <sup>210</sup>Po/<sup>210</sup>Pb ratio at equilibrium in soft tissues, in the absence of any intake of <sup>210</sup>Po, is 0.5 (162). The <sup>210</sup>Po inventory in soft tissues obtained in this way is 190 pCi. Considering the uncertainties attached to the values of the parameters used, this result is in good agreement with the value of 170 pCi given in the preceding paragraphs.

144. The <sup>210</sup>Po activity in man being about 500 pCi (320 pCi in bone and 170 pCi in soft tissues) and the contribution to that activity due to the <sup>210</sup>Po dietary intake being only about 75 pCi, it is clear that the <sup>210</sup>Po activity in man depends little on the amount present in diet. It is determined mainly by the concentration of <sup>210</sup>Pb in the body, since approximately 85 per cent of

the <sup>210</sup>Po body content arises from the decay of <sup>210</sup>Pb. This view has also been expressed by Holtzman (136) and by Parfenov (267).

145. Although in most of the soft tissues, the <sup>210</sup>Po/<sup>210</sup>Pb activity concentration ratio is about 1, it is clearly greater than 1 in a few organs such as the liver and kidney. The excess <sup>210</sup>Po is probably taken up directly from food and would be partly attributable to a higher rate of incorporation for <sup>210</sup>Po than for <sup>210</sup>Pb in those organs (162). It has been suggested (80, 131) that the distribution of polonium might be similar to that of sulphur, which might be replaced by polonium in several chemical compounds of the body.

146. *Absorbed doses.* The absorbed doses from the <sup>210</sup>Pb chain depend mainly on the highly energetic alpha particles of <sup>210</sup>Po, the contribution from the beta emissions of <sup>210</sup>Pb and <sup>210</sup>Bi being at most 30 per cent of the dose from <sup>210</sup>Po. For non-smokers, the annual absorbed doses in the lungs and gonads are about 0.3 and 0.6 mrad, respectively; those in tissues in bone, calculated using the dosimetric factors presented in figures IX and X, are found to be 3 mrad for bone lining cells and 0.7 mrad for the red marrow (table 23). The annual average whole-body dose is about 0.7 mrad.

TABLE 23. ESTIMATED TISSUE CONCENTRATION AND ANNUAL ABSORBED DOSE DUE TO <sup>210</sup>Pb, <sup>210</sup>Bi AND <sup>210</sup>Po IN AREAS OF NORMAL AND HIGH DIETARY INTAKE

Area and radionuclide	Average tissue concentration (pCi kg <sup>-1</sup> )				Annual tissue absorbed dose (mrad)			
	Gonads	Lung	Can-cellous bone	Red bone marrow	Gonads	Lung	Red bone marrow	Bone lining cells
<i>Areas of normal dietary intake</i>								
Non-smokers								
<sup>210</sup> Pb	6	6	100	5	6 10 <sup>-4</sup>	6 10 <sup>-4</sup>	5 10 <sup>-4</sup>	8 10 <sup>-4</sup>
<sup>210</sup> Bi	6	6	100	5	4 10 <sup>-2</sup>	4 10 <sup>-2</sup>	2 10 <sup>-1</sup>	4 10 <sup>-1</sup>
<sup>210</sup> Po	6	3	80	4	6 10 <sup>-1</sup>	3 10 <sup>-1</sup>	7 10 <sup>-1</sup>	3
Smokers								
<sup>210</sup> Pb	8	9	130	6	8 10 <sup>-4</sup>	8 10 <sup>-4</sup>	6 10 <sup>-4</sup>	1 10 <sup>-3</sup>
<sup>210</sup> Bi	8	9	130	6	6 10 <sup>-2</sup>	7 10 <sup>-2</sup>	3 10 <sup>-1</sup>	6 10 <sup>-1</sup>
<sup>210</sup> Po	8	9	100	5	8 10 <sup>-1</sup>	9 10 <sup>-1</sup>	9 10 <sup>-1</sup>	4
<i>Areas of high dietary intake</i>								
Reindeer or caribou eaters								
<sup>210</sup> Pb	15	15	250	12	1.4 10 <sup>-3</sup>	1.4 10 <sup>-3</sup>	1.3 10 <sup>-3</sup>	1.9 10 <sup>-3</sup>
<sup>210</sup> Bi	15	15	250	12	1 10 <sup>-1</sup>	1 10 <sup>-1</sup>	6 10 <sup>-1</sup>	1
<sup>210</sup> Po	72	36	200	48	7	4	5	10

147. *Differences between smokers and non-smokers.* The additional intake due to smoking leads to increased concentrations of <sup>210</sup>Pb and <sup>210</sup>Po in organs and tissues. As expected, it is in the lung that the increase is most clearly marked. The concentrations in that organ exceed on the average the levels found in non-smokers by factors of about 1.5 for <sup>210</sup>Pb and 3 for <sup>210</sup>Po (35, 131, 267, 289). However, in spite of the fact that the daily intake from smoking is at least 20 times the natural intake from atmospheric air, the ratio of the amounts contained in the lungs of smokers and non-smokers is relatively small. This strongly suggests that <sup>210</sup>Po inhaled during smoking is rapidly removed from the lungs (267).

148. Data on the degree of non-uniformity of <sup>210</sup>Po in the individual tissues of the lungs of smokers are contradictory. One school of thought holds that <sup>210</sup>Po can be concentrated in the bronchial epithelium, particularly at points of bifurcation (207, 287), whereas the other considers that the levels in the bronchial epithelium do not exceed those in the alveolar region (131, 289). As a result, the estimates of the annual absorbed dose in the bronchial epithelium as compiled in reference (267), range from 4 to 3000 mrad.

149. The increase due to smoking is less clear in organs other than lung. Parfenov (267), summarizing the

relevant published data, shows that on the average the  $^{210}\text{Po}$  concentrations in the soft tissues of cigarette smokers is higher than the corresponding concentrations in non-smokers by about 30 per cent, but points out that a number of studies have failed to reveal a statistically significant difference (19, 35, 206).

150. An estimate of the increase of the  $^{210}\text{Pb}$  and  $^{210}\text{Po}$  concentration in smokers can be made from the intake and metabolism information presented above. An additional daily intake of 1.6 pCi of  $^{210}\text{Po}$  from smoking would yield at equilibrium an additional content of 32 pCi in the soft tissues, which would increase the average value by about 20 per cent. A more substantial increase would arise from the additional daily intake of 1.2 pCi of  $^{210}\text{Pb}$ , which would result in an additional bone content of 300 pCi at equilibrium and in an excess of 75 per cent above the average value. It should be pointed out, however, that, under conditions of steady smoking, a few months are sufficient for  $^{210}\text{Po}$  to approach its equilibrium value in the soft tissues, while tens of years would be required for  $^{210}\text{Pb}$ . The full effect of cigarette smoking on the body contents of  $^{210}\text{Pb}$  and  $^{210}\text{Po}$  in smokers can thus only be experienced after a long period of steady smoking. Shorter periods would cause the excess to lie in the range from 20 to 95 per cent, which is in agreement with the average value of 30 per cent derived from experimental studies and used here to calculate the doses in smokers (table 23).

151. *Reindeer or caribou eaters.* Measurements carried out on the blood, placenta and bone tissue of inhabitants of the northern regions who consume caribou or reindeer meat regularly show levels higher than those in the populations of the temperate latitudes (table 22). The increase is by a factor of about 2 for  $^{210}\text{Pb}$  in all tissues and a factor of about 10 for  $^{210}\text{Po}$  in the placenta, which is taken to be representative of all the soft tissues. On the basis of their own measurements, Kauranen and Miettinen (180) estimated the factors of increase to be 2.5 for  $^{210}\text{Pb}$  and 12 for  $^{210}\text{Po}$ . The use of these values leads to the doses indicated in table 23. It is interesting to note that the factors are estimated to be 1.6 for  $^{210}\text{Pb}$  and 14 for  $^{210}\text{Po}$  when calculated from estimated dietary intakes of 6 pCi d<sup>-1</sup> for  $^{210}\text{Pb}$  and 100 pCi d<sup>-1</sup> for  $^{210}\text{Po}$ , using the values of the metabolism parameter indicated in previous paragraphs.

## C. RADON-222, RADON-220 AND THEIR SHORT-LIVED DECAY PRODUCTS

### 1. Inhalation

152. In the decay chains of  $^{238}\text{U}$  and  $^{232}\text{Th}$ ,  $^{222}\text{Rn}$  (radon) and  $^{220}\text{Rn}$  (thoron) are the only isotopes of noble gases. This property allows them to emanate from the ground and to be present in the atmosphere in much larger concentrations than their precursors. Exposure to the inhaled short-lived decay products of radon and thoron constitutes the main natural irradiation of the various parts of the human respiratory tract. The major part is normally caused by radon daughters rather than by thoron daughters, and by indoor exposure. Although outdoor exposure is normally smaller, the occurrence of

radon and thoron and their daughters outdoors has been extensively studied since they are also of interest as tracer elements in meteorological studies. The following paragraphs summarize the data of interest on levels and doses and the factors which explain these levels and doses.

### (a) Exposure-dose relationship

153. Radon and thoron emanate from soil, water, building materials etc. and become dispersed in the air in the gaseous phase. The decay products, radon and thoron daughters, are produced as free atoms, usually as positive ions since the alpha particles carry electrons away from the atom during the decay process. These ions tend to form clusters very rapidly with water, oxygen or other trace gases. Soon afterwards, in a matter of seconds to minutes, these clusters tend to attach themselves to aerosol particles. The dimensions of the aerosol particles being much larger than those of the clusters, the aerosols inhaled do not deposit in the same region of the respiratory tract as the clusters. It is thus important to make a distinction between the fraction of the activity of the short-lived decay products of radon carried by clusters, which is called the unattached fraction, and the fraction fixed on aerosol particles, called the attached fraction.

154. The concentration of radon and thoron daughters in air may be expressed in terms of activity concentration (unit: pCi l<sup>-1</sup>), or in terms of potential alpha-energy concentration, which is defined as the total alpha energy released per unit volume by the short-lived daughters in their decay (unit: MeV l<sup>-1</sup>). A unit which has been used in mines to describe the radon decay-product activities in air in terms of potential alpha energy is the working level (WL). It is defined as any combination of short-lived radon daughters (through  $^{214}\text{Po}$ ) per litre of air that will result in the emission of 1.3 10<sup>5</sup> MeV of alpha energy. An activity concentration of 100 pCi l<sup>-1</sup> of  $^{222}\text{Rn}$ , in equilibrium with its daughters, corresponds to a potential alpha-energy concentration of 1 WL. The WL unit could also be used for thoron daughters. In this case, 1.3 10<sup>5</sup> MeV of alpha energy (1 WL) is released by the thoron daughters in equilibrium with 7.5 pCi of thoron per litre. Table 24 shows the potential alpha-energy concentrations of radon and thoron daughters (157).

155. Radon and thoron daughters in air are very seldom in equilibrium with radon and thoron, respectively. The equilibrium factor  $F$  is defined as the ratio of the total potential alpha energy of the given daughter concentrations to the total potential alpha energy of the daughters if they are in equilibrium with radon and thoron, respectively.

156. It follows from the definition of the WL that the equilibrium factor  $F$  for radon or thoron (Tn) can be calculated as

$$F_{\text{Rn}} = a \langle a \rangle_{\text{Rn}} / \langle \text{Rn} \rangle; F_{\text{Tn}} = b \langle a \rangle_{\text{Tn}} / \langle \text{Tn} \rangle$$

where  $\langle a \rangle_{\text{Rn}}$  and  $\langle a \rangle_{\text{Tn}}$  are the potential alpha-energy concentrations, in WL, of Rn daughters and Tn daughters, respectively;  $\langle \text{Rn} \rangle$  is the activity concentration, in pCi l<sup>-1</sup>, of radon;  $\langle \text{Tn} \rangle$  is the activity concentration, in pCi l<sup>-1</sup>, of thoron; and  $a$  and  $b$  are constants ( $a = 100$  pCi/WL,  $b = 7.5$  pCi/WL).

TABLE 24. POTENTIAL ALPHA ENERGY OF THE SHORT-LIVED DECAY PRODUCTS OF  $^{222}\text{Rn}$  AND  $^{220}\text{Rn}$ 

Radio-nuclide	Radio-active half-life	Number of atoms per picocurie	Potential alpha energy (MeV)		Conversion factor	
			Per atom	Per picocurie	$\text{MeV l}^{-1}$ $\text{pCi l}^{-1}$	$\text{WL}$ $\text{pCi l}^{-1}$
$^{218}\text{Po}$ (Ra A)	3.05 min	9.77	13.68	134	134	0.00103
$^{214}\text{Pb}$ (Ra B)	26.8 min	85.3	7.68	659	659	0.00507
$^{214}\text{Bi}$ (Ra C)	19.7 min	63.1	7.68	485	485	0.00373
$^{214}\text{Po}$ (Ra C')	$1.6 \cdot 10^{-4}$ s	$10^{-5}$	7.68	$7.68 \cdot 10^{-5}$	$7.68 \cdot 10^{-5}$	$6 \cdot 10^{-10}$
$^{216}\text{Po}$ (Th A)	0.158 s	0.00844	14.57	0.123	0.123	$9.5 \cdot 10^{-7}$
$^{212}\text{Pb}$ (Th B)	10.6 h	2040	7.79	15 900	15 900	0.1223
$^{212}\text{Bi}$ (Th C)	60.5 min	194	7.79	1 510	1 510	0.0116
$^{212}\text{Po}$ (Th C')	$3 \cdot 10^{-7}$ s	$1.6 \cdot 10^{-8}$	8.78	$1.4 \cdot 10^{-7}$	$1.4 \cdot 10^{-7}$	$1 \cdot 10^{-12}$

157. If in a given atmosphere radon (or thoron) is not in equilibrium with its daughters and the concentration of radon (or thoron) is  $C$ , the product  $CF$  corresponds to a concentration of radon (or thoron) for which the daughters in equilibrium would have the same potential alpha-energy concentration as the actual atmosphere of interest. The product  $CF$  will be referred to in this report as the equilibrium equivalent concentration of radon (or thoron).

158. For the purpose of this report, exposure to radon and its daughters is defined as the integral of the activity concentration in air over the exposure time. The unit, working level month (WLM), is often used in connection with radon in mines, and means an exposure during 170 working hours in a radon daughter concentration of 1 WL. One WLM corresponds to a time-integral of the equilibrium equivalent concentration of  $1.7 \cdot 10^4 \text{ pCi h l}^{-1}$  for occupational exposure in mines. For thoron daughters, 1 WLM corresponds to an exposure during 170 working hours in a thoron daughter concentration of 1 WL, which is equivalent to a time-integral of the equilibrium equivalent concentration of  $1.3 \cdot 10^3 \text{ pCi h l}^{-1}$  for occupational exposure in mines.

159. The deposition in the respiratory system of radon and thoron daughters attached to aerosol particles depends on, among other things, the size distribution of the radioactive aerosol, this size distribution being closely related to the size distribution of the inactive aerosol present. In both free air and room air this size distribution is relatively constant. Figure XV shows the typical size distribution of the natural aerosols carrying short-lived radon daughters (146, 242a). When these aerosols are inhaled, up to 60 per cent of the particles are deposited in different regions of the respiratory system. The attached radon and thoron daughters are mainly deposited in the pulmonary region. The unattached daughters are deposited in the upper respiratory tract on account of their high diffusion coefficient. Because of the efficient deposition of unattached daughters in the respiratory tract, experimentally proved with a model by Chamberlain and Dyson (55), the unattached fraction has since been given great attention. However, the fraction of unattached daughters in air is often small and a major proportion (up to 60-70 per cent) of the unattached daughters in the inhaled air is removed by nasal deposition (93).

160. In indoor air the degree of equilibrium between radon (or thoron) and its daughters and the fraction of

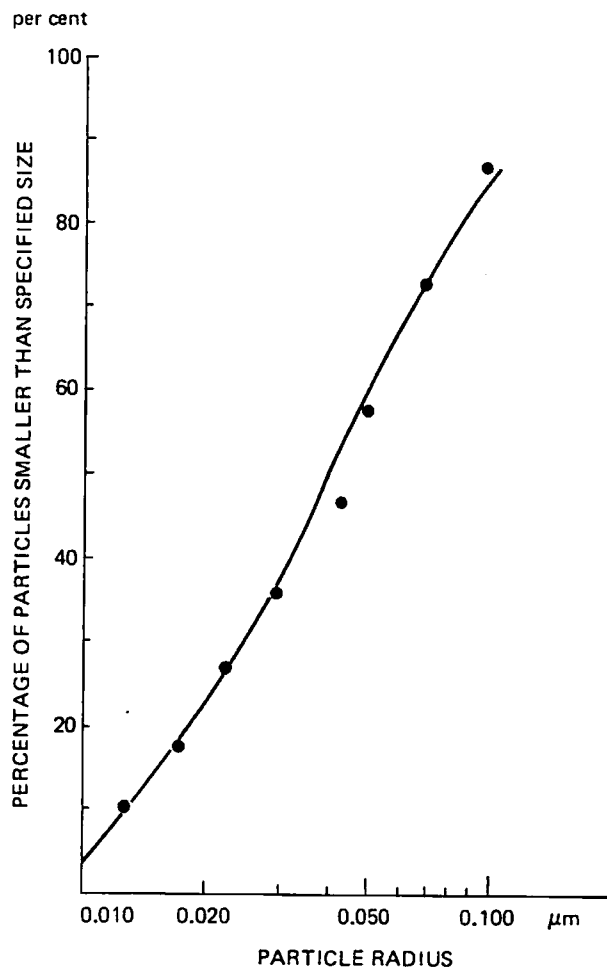


Figure XV. Size distribution of the natural carriers of  $^{214}\text{Pb}$  and  $^{214}\text{Bi}$  (149, 242a)

unattached daughters are affected by the ventilation rate (126), by the deposition on walls (371), and by attachment to aerosols. The relative influence of these factors has been considered on a theoretical basis by Jacobi (157). It was found that the fraction of unattached daughters increases markedly with decreasing aerosol concentration and decreasing residence time of the air. Since enhanced ventilation reduces the residence time of the air and also usually the aerosol concentration, the effect on the fraction of unattached daughters is considerable. However, the net effect of increased ventilation is a reduction of dose due to a large decrease of the potential alpha-energy concentration. In

a poorly ventilated room with a low aerosol concentration, wall deposition of unattached daughters plays an important role in reducing their concentration in air.

161. Inhalation of radon and thoron daughters results in an inhomogeneous internal irradiation of the respiratory tract, with the dose absorbed primarily in the bronchial region. The factors which influence the deposition and fate of inhaled activity and the doses, apart from the physical characteristics of the radioactive aerosol, are:

Way of breathing, i.e., mouth breathing or nose breathing and the rate and the depth of respiration

Geometrical parameters of different regions of the respiratory system

Translocation and clearance of deposited activity

Several models have been used to calculate the resultant doses in the respiratory system, assuming different characteristics of the radioactive aerosol, including the fraction of unattached activity.

162. A recent study was made by Harley and Pasternack (123), who performed experimental stopping-power measurements with tissue equivalent material using radon daughters. In the calculation of doses it was assumed, on the basis of the experimental results of Kirichenko *et al.* (184), that the activity was homogeneously distributed in the mucous layer. The lung geometry used in the calculations was based on the Weibel lung model (360), and the fractional retention was tabulated by applying the Gormley-Kennedy equations (104).

163. The removal of unattached daughters in the nose was assumed to be 60 per cent (93) and of the attached

daughters, 1.3 per cent. Taking into account the deposition and translocation rates, the doses in different regions of the bronchial tree were calculated. With an aerosol size distribution with an activity median aerodynamic diameter (AMAD) of  $0.3 \mu\text{m}$ , the highest regional activities were found in the segmental bronchioles (tertiary bronchi generation 4 of the Weibel model). The dose-to-exposure quotient was estimated for different depths of the airway wall. In basal cell nuclei at a depth of  $22 \mu\text{m}$ , it was found to be  $0.2 \text{ rad (WLM)}^{-1}$  for a breathing rate of  $15 \text{ l min}^{-1}$ , an equilibrium factor  $F = 1$ , and 4 per cent of unattached  $^{218}\text{Po}$  atoms. However, if these parameters change, so also does the relationship between the dose and the exposure. For example with  $F = 0.3$  and 4 per cent unattached  $^{218}\text{Po}$ , the value is  $0.4 \text{ rad (WLM)}^{-1}$ .

164. Corresponding calculations concerning thoron daughters have been made (124). The highest regional activities were found in the terminal bronchioles (generation 10 of the Weibel model). For that region, and for an AMAD of  $0.15 \mu\text{m}$  and 2.2 per cent unattached  $^{212}\text{Pb}$ , a factor of  $0.7 \text{ rad (WLM)}^{-1}$  may be calculated from Harley's data (124). The contribution from the unattached activity is about 20 per cent.

165. Another recent study of doses from inhaled radon and thoron daughters has been made by Jacobi (158, 159) as a continuation of his studies on the characteristics of the inhaled aerosol, activity and potential alpha-energy of radon and thoron daughters. He calculated the doses in the tracheo-bronchial region (T-B) and in the pulmonary region (P) assuming the masses to be 45 g and 955 g, respectively. The doses were derived as a function of the unattached fraction  $f_p$  of the total potential alpha energy in the inhaled air. The mean dose from alpha particles is shown in table 25 for a breathing rate of  $20 \text{ l min}^{-1}$ .

TABLE 25. MEAN DOSE FROM ALPHA PARTICLES IN THE TRACHEO-BRONCHIAL AND PULMONARY REGIONS AS A FUNCTION OF THE UNATTACHED FRACTION  $f_p$  OF THE POTENTIAL ALPHA ENERGY IN AIR

	Nose breathing	
	Dose-to-exposure quotient	
	Dose to time-integral of potential alpha energy (rad per WLM)	Dose to time-integral of equilibrium equivalent concentration (rad per pCi h l <sup>-1</sup> )
<i>Tracheobronchial region</i>		
Radon daughters	0.31 (1 + 6 $f_p$ )	$1.9 \cdot 10^{-5}$ (1 + 6 $f_p$ )
Thoron daughters	0.012 (1 + 5 $f_p$ )	$10^{-5}$ (1 + 5 $f_p$ )
<i>Pulmonary region</i>		
Radon daughters	0.16 (1 - $f_p$ )	$10^{-5}$ (1 - $f_p$ )
Thoron daughters	0.087 (1 - $f_p$ )	$7.6 \cdot 10^{-5}$ (1 - $f_p$ )

166. It was concluded that the mean dose-to-exposure quotient in the T-B region increases with increasing ventilation rate and decreases with increasing aerosol concentration. For the P region the variation is reversed. As seen in table 25, the mean dose-to-exposure quotient for thoron daughters is higher in the P region than in the T-B region with low values of  $f_p$ . A large fraction of the alpha energy deposited in the T-B region is deposited in

the mucous sheet, ciliated cells and goblet cells on the bronchial epithelium. The dose in the underlying basal cells, where bronchogenic lung cancer is assumed to originate, was derived from different lung models. If the fraction  $f_p$  of the total potential alpha energy contributed by unattached radon daughters varied between 0.02 and 0.1, the factor estimated from different models covered a range from 0.2 to 10 rad

(WLM)<sup>-1</sup>, assuming nose breathing at a rate of 20 l min<sup>-1</sup>.

167. The lung cancer among uranium miners predominantly appearing in the area of the large bronchi (217) presumably originates in the basal cells in the basement membrane of the upper bronchial epithelium. It seems reasonable to regard the doses in these cells as the most relevant in the discussion of the correlation between dose and effect. However, there is still incomplete knowledge of the distribution of dose and the genesis of cancer in the basal cells and it is not yet

considered appropriate to use only the dose in the basal cells as the basis for the risk assessments. As discussed in Annex G, most risk assessments are based on the direct relationship between lung cancer incidence among uranium miners and exposure as expressed in WLM. In addition, for purposes of comparison with other irradiation conditions of the lung, the mean dose in the lung is also calculated in this report.

168. The distribution of the values of the dose-to-exposure quotient for radon daughters, derived from different models is shown in table 26 (171). From the

TABLE 26. DOSE-TO-EXPOSURE QUOTIENT FOR RADON DAUGHTERS  
Segmental bronchial epithelium

Relative activity concentration Rn : Ra A : Ra B : Ra C	Equilibrium factor F	Exposure conditions	Lung model	Dose-to-exposure quotient (rad per WLM)	Reference
10 : 10 : 10 : 10 4% free Ra A	1	0.3- $\mu$ m particles	Weibel (A), 15 l min <sup>-1</sup>	0.2	123
10 : 6 : 3 : 2 4% free Ra A	0.3	0.3- $\mu$ m particles	Weibel (A), 15 l min <sup>-1</sup>	0.4	123
10 : 9 : 6 : 4	0.6	0.3- $\mu$ m particles	Landahl	1.7	123
Nonequilibrium; little free Ra A	< 1			0.5-1	247
Nonequilibrium; 1-2% free Ra A	< 1	Clean air	Revised ICRP	0.3-1	158
10 : 10 : 6 : 4	0.6	1 h <sup>-1</sup> air change; 0.09- $\mu$ m particles, 10 <sup>4</sup> cm <sup>-3</sup>	Findeisen-Landahl, 14 l min <sup>-1</sup>	1.7	156
10 : 10 : 10 : 10	1	0.09- $\mu$ m particles	Findeisen-Landahl, 14 l min <sup>-1</sup>	2.7	156
10 : 9 : 6 : 4	0.6	0.3- $\mu$ m particles	Landahl, 15 l min <sup>-1</sup> , mouth breathing	2.0	217 8
10 : 9 : 6 : 4 8.5% free Ra A	0.6	0.3- $\mu$ m particles	Nose breathing	1.1	8
10 : 9 : 5 : 3.5	0.5	Adequately ventilated room	Weibel, 15 l min <sup>-1</sup> , mouth breathing	1.7-12	120
10 : 9 : 6 : 4	0.6	0.1- $\mu$ m particles	15 l min <sup>-1</sup>	2.2	49

calculations described above, it is believed (159) that in the case of mining conditions ( $f_p < 0.1$ ) the alpha dose in the basal cell layer of the critical bronchial region lies at the lower end of the range of 0.2-10 rad (WLM)<sup>-1</sup> and that a value of 1 rad (WLM)<sup>-1</sup> could be used in the assessments of dose. One rad per WLM corresponds to 60  $\mu$ rad per pCi h l<sup>-1</sup> for occupational exposure in mines. In the case of exposure in houses and outdoor air, taking into account the lower mean breathing rate, the conversion factor would be 45  $\mu$ rad per pCi h l<sup>-1</sup>. However, it is recognized that such important parameters as the size distribution of the aerosols carrying the short-lived radon daughters, the way of breathing and the rate of ventilation might differ from what is found in mining conditions. With regard to the mean dose in the lung, from the data in table 25 a mean value of 0.2 rad (WLM)<sup>-1</sup> can be derived, corresponding to dose-to-exposure quotients of 9  $\mu$ rad per pCi h l<sup>-1</sup> in houses and outdoor air and 12  $\mu$ rad per pCi h l<sup>-1</sup> under occupational conditions.

169. In the case of thoron daughters, the highest doses occur in the terminal broncholi and the alveolar region.

It seems reasonable therefore to estimate only the mean lung dose for the purpose of this report. From the data in table 25, a value of 0.1 rad (WLM)<sup>-1</sup> can be derived, corresponding to 60  $\mu$ rad per pCi h l<sup>-1</sup> for exposure outdoors and in houses.

(b) Exposure outdoors

(i) Sources

170. Radon and thoron in the atmosphere originate mainly from emanation from the soil. Wilkening *et al.* (366) reviewed the results of about a thousand measurements of the <sup>222</sup>Rn emanation rate from soil and obtained an overall mean value of 0.42 pCi m<sup>-2</sup> s<sup>-1</sup>, with a range from 6 10<sup>-3</sup> to 1.4 pCi m<sup>-2</sup> s<sup>-1</sup>. Their world-wide estimate for the total <sup>222</sup>Rn emanation rate from the land areas of the globe is about 50 Ci s<sup>-1</sup>. The contribution from the oceans is one to two orders of magnitude smaller (122, 386), the other sources are negligibly small. Even though the concentrations of <sup>238</sup>U and <sup>232</sup>Th in the soil are about the same, the emanation rate of thoron in terms of activity is about a

hundred times higher than that of radon because of its higher decay constant (33, 122).

171. The equilibrium activity of radon in the atmosphere is estimated to be  $2.5 \cdot 10^7$  Ci (366), and the average surface air concentration,  $0.07 \text{ pCi l}^{-1}$  (122). The total inventory of thoron in the atmosphere is much less because of the short half-life of thoron. However, in the first few metres above ground level, the thoron concentrations are of the same order of magnitude as those of radon.

172. The only significant sources of radon and thoron daughters in the atmosphere are the radon and thoron in the air. The concentration of the daughter products depends on the concentration of radon and thoron, the height above earth and the meteorological conditions. Because of wash-out effects in connection with precipitation and deposition, the concentration of radon daughters is often lower than that of radon and the concentration of thoron daughters is much lower than that of thoron near the ground.

(ii) *Emanation from the soil*

173. The emanation rate of radon is influenced by the condition of the soil, its porosity, moisture content and temperature (77, 229, 285). The emanation is reduced by snow cover, increasing atmospheric pressure, and heavy rainfall (193, 229, 338). Light rainfall does not affect the emanation since it only moistens a thin surface layer of soil. Diurnal variations of the emanation, within a factor of 2, may occur with maxima at night and minima during the afternoon (310). The variations are influenced by two opposing factors. Temperature differences in the soil during the night cause convective flow in the top layer leading to an increased nocturnal emanation. On the other hand, the greater turbulent mixing in the atmosphere in daytime enhances the daytime emanation and the diurnal fluctuations are smoothed out (229, 310). The seasonal variations of the emanation rate depend on the climatic conditions. Where there is no snow and temperatures are normally above  $0^\circ\text{C}$  all year, only small seasonal variations have been found (229), probably because of the relatively constant moisture content of the deeper soil levels.

174. Because of the very short radioactive half-life of thoron (55s), the emanation of thoron is more dependent on the soil conditions and on meteorological factors than is that of radon. The effective emanating soil thickness is of the order of a few centimetres. The emanation decreases rapidly when the moisture increases. The thoron emanation in summer seems to be about twice that in winter mainly because of higher moisture in the soil in the winter than in the summer. When the soil surface is warmer than the air, the emanation of thoron increases because of convection. This explains the diurnal variations of the emanation of thoron on dry summer days with maxima at sunset and at night and minima at sunrise and early in the day. The variations have been found to be within 30 per cent of the mean. The influence of several other factors on the emanation rate of thoron have been reported in the literature (75, 108, 220, 229, 331).

(iii) *Variations in air concentration*

175. The concentration of radon and thoron in the air depend on their emanation rate from the soil, meteorological factors, geographical factors and the height of observation. The vertical distribution of radon and its daughters has been studied by several investigators (10, 34, 44, 183, 198, 238, 364, 365). Normally, the radon concentration decreases with increasing altitude, but there are different profiles of radon concentration at different locations and times. The reported values are in the range  $0.1\text{-}0.01 \text{ pCi l}^{-1}$  from about 0.1 km above ground to an altitude of 2-3 km; above this height the concentration is less than  $0.01 \text{ pCi l}^{-1}$ . The results of measurements of the vertical distribution of radon in Illinois (United States) are shown in figure XVI (44). Figure XVII shows a typical

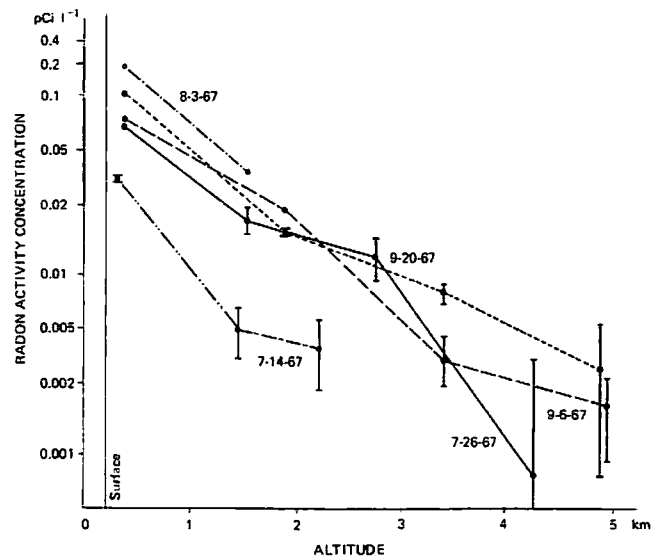


Figure XVI. Variation of radon concentration with altitude (44)

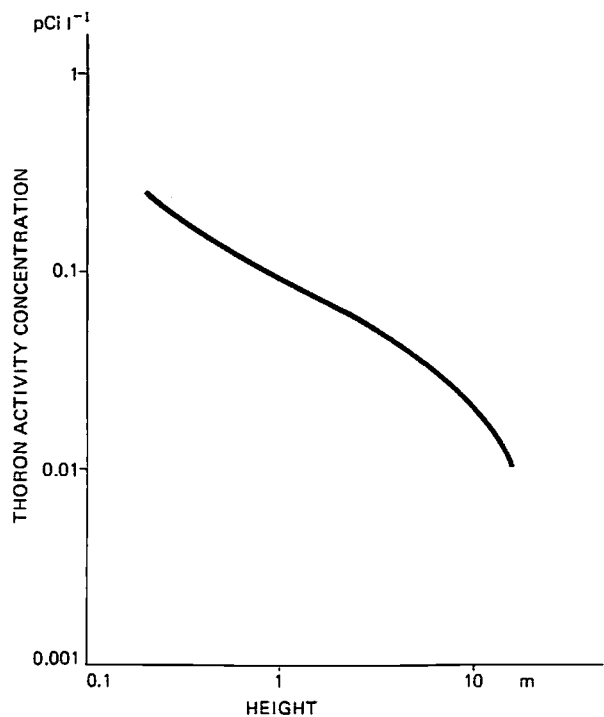


Figure XVII. Vertical profile of thoron in the atmosphere for wind speeds ranging from 4 to  $12 \text{ m s}^{-1}$  (75)

vertical profile of thoron below a height of 10 m for wind speeds ranging from 4 to 12 m s<sup>-1</sup> (75). The vertical distributions of radon and thoron close to the ground are also shown in figures XVIII and XIX which

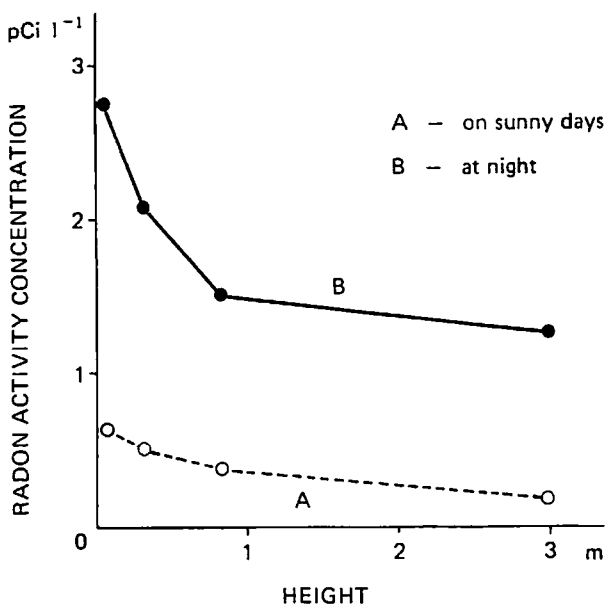


Figure XVIII. Vertical distribution of radon concentration

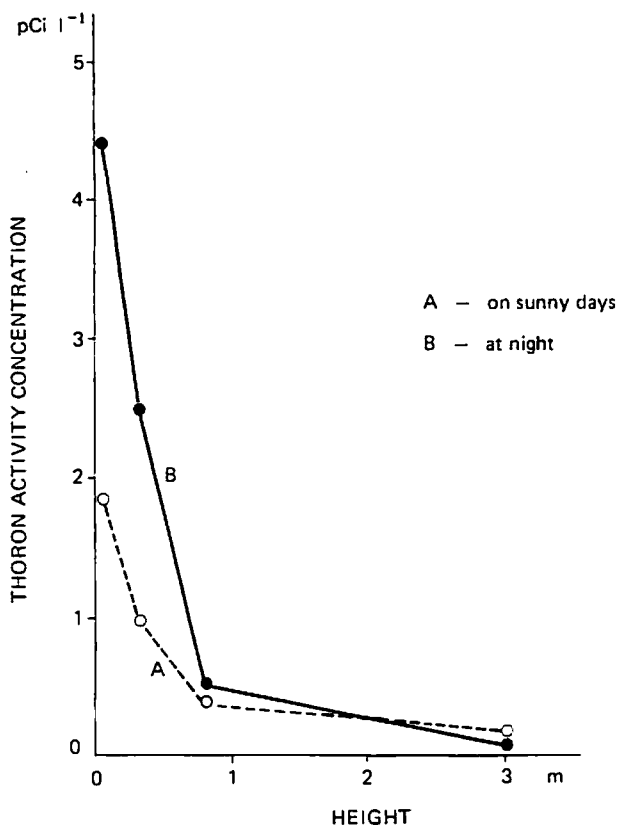


Figure XIX. Vertical distribution of thoron concentration

illustrate the influence of turbulent transfer on the radon and thoron profiles. The greater turbulence in the daytime causes smaller gradients and smaller absolute levels of radon and thoron than at night. At 1 m and above, the concentrations of thoron are about the same night and day.

176. The diurnal and seasonal variations of radon and thoron at ground level have been studied by several investigators (37, 141, 154, 155, 220, 310, 317). Eddy diffusion is the mechanism by which radon and thoron and their daughter products are transferred upward from ground level. The diurnal variation of the diffusion coefficient may be two orders of magnitude (298). The corresponding diurnal variation of radon is normally less, within one order of magnitude. As a rule, a maximum occurs towards the end of the night, and a minimum in the afternoon.

177. The seasonal variation of radon concentration depends mainly on the seasonal variation of turbulence. A maximum value of the radon concentration at ground level is reported to occur in the autumn and early winter, corresponding to a minimum in turbulent transfer. The minimum occurs in the spring. The local seasonal variations are normally less than a factor of five. The concentration of thoron in ground-level air is of the same order of magnitude as that of radon.

178. As the emanation rates of radon and thoron are much smaller over sea than over land, the concentrations of radon and thoron in ground-level air depend on the wind direction and on geographical factors. The concentration of radon at ground level is of the order of 0.1 pCi l<sup>-1</sup> in continental air, 0.01 pCi l<sup>-1</sup> in coastal areas and islands, and of the order of 0.001 pCi l<sup>-1</sup> in oceans and arctic areas (347). In coastal areas, the diurnal variation is increased by the much smaller radon concentration during the day under sea-breeze conditions than at night with offshore winds. Inland, far away from the coast, there seems to be no correlation between radon concentration and wind direction (141). On the other hand, air which has passed over land can be identified thousands of kilometres from the coast at sea, where the emanation rates are very low (286). The concentrations of radon and thoron are reported to be very dependent on wind speed and temperature stratification (155). This correlation is probably caused by the close connection between wind speed and the intensity of turbulent transfer (141, 155). Maximum values of the radon and thoron concentrations occur during light-wind conditions, but the relation between the concentration of radon and thoron and the wind speed seems to be greatly affected by the stability of the atmosphere (146).

#### (iv) Levels and doses

179. As discussed in previous paragraphs, there are variations of the radon and thoron concentrations in air depending on local conditions. Similar variations are found for the daughters of radon and thoron, the variation being enhanced by wash-out and deposition effects. It is therefore very difficult to estimate representative values for the concentration of radon and thoron daughters in air, unless long-duration measurements are made. To estimate the resultant doses, it is also important to know the characteristics of the aerosols inhaled, and also the proportion of time spent out of doors. This proportion varies for different people depending on season, country, age, habits and type of work. For the purpose of this report it will be assumed that 20 per cent of the time is spent out of doors (4.5 h per day).

180. The equilibrium factor  $F$  for radon has been considered by several authors directly or indirectly. By comparing the activities of  $^{214}\text{Pb}$  and  $^{214}\text{Bi}$  and radon in the summer, autumn and winter at a height of 1 m above the ground, it was concluded that the deviation from equilibrium was less during the winter than in the autumn or summer (310). In another study (376) in Boston (United States) the concentrations of  $^{218}\text{Po}$ ,  $^{214}\text{Pb}$  and  $^{214}\text{Bi}$  were measured. If  $^{218}\text{Po}$  is assumed to be in equilibrium with radon, the values of  $F$  vary between about 0.6 and 0.9 with an average of 0.8. Measurements in France in March 1970 showed that the ratio between  $^{214}\text{Pb}$  and radon varied between about 0.6 and 0.7 at 1 m above the ground and between 0.8 and 1.0 at 13 m above the ground (41). Measurements made on the air in the city of New York (United States) from July 1973 through June 1974 gave an average radon concentration of  $0.1 \text{ pCi l}^{-1}$  (range  $0.06\text{--}0.17 \text{ pCi l}^{-1}$ ), average radon-to-radon daughters ratios ( $^{222}\text{Rn}:\text{}^{218}\text{Po}:\text{}^{214}\text{Pb}:\text{}^{214}\text{Bi}$ ) of 1:0.9:0.7:0.7 and an average value of  $F$  of 0.7 (84). Measurements at the same place in June and July 1972 gave an average radon concentration of  $0.2 \text{ pCi l}^{-1}$  (range  $0.10\text{--}0.22 \text{ pCi l}^{-1}$ ), average radon-to-radon daughters ratios of 1:0.8:0.5:0.3 and an average value of  $F$  of 0.4 (range  $0.18\text{--}0.73$ ) (94). Similar measurements in a rural atmosphere at Sterling Forest, 80 km north of New York, in July 1972 gave an average radon concentration of  $0.2 \text{ pCi l}^{-1}$  (range  $0.16\text{--}0.26 \text{ pCi l}^{-1}$ ), average radon-to-radon daughters ratios of 1:0.8:0.5:0.4, and an average value of  $F$  of 0.42 (range  $0.08\text{--}0.56$ ) (94). The lowest value, 0.08, occurred on a rainy day when the radon daughter activity dropped by a factor of almost 10.

181. The fraction of unattached radon daughters<sup>2</sup> out of doors varies primarily with the concentration and size distribution of the aerosols in the atmosphere. Measurements at Sutton, England (United Kingdom) indicated no consistent difference in the unattached fraction of  $^{218}\text{Po}$  indoors and out of doors (76). It varied between 0.07 and 0.40 (relative to  $^{218}\text{Po}$ ). In two series of measurements in New York City the averages of the unattached fraction relative to radon were found to be 0.04 (range  $0.01\text{--}0.06$ ) (94) and 0.09 (range  $0.05\text{--}0.12$ ) (84). The average value for unattached  $^{212}\text{Pb}$  was 0.02 at an average  $^{212}\text{Pb}$  concentration of  $9 \times 10^{-4} \text{ pCi l}^{-1}$  (84). In Sterling Forest the unattached fraction of  $^{218}\text{Po}$  was, on the average, 0.08 relative to radon (range  $0.04\text{--}0.10$ ). The lowest value, 0.04, was found on a rainy day. The average aerosol concentration was  $7.5 \times 10^3 \text{ particles cm}^{-3}$  compared to  $1.9 \times 10^5 \text{ particles cm}^{-3}$  in New York (94).

182. As the fraction of unattached  $^{218}\text{Po}$  is as a rule less than 0.1, it is possible to estimate the absorbed doses in the basal cells of the segmental bronchioles using a value of  $45 \mu\text{rad per pCi h l}^{-1}$  for the quotient

<sup>2</sup>The unattached fraction of  $^{218}\text{Po}$  is either expressed relative to the total number of atoms of  $^{218}\text{Po}$  measured in the atmosphere ("relative to  $^{218}\text{Po}$ ") or to the total number of atoms of  $^{218}\text{Po}$  that would be present at equilibrium with  $^{222}\text{Rn}$  ("relative to  $^{222}\text{Rn}$ "). Since the atmospheric activity concentration of  $^{218}\text{Po}$  is usually more than 80 per cent of its equilibrium value with  $^{222}\text{Rn}$ , the difference between the two values of the unattached fraction of  $^{218}\text{Po}$  is at most 25 per cent.

between the dose and the time-integral of the equilibrium equivalent concentration of radon (para. 168). The mean radon concentration in continental air is about  $0.1 \text{ pCi l}^{-1}$  (347), with a mean  $F$  of 0.6. Using an occupancy factor of 0.2 for outdoor exposure, the resulting annual dose in the basal cells is about 5 mrad, with a range of 1-25 mrad for different persons located in different places.

183. In order to assess the relative importance of the various natural radionuclides considered in this Annex, the doses from the radon decay products in the pulmonary region of the lung, the gonads, the bone marrow and the bone lining cells also have to be estimated. With regard to the mean dose in the lung, using a dose-to-exposure quotient of  $9 \mu\text{rad per pCi h l}^{-1}$  (para. 168), an annual dose of about 1 mrad is calculated. The doses in organs and tissues outside the respiratory system have been evaluated, as in the 1972 report, from the measurements in guinea-pigs (281, 282). As the ventilation volume and the weight of blood are about the same for man and for guinea-pigs when divided by their respective body weight, the results can be taken as an estimate of the absorbed doses in man. They are calculated to be 0.007 mrad in the gonads, and 0.008 mrad in the bone marrow and the bone lining cells.

184. The thoron daughter concentration in air is mainly measured as the concentration of  $^{212}\text{Pb}$ . In continental air the measured concentrations of  $^{212}\text{Pb}$  are on the average about  $0.001 \text{ pCi l}^{-1}$  (37, 84, 209). This average is based on several long-term measurements (months to years) and the range of the results of these measurements is  $0.0001\text{--}0.003 \text{ pCi l}^{-1}$ . Assuming equilibrium between  $^{212}\text{Pb}$  and  $^{212}\text{Bi}$ , a dose-to-exposure quotient of  $60 \mu\text{rad per pCi h l}^{-1}$  can be used to assess the annual absorbed dose in the whole lung (para. 169). Assuming an occupancy factor of 0.2 for outdoor exposure, the annual dose in the lung is estimated to be 0.1 mrad.

185. More than 90 per cent of the  $^{212}\text{Pb}$  atoms deposited in the bronchial tree are eliminated by swallowing before their decay. Those deposited in the pulmonary region are transferred to the blood with a biological half-life of around 10 h, which means that about 50 per cent of the potential decay energy of  $^{212}\text{Pb}$  is released outside the lung, whereas the corresponding figure for  $^{214}\text{Pb}$  is only 4 per cent (347). The annual doses in tissues outside the respiratory system, as estimated from experiments on guinea-pigs, are  $2 \times 10^{-4}$  mrad in the gonads and  $3 \times 10^{-3}$  mrad in bone marrow and in bone lining cells.

### (c) Exposure indoors

186. As the indoor concentrations of thoron daughters are low compared to those of radon daughters, the main emphasis in this Annex will be on radon. The main contribution to radon indoors is from the building materials. Other sources of significance may be the soil under the building, natural gas and radon-rich water. The radon level outdoors may sometimes also be of significance for the radon level indoors. Even if many measurements have been made on natural radiation



indoors, most indoor measurements have been concerned with the external irradiation and there are only a few extensive surveys of radon and radon daughter levels indoors.

(i) Sources

187. Factors influencing radon levels in a room. The radium content of the building materials constitutes the source of the emanation of radon. High radon levels may be found in buildings with high radium content in the building materials (142), and it has been shown that particularly low radium contents result in low levels (205).

188. However, it is not possible, on a general basis, to correlate the radon levels in a building to the radium content of the building material, mostly because of the strong influence of ventilation conditions. Furthermore, variations may occur even with the same building material, depending on the distance from the ground level (342) and whether there is a cellar or not. The higher radon levels in cellars and lower storeys are believed to be due to radon emanation from the soil, but they may also be influenced by the lower ventilation. It is not unusual for different building materials with different radium contents to be used in houses, for outer walls, for inner walls and for insulation.

189. The diffusion of radon from the building materials into a room is influenced by the moisture content of the material, its density, whether or not sealants are used

and the nature of the material itself. When the moisture content in concrete increases by a factor of 2 from about 3 to 7 per cent by weight, the radon emanation may increase by 10 to 20 per cent (15). This effect has also been found with soil samples (230) and it depends on a decreased adsorption power of the particles in the soil and concrete. If, however, the moisture content increases further, the emanation rate decreases. The temperature effect between 20° and 45°C on the emanation rate from concrete has been found to be insignificant (15). At temperatures lower than 0°C the emanation of radon is expected to decrease (21). It has been suggested (119) that the diurnal variations of radon levels found in some buildings depend on the higher temperature during the afternoon, causing higher emanation rates of radon from the walls than during the night. A possible dependence of the radon emanation rate on the atmospheric pressure has also been suggested (170).

190. Few data for the rate of emanation from building materials can be found in the literature. They are presented as diffusion coefficient (unit:  $\text{cm}^2 \text{s}^{-1}$ ), as emanation rate per unit area ( $\text{pCi m}^{-2} \text{s}^{-1}$ ) or as fractional escape ( $\text{pCi escaped per pCi produced}$ ). However, both the fractional escape and the emanation per unit area depend on the thickness of the material. As a rule of thumb the fractional escape is of the order of 1 per cent for building materials in walls and ceilings. Table 27 shows the estimated emanation rate per unit activity concentration of  $^{226}\text{Ra}$  of different materials based on data given in the references.

TABLE 27. RADON EMANATION RATES OF VARIOUS MATERIALS

Material	Emanation rate of $^{222}\text{Rn}$ per unit activity concentration of $^{226}\text{Ra}$ ( $\text{pCi m}^{-2} \text{s}^{-1}$ per $\text{pCi g}^{-1}$ )	Comments	Reference
By-product gypsum	0.01	Internal walls 76 mm thick	265
By-product gypsum	0.001	Ceilings 13 mm thick	265
Concrete	0.005	10 cm thick	306
Uranium mill tailings	0.2	10 cm thick	306
Uranium mill tailings	1.6	"Infinite" thickness	306
Soil	0.5	"Infinite" thickness	33
Light concrete	0.02	20 cm thick	195
Heavy concrete	0.01	8 cm thick	195

191. The effect of paints and sealants on the emanation rate is quite variable. Cement plaster and asphalt coating on the walls does not reduce the emanation rate (15). However, by heavily coating with epoxy paint the emanation rate can be reduced by a factor of 4. Furthermore, three layers of oil paint reduce the radon emanation rate by about an order of magnitude (195). Several sealants have been tested both in the uranium industry (297) as well as for buildings incorporating uranium mill tailings in the construction (64).

192. The most effective factor influencing the radon level in houses is the ventilation rate, defined as the fractional change of air per unit time. The equilibrium radon concentration in a room varies with the ventilation rate  $\lambda_v$  (unit: air changes per hour,  $\text{h}^{-1}$ ) according to the formula

$$C = C_0 + eT/(\lambda_v + \lambda)V$$

where  $e$  is the emanation rate (in  $\text{pCi m}^{-2} \text{h}^{-1}$ );  $T$ , the area (in  $\text{m}^2$ ) of the emanating surfaces;  $V$ , the volume

(in  $\text{m}^3$ ) of the room;  $\lambda$ , the decay constant ( $0.00755 \text{ h}^{-1}$ ); and  $C_0$ , radon concentration (in  $\text{pCi m}^{-3}$ ) of the ventilation air (outdoor air). Changes in the ventilation of a poorly ventilated room influence the radon level considerably. Conversely, the radon level in a room in which the ventilation ceases may increase to 100 times an earlier level obtained with an air change rate of  $1 \text{ h}^{-1}$ . For example, in a room with  $V = 30 \text{ m}^3$ ,  $T = 50 \text{ m}^2$  (walls and ceiling),  $\lambda_v = 1 \text{ h}^{-1}$ ,  $e = 0.005 \text{ pCi m}^{-2} \text{ s}^{-1}$  per picocurie of  $^{226}\text{Ra}$  in each gram of concrete (table 27), and concrete with a  $^{226}\text{Ra}$  content of  $5 \text{ pCi g}^{-1}$ , the radon activity concentration will be about  $0.15 \text{ pCi l}^{-1}$ . If the room is unventilated, the radon activity concentration increases to about  $20 \text{ pCi l}^{-1}$ .

193. The ventilation differs in different types of houses, depending on age, number of storeys and number of apartments, and in different parts of a building. It is frequently found that the basement of a house has less ventilation than the higher floors and that consequently the radon levels are higher. The ventilation rate in houses is different in different countries owing to differences in climate, heating systems and building standards. Air change rates of  $2.5 \text{ h}^{-1}$  are not unusual in many countries (347). However, in countries with cold climates the ventilation rate may be much less; it has been found to be in the range  $0.1\text{--}0.9 \text{ h}^{-1}$  in central Sweden in houses built after 1970 (251). Central heating and good insulation reduce air exchange rates and increase radon concentrations. In some houses, there is often only natural draught ventilation, which is less efficient than the forced ventilation found in tall buildings. In the case of recirculated forced-air heating or recirculation of ventilation air, only a fraction  $p$  of fresh air is admitted, and the true air exchange rate will be reduced to  $\lambda_v p$ .

194. Diurnal variations of the indoor radon levels may occur because of variations in the outdoor concentration and the opening or closing of windows. In measurements in residential structures in Grand Junction (United States), diurnal variations of a factor of 2-3 were found (322). Variations occurred even in vacant houses, with maxima in the afternoon and decreasing levels during the night, and no correlation was found with either the barometric pressure or the indoor and outdoor temperatures. Other long-term measurements of radon concentrations in a house have shown an increase of radon level during the night up to levels much greater than those outdoors (67). The great effect of closing and opening doors between rooms has also been demonstrated in apartments with natural, as well as forced, ventilation (333). Opening doors could lead to reductions in the radon levels by a factor of 5.

195. Temperature, wind direction and wind speed influence the ventilation rate. It has been shown that a mere change in wind direction to a direction at right angles to the outer wall of a badly ventilated room reduces the radon level by a factor of 3 (333). In rooms with open vents the reduction is even greater (73). If the radon levels indoors are of the same order as the levels outdoors, the variation indoors follow the pattern outdoors, but the variations are smaller (119).

196. *Levels and doses.* For the estimation of doses, use has to be made of the results of a limited number of measurements. Since large variations may occur, as already described, it may be very difficult to judge how representative the results are. It has been suggested (369), as a criterion for determining the radon daughters concentration, that four to six samples of several weeks' duration spread throughout the year should be necessary to provide representative values. Results of radon and radon daughter measurements are shown in table 28. The measurements by Fisenne, Harley and George (84, 94) show the effect of recirculation (high fraction of unattached Ra A, low value of  $F$ ) and show that even with a low ventilation rate the value of  $F$  is fairly low (0.4). The radon activity concentrations in the Hungarian houses (342) are assumed to be numerically equal to the  $^{218}\text{Po}$  activity concentrations (according to the reference). This results in a rather high value of  $F$ .

197. There are no direct measurements reported on radon and radon daughters in houses which give values of  $F$  higher than 0.5. This value is used in this report for the purpose of assessing doses in cases in which only the radon values have been given. As indicated in paragraph 168, the quotient of bronchial dose to the time-integral of the equilibrium equivalent concentration of radon is taken to be  $45 \mu\text{rad per pCi h l}^{-1}$ , as the unattached fraction is of the order of 0.1 or less. The occupancy factor is assumed to be 0.8.

198. The difficulty in estimating mean annual bronchial doses to the population is illustrated by the Hungarian and the Swedish values. As regards the Hungarian data, the weighted mean dose, taking into account the use of different types of apartments, differs a great deal from the unweighted mean. The weighted mean annual dose is 1050 mrad while the unweighted mean annual dose is 700 mrad. Regarding the Swedish data, the mean annual dose obtained from the levels of radon and radon daughters measured in the "new buildings" (houses built after 1970) is 480 mrad, which is twice the result obtained from the measurements performed in the "old buildings" (houses built before 1956). Possible reasons for that difference are that, in modern houses, (a) the ventilation rate is lower, (b) more concrete is used, and (c) the activity concentration of  $^{226}\text{Ra}$  in the concrete is higher (334). Taking into account the proportion of the "new buildings", the mean annual dose in the segmental bronchial epithelium is estimated to be about 320 mrad.

199. The differences between the doses calculated in this chapter (and in table 29) and those given in the references depend on different assumptions concerning the occupancy factors and the dose-to-exposure quotients. The arithmetic mean of the annual doses obtained for the five countries listed in table 29 is about 250 mrad. Since a substantial fraction of the measurements were taken in unventilated buildings, this mean is believed to be an overestimate of the average dose.

200. Another estimate can be tentatively derived from the information contained in table 28 and the paragraphs above. Assuming that a representative value of the average  $^{222}\text{Rn}$  concentration indoors is  $1 \text{ pCi l}^{-1}$